FINAL REPORT

ACOUSTIC EMISSION MONITORING OF STEEL BRIDGE MEMBERS

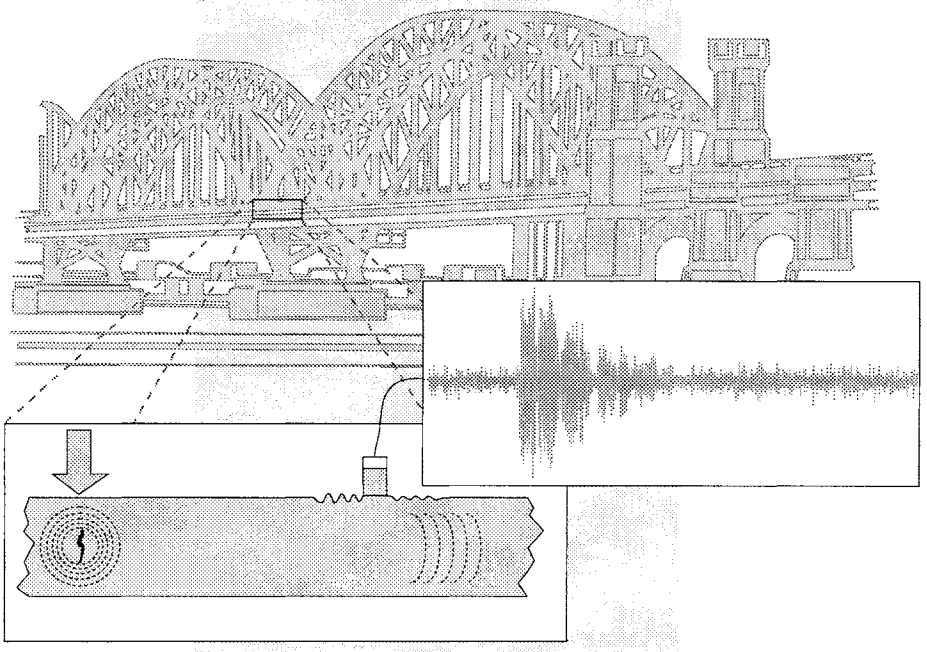

MARGARIT G. LOZEV, Ph.D.
Senior Research Scientist

GERARDO G. CLEMEÑA, Ph.D.
Principal Research Scientist

JOHN C. DUKE, Jr., Ph.D.
Professor

MIGUEL F. SISON, Jr.
Graduate Research Assistant

MICHAEL R. HORNE
Graduate Research Assistant

V · I · R · G · I · N · I · A
VTRC
TRANSPORTATION RESEARCH COUNCIL

VIRGINIA TRANSPORTATION RESEARCH COUNCIL

Standard Title Page - Report on Federally Funded Project

1. Report No. FHWA/VTRC 97-R13	2. Government Accession No.	3. Recipient's Catalog No.
4. Title and Subtitle Acoustic Emission Monitoring of Steel Bridge Members		5. Report Date April 1997 6. Performing Organization Code
7. Author(s) M.G. Lozev, Ph.D., C.G. Clemena, Ph.D., J.C. Duke, Ph.D., M.F. Sison, and M.R. Horne		8. Performing Organization Report No. VTRC 97-R13
9. Performing Organization and Address Virginia Transportation Research Council 530 Edgemont Road Charlottesville, VA 22903		10. Work Unit No. (TRAIS) 11. Contract or Grant No. 0569-010
12. Sponsoring Agencies' Name and Address Virginia Department of Transportation 1401 E. Broad Street Richmond, VA 23219 FHWA 1504 Santa Rosa Road Richmond, VA 23239		13. Type of Report and Period Covered Final Report 14. Sponsoring Agency Code
15. Supplementary Notes		

16. Abstract

This report describes the results of a study to characterize the acoustic emission (AE) associated with steel cracking and various sources of noise in a typical bridge environment. It summarizes previous applications of AE monitoring of steel bridges and describes the AE field testing of five bridges in Virginia, including extensive data and discussion of the field testing of the active cracking of a hanger on the Rte. 29 bridge over the Robinson River in Madison County.

The study revealed that AE monitoring is sensitive to the acoustic energy emitted by steel bridge members during the formation and growth of cracks. It is the only method that can distinguish between active and benign cracks. It is also possible to discriminate between AE caused by crack growth and irrelevant noise. AE information can be significant in making repair or replacement decisions, and AE could be used for the continuous remote monitoring of critical bridge members or even entire bridges. A database developed from AE studies would allow the integration of real-time monitoring of the deterioration of steel bridge members into bridge management and decision making in lieu of frequent visual inspections.

17 Key Words	18. Distribution Statement
acoustic emission, bridge, crack monitoring, noise, steel	No restrictions. This document is available to the public through NTIS, Springfield, VA 22161.

19. Security Classif. (of this report)	20. Security Classif. (of this page)	21. No. of Pages	22. Price
Unclassified	Unclassified	91	

Form DOT F 1700.7 (8-72) Reproduction of completed page authorized

FINAL REPORT

ACOUSTIC EMISSION MONITORING OF STEEL BRIDGE MEMBERS

Margarit G. Lozev, Ph.D.
Senior Research Scientist

Gerardo G. Clemeña, Ph.D.
Principal Research Scientist

John C. Duke, Jr., Ph.D.
Professor

Miguel F. Sison, Jr.
Graduate Research Assistant

Michael R. Horne
Graduate Research Assistant

Virginia Transportation Research Council
(A Cooperative Organization Sponsored Jointly by the
Virginia Department of Transportation and the
University of Virginia)

In Cooperation with the U.S. Department of Transportation
Federal Highway Administration

Charlottesville, Virginia

April 1997
VTRC 97-R13

EXECUTIVE SUMMARY

Although the acoustic emission (AE) method has existed for decades, the use of AE in bridge integrity assurance applications has been limited in comparison to other nondestructive testing methods that have become standard tools for bridge engineers and inspectors. The existence of sources of emissions other than crack growth on a structure as inherently noisy as a bridge has been the main impediment to the successful and regular use of AE in bridge inspection. The advent of more powerful yet portable computers give added encouragement that the problem of noise discrimination and filtering in field applications can finally be resolved.

Past studies of AE have not fully developed the engineering application of AE to bridge monitoring. Typically, these studies have been directed at extensive AE testing approaches designed to use AE to detect and monitor deterioration. In particular, to monitor critical regions of a structure reliably, unwanted noises associated with bolt fretting and rubbing or traffic must be distinguished systematically from sounds associated with crack initiation or growth. Strategies that can accomplish this discrimination for all critical areas of a typical bridge structure require impractical, expensive instrumentation systems. By focusing on defined critical areas, as this study does, the advantages of AE monitoring may be fully exploited.

The objective of this study was to study and characterize the AE associated with various sources of noise in a typical bridge environment.

This report summarizes previous applications of AE monitoring of steel bridges and describes the AE field testing of five bridges in Virginia, including extensive data and discussion of the field testing of the active cracking of a hanger on the Rte. 29 bridge over the Robinson River in Madison County. Six appendixes provide an introduction to the AE theory, detail the laboratory fatigue testing of bridge steels and the simulated environmental exposure of AE transducer-monitoring adhesives, provide an executive summary about remote AE field monitoring systems, and provide a procedural outline for applying AE monitoring of steel bridge members.

This study demonstrated that a pattern recognition process involving source location, strain magnitude, location on strain cycle, and uniqueness of waveforms could be used to distinguish between primary and secondary AE and spurious noise.

A large majority of detected emissions from the cracks were repetitive, with nearly identical AE waveforms. These emissions were attributable to crack face rubbing and the crushing of dirt and corrosion products between the crack faces.

Very few probable crack-growth AE were recorded. Secondary AE, especially repetitive emissions, were high-amplitude, readily detectable signals. In the absence of actual crack growth AE, secondary emissions can aid in identifying and locating flaws in steel bridge structures.

Crack activity varies from time to time, with quiet intervals occurring between periods of discernible activity. It is, therefore, necessary that continuous monitoring be performed over a significant length of time to ensure that all loading and environmental conditions that could affect crack activity are covered during the period of testing.

The progress of a crack can be assessed qualitatively using the apparent longevity of repetitive AE attributable to crack face rubbing. The presence, for example, of AE waveforms that appear unchanged from one monitoring period to another is an indication that significant flaw growth could not have taken place between the tests.

The nature of repetitive emissions, wherein a single type of nearly identical waveforms had signal strengths that varied in magnitude by as much as 22 dB, make it unlikely that time domain analysis of AE from bridge members alone can accurately distinguish between noise and crack growth emissions.

Wideband sensors should be used in conducting preliminary AE tests on bridges since they are more capable of distinguishing between different AE source types than resonant sensors.

AE waveforms not originating from the cracks such as traffic, mechanical, and fretting noise are distinguishable from crack-related AE because of their lower frequency content and much longer rise times and durations.

Since secondary emissions are far easier to detect, whether they could be used as indirect yet reliable indicators of crack severity should be investigated. A particular challenge with regard to this issue is the difficulty associated with accurately simulating the causes for such emissions in the laboratory or systematically studying these effects in the field.

Bridge management should use AE monitoring in accordance with the procedural guidelines for applying AE monitoring to steel bridge components provided in Appendix F.

FINAL REPORT

ACOUSTIC EMISSION MONITORING OF STEEL BRIDGE MEMBERS

Margarit G. Lozev, Ph.D.
Senior Research Scientist

Gerardo G. Clemeña, Ph.D.
Principal Research Scientist

John C. Duke, Jr., Ph.D.
Professor

Miguel F. Sison, Jr.
Graduate Research Assistant

Michael R. Horne
Graduate Research Assistant

INTRODUCTION

Although corrosion loss is the biggest cause of deterioration in steel bridges, the few cases of recorded failures in service have been due to fatigue crack growth. The danger to motorists and the economic consequences that the failure of a bridge would create are self-evident. Currently, the primary method of ensuring the integrity of bridges is through periodic visual inspections of the entire structure with emphasis on details that are known to be prone to developing defects. Successful implementation of an inspection program is therefore heavily dependent on the skill and experience of the personnel performing the inspections. As valuable aids in the inspection process, nondestructive evaluation (NDE) methods such as ultrasonic flaw detection have been used for years to detect, confirm, and measure damage to structural members. Each method has particular advantages and limitations that determine its appropriateness for a specific inspection application.

Although the method itself has existed for decades, the use of acoustic emission (AE) in bridge integrity assurance applications has been limited in comparison to other NDE methods that have become standard tools for bridge engineers and inspectors, despite its many advantages. Among the most important in terms of applicability to highway bridge testing are:

- *AE detects actively growing flaws.* Since repair of existing cracks can at times do more harm than good to a structure, it is necessary to determine whether a defect is benign or active before repairs are made. Other methods require periodic crack length measurements to ascertain whether a crack is active.

- *AE can locate remote or hidden flaws as long as a propagation path exists between the flaw and the detecting sensors.* This precludes the need for direct and close access to the location of a defect. For example, AE can detect flaws under paint layers without removal of the coatings.

- *AE is the only NDE method amenable to long-term continuous monitoring of flaws.* AE is significantly more sensitive than other NDE methods and can detect even incipient flaws. Other methods, which are highly dependent on defect size or surface opening, can reliably detect defects only after they have progressed beyond a certain size.

The existence of sources of emissions other than crack growth on a structure as inherently noisy as a bridge has been the main impediment to the successful and regular use of AE in bridge inspection. However, for an NDE method that relies heavily on instrumentation, continued advances in electronics that have resulted in systems with faster microprocessors, better background noise filtering, and waveform recording and processing capabilities promise better chances of improving the reliability of AE bridge testing. The advent of more powerful yet portable computers gives added encouragement that the problem of noise discrimination and filtering in field applications can finally be resolved.

This report presents the findings of a comprehensive study that combined laboratory testing, short-term field monitoring, and long-term continuous, remote field monitoring of AE from steel bridge members. A strategy for deciding when to use AE monitoring of steel bridges is recommended, and specific guidelines for implementation and data analysis are provided.

PROBLEM STATEMENT

Past studies of AE did not fully develop the engineering application of AE to bridge monitoring. Typically, these studies were directed at extensive AE testing approaches designed to use AE to detect and monitor deterioration. In particular, to monitor critical regions of a structure reliably, unwanted noises associated with bolt fretting and rubbing or traffic must be distinguished systematically from sounds associated with crack initiation or growth. Strategies that can accomplish this discrimination for the critical areas of a typical bridge structure require impracticably expensive instrumentation systems. By focusing on defined critical areas, as this study does, the advantages of AE monitoring may be fully exploited.

PURPOSE AND SCOPE

The objectives of this study were (1) to study and characterize the AE associated with various sources of noise in a typical bridge environment, and (2) to develop relevant expertise in the

Virginia Department of Transportation (VDOT) consistent with guidelines on AE soon to be released by the Federal Highway Administration (FHWA).

REVIEW OF RELATED LITERATURE

Appendix A is a discussion of AE technology for the reader not familiar with this NDE method.

Overview of Acoustic Emission

One of the most useful applications of AE in NDE work is in the location of active defects. The most common method of source location involves measuring the differences between arrival times of a signal at two or more transducers carefully positioned in a geometric pattern around a source. The simplest configuration, the zone method, assigns a signal to the location zone covered by the sensor that first detects it. Linear flaw location is calculated from the formula

$$x = \frac{v\,(t_a - t_b)}{2}$$

where x is the distance between the source to the midpoint between two transducers, t_a is the arrival time at transducer a, t_b is the time of arrival at transducer b, and v is a constant determined from the speed of wave propagation through the material. Other configurations range from three sensors in a triangle to multiple sensors arranged in complex 3D configurations. The accuracy of location is dependent on the geometry of the test specimen, signal characteristics of the emission, and sensor spacing.

Another timing method of locating an AE source makes use of cross correlation techniques to measure the time delay between two waveforms. The cross correlation function between a given waveform detected at one sensor, $A(t)$, and the same waveform as detected at another sensor, $B(t)$, is given by

$$C_{AB}(\tau) = \int_0^T A(t)\, B(t + \tau)\, dt$$

where t is a time delay or lag and T is the time interval corresponding to the length of the waveform record used for the analysis. The function is a maximum at the value of lag that coincides with the time difference of arrival of the waveform at the two sensors. Unlike timing methods, cross correlation is not threshold dependent and can be used for locating continuous emissions that have no distinct sensor arrival times.

Improvements in instrumentation in recent years have made it possible to record signal waveforms not only in the well-controlled environments of laboratories but also in actual AE field tests. The ability to capture waveform records using high-speed analog-to-digital converters provides the AE investigator with more information about an AE event and better accuracy and reliability in interpreting results. Gorman pointed out that analysis of AE using waveform processing has a better theoretical basis than simple parameter-based analyses and may serve to reconcile conflicting conclusions that have resulted from the older method.[1]

Consequent with the ability to record waveforms is the ability to extract full-frequency domain information from a waveform. The frequency spectra of individual emissions are obtained through use of algorithms such as the fast Fourier transform (FFT) implemented in software or hardware-based spectrum analyzers. Graham and Alers discovered from tests on A533-B steel that frequency content could be used to distinguish between the two major types of damage mechanisms: plastic deformation and crack propagation.[2] In a separate study, they found that frequency spectra are not substantially affected by specimen size and shape or mode conversion because of multiple wave reflections.[3] Hartman and Kline attributed the three distinct frequency spectra they observed from tensile loading of HF-1 steel to microplasticity, plasticity, and deformation after recovery.[4] Crostack demonstrated that frequency analysis could be used to identify the different source mechanisms present in welding processes.[5]

Acoustic Emission in Fatigue Studies

A majority of the applications of the AE technique as an NDE tool for evaluating structures has been to detect and monitor fatigue cracks. Numerous studies can be found in the literature that involve finding correlations between fatigue crack growth and the nature of the consequent acoustic emissions. In 1973, Morton et al., working on aluminum alloy specimens, reported a power law relationship between the total AE counts per cycle, dN/dn, and the range of stress intensity factors, Dk, i.e.,

$$dN/dn = A\, Dk^{n}$$

where A and n are material constants.[6] The equation bears a strong resemblance to the Paris law for crack propagation in fatigue,

$$da/dn = C\, Dk^{m}$$

where C and m are also material constants. Emissions were determined to be more closely related to the volume of the plastic zone ahead of the crack tip than to crack extension. A year later, the same team published their investigation of the effect of loading variables on the AE produced by fatigue crack growth on aluminum and magnesium alloys.[7] They found that variations in the cyclic loading frequency and load ratio had no effect on the AE count rate. That

same year, Harris and Dunegan determined that AE counts per cycle are closely related to the energy released by crack extension per cycle.[8] Lindley et al. would later add that deformation and fracture events within the plastic zone contribute to detected AE.[9]

In addition to damage mechanisms directly associated with crack propagation, other processes that are a consequence of fatigue crack growth are potential sources of AE. Crack closure resulting in friction between crack surfaces and fracture of corrosion products in the case of environmentally exposed flaws also generate some forms of elastic waves that are detected as AE.

The point of occurrence of emissions in the load cycle has been a principal means of distinguishing between damage-related, or primary, and non-damage related, or secondary, emissions. Morton et al. found from high-cycle fatigue testing of aluminum that emissions were detected close to maximum load and near minimum load during both rising and decreasing loads.[7] The low-load emissions, which they tentatively attributed to crack closure, had slower rise times and larger amplitudes than the emissions near maximum load. Sinclair et al. found that the major sources of AE from fatigue loading of the three types of steel they studied were microfracture processes just ahead of the crack and the "unsticking" of partially repaired areas of the crack face upon increasing load.[10]

Lindley et al. reported in 1978 the first detailed investigation of the crack closure phenomena with respect to the detection of AE.[9] Closure emissions were seen to be repetitive and, although also detected during falling loads, mostly occurred on the rising part of the cycle. These emissions were produced generally below mean load but were also sometimes found to occur at the top 20 to 30 percent of the load range. The effects of overloads on emissions were also investigated. It was found that these resulted in a decrease in both crack growth and crack closure emissions.

Kim et al. detected crack rubbing signals only at low, increasing loads, and Cherfaoui et al. found them to occur at low decreasing loads.[11,12] Both teams of investigators reported detecting crack growth AE only near peak loads at the rising part of the cycle. Similar results were obtained by Weatherly et al.[13] However, unlike in other studies, crack closure emissions were sometimes detected close to maximum loads. This led the authors to conclude that the practice of load gating to ignore emissions occurring at lower parts of the cycle is not sufficient to exclude all crack closure AE.

Using results from previous investigations on crack growth and crack closure AE, Bowles performed fatigue tests on a Mirage aircraft to determine in part the load dependence of the two types of AE under complex loading cycles.[14] The aircraft parts monitored produced AE mostly at

load regions where crack growth was not expected to occur. It was also determined that crack rubbing emissions have no load cycle dependence, i.e., can occur anywhere in a fatigue load cycle.

Noise Discrimination in Acoustic Emission

The most serious obstacle to the successful application of AE to the surveillance of structures is in the reliable detection of damage growth-related emissions over a background of various noise signals. In 1971, Nakamura developed a system capable of isolating AE coming from a region of interest.[15] Noise signals originating outside this region are detected by a "slave" sensor that closes a gate that is normally open and prevents the "master" sensor from producing an output attributable to the emission. Horak and Weyhreter further improved this design in 1976 by incorporating a rise time criterion.[16] Knowing that the rise time of a waveform increases with distance from a source, they developed an algorithm to reject emissions having rise times greater than a preset value.

In 1984, McBride and Maclachlan, as a result of tests conducted on aluminum specimens attached to the frame of an aircraft, recommended a three-point criteria for distinguishing sources of emissions[17]: (1) analysis of signal characteristics, (2) location of source, and (3) measurement of an external parameter such as load or strain. Based on these guidelines, emissions were classified as being attributable to either crack growth, crack face rubbing, or structural noise. The first two types were found to have much shorter rise times than the noise signals. Although they had comparable rise times, crack growth emissions had a much longer duration than emissions attributable to crack face rubbing.

Working on a specimen with a simulated pin joint, Friesel collected AE waveforms from cracks growing at the edges of the pinhole and fretting noise produced by the joint.[18] Several waveform features were derived from which rise time, signal mean, and signal skewness were found best in distinguishing crack growth from fretting emissions. AE from the fracture of pencil lead were used to calibrate the test setup since these appeared to have features similar to crack growth signals.

Scala and Coyle employed a semiadaptive AE processing method to identify AE attributable to fatigue crack propagation on a Mirage aircraft subjected to full-scale fatigue testing.[19] The method involved comparing features of AE waveforms collected during testing to predicted features based on waveforms produced by the fracture of pencil lead at designated locations on the structure. Rise time characteristics and the autocorrelation function of the waveforms were found effective in rejecting spurious emissions.

Deuster et al. similarly found that rise time was an effective discriminator.[20] It was believed that this parameter is directly related to the duration of the source lifetime. Microscopic crack growth had earlier been determined to have very short lifetimes, whereas crack surface friction had longer source lifetimes. Results were consistent among the three fatigue tests conducted: cyclic pressurization of a pressure vessel, cyclic thermal shock of a nozzle, and cyclic fatigue tests of compact tension specimens.

In a two-part study on the fatigue of aluminum alloys, Buttle and Scruby employed extremely accurate wideband sensors to locate and characterize crack-related and noise AE.[21,22] Several waveform features were found useful in discriminating among crack growth, fretting, and spurious emissions. Compared to the other two types, crack growth emissions have a higher frequency bandwidth and shorter rise times. Fretting signals appeared to have much higher signal amplitudes than crack growth or spurious emissions. Reproducibility of the waveforms was also distinctly different among the three groups. Whereas crack growth waveforms had similar characteristics but different details, fretting waveforms were nearly identical. Spurious waveforms were not reproducible.

In 1990, Scruby et al. hydrotested and pressure cycled a scaled-down PWR vessel and reported a comprehensive analysis of AE from crack face rubbing.[23] Like the fretting emissions reported by Buttle and Scruby, closure emissions were highly reproducible and repetitive and accounted for the vast majority of detected AE events. Though these occurred mostly on falling pressure, they were also detected on the rising part of the cycle from low to relatively high pressures. Most emissions repeated from cycle to cycle at identical pressure levels and positions on the pressure cycle. The researchers concluded that non-repeatability should be the main criterion in determining damage-related AE consistent with the irreversible nature of crack growth. No recorded waveforms from the test were positively identified as being attributable to crack growths, which were believed to have much weaker intensities than closure emissions.

Various investigators have employed statistical pattern recognition techniques to classify and discriminate between crack growth AE and different types of noise emissions. Pattern recognition in AE waveform analysis involves the use of statistical methods to select an optimal set of derived signal features from a larger feature set that may include time and frequency domain characteristics and other quantifiable information about the AE event. This optimal feature set provides the strongest ability to distinguish between the different types of waveforms. A classifier, often a computer algorithm, is then trained to classify events of known class membership automatically. The final step involves using the trained classifier to sort events that have no *a priori* information on class membership.

Harrington and Doctor applied three classifier algorithms to distinguish fatigue crack signals from mechanical noise.[24] Time and frequency domain features of recorded waveforms were derived. From these features, the frequency of the maximum response by itself was found capable of correctly classifying 78 percent of the waveforms. The autocorrelation function also turned out to be an effective discriminator.

Scala and Coyle emphasized the need for using wideband sensors to obtain source-related signal characteristics that can be significant discriminators.[25] The autocorrelation function of the waveforms was determined to be the best feature for distinguishing damage-related AE from emissions attributable to gas flow, electromagnetic interference, and mechanical and electronic noise. Its effectiveness was such that complex algorithms for classifying the two main classes were found unnecessary.

Hutton and Lemon and Graham and Elsley performed fatigue experiments on aluminum specimens that simulated aircraft rivet joints.[26,27] By varying test parameters and using load position information, they were able to produce and distinguish signals attributable to fretting, crack face rubbing, and crack extension. The use of features taken from the spectral energies of waveforms detected by two transducers resulted in a 95 percent success rate in separating fretting noise from crack-related AE.

The effect of varying the test setup on the performance of a classifier was investigated by Horvath and Cook.[28] Classifiers developed using a particular sensor and experiment were found to perform poorly when applied to data collected from other sensors or experiments. Similar results were reported by Melton et al., who used a classifier trained in using data from one specimen to classify signals from another specimen.[29] Fretting signals were classified satisfactorily, but performance was poor in distinguishing crack-related AE. Both studies indicated the strong dependence of AE data on instrumentation and the part being tested.

Acoustic Emission Testing of Steel Bridges

In what was perhaps the first application of instrumented AE monitoring on bridges, Pollock and Smith in 1971 collected AE data during proof testing of a portable military tank bridge.[30] They demonstrated that AE signals recorded in the field could be associated with results of tests on laboratory specimens.

In 1977, Hutton and Skorpik developed a portable digital AE monitor (DAEM) system for use in testing bridges.[31] The system featured an erasable, programmable, read only memory (EPROM) and a zone isolation method that screened out signals originating outside the area of interest. Field testing was performed on two inservice steel highway bridges and box girder fabrication welds at a steel plant.

In 1978, Hopwood and Havens attempted to determine the loading history of demolished bridges by AE testing of tensile specimens fabricated from the bridge materials.[32] However, no difference in AE activity was detected between steels that were new and not yet fatigued and steels that had been through extended service.

Using an electrohydraulic actuator, Salane et al. monitored AE in conjunction with dynamic testing on a full-scale three-span highway bridge cycled in fatigue.[33] An increase in amplitude count was detected when one girder fractured. The detection of AE signals was hampered by noise from the actuator and bridge supports.

The first long-term continuous monitoring of a bridge was begun by the Dunegan Corporation in February 1982 and lasted for 10 months.[34] Planar source location using guard sensors in conjunction with analysis of time domain feature distributions wa used to identify probable crack-related events. The study examined the practical difficulties and the overall feasibility of long-term remote AE monitoring of a bridge. A directional sensor, developed exclusively for this project, was used to study the characteristics of background noise.

The characteristics of wave propagation through a riveted bridge girder were investigated by Noyes et al. in 1983.[35] Using simulated AE from the fracture of pencil lead, they determined that surface conditions had a minimal effect on the velocity of wave propagation. Unclean surfaces, however, tended to increase the attenuation of surface waves.

Miller et al. performed laboratory and field tests to characterize AE signals from flaws and various noise-related emission sources in bridge components.[36] Different approaches were explored using both time and frequency domain representations of AE signals. The use of pattern recognition and source classification for filtering out noise emissions and discriminating between damage-related AE events such as brittle fracture and fatigue was demonstrated. The study highlighted the need to use sensors that reproduce detected AE signals with minimal distortion. To this effect, a point contact, field-worthy broadband transducer was constructed for use in the study.

Prine and Hopwood developed an AE weld monitoring (AEWM) system that was used to perform survey-type inspections of nine steel bridges.[37,38] The system employed a three-step filter that used ringdown counts, event rate, and source location information in conjunction with a frequency bias classifier to distinguish crack-related AE from noise.

In 1987, Vannoy et al. monitored a bridge on the Maryland-Virginia border and found that the predominant peak frequency of noise emissions is distinctly lower than that of crack-related AE.[39] They concluded that most noise signals can be eliminated using software filters designed to exclude emissions having time domain parameters outside an established range of parameters for crack-related AE.

In a study completed in 1991, the same team conducted extensive laboratory tests on full-size A588 bridge beams.[40] Crack-related and noise AE from rolled, welded, and cover-plated beams fatigue loaded to failure were characterized in both the time and frequency domains. Corrosion was found to have no effect on the time domain parameters of crack-related AE.

In a related study, Hariri sought to develop a database of AE signal characteristics from different types of bridge steels of various material conditions, part geometry, and thickness and subject to different loading conditions for application to AE testing of steel bridges.[41] Filters for eliminating noise signals can thus be developed using the ranges of time domain parameters of crack-related AE signals provided by such a database. These parameters were found to be dictated by the type of material, thickness, paint layer and corrosion conditions of the parts monitored; a surface paint layer does not significantly attenuate AE signals.

A series of field tests by the Physical Acoustics Corporation on various structural details of several bridges emphasized the need for source location using guard sensors to filter out irrelevant AE events.[42] AE testing was demonstrated to be well suited for determining the effectiveness of retrofits and discovering new cracks.

In Canada, Gong et al. conducted AE monitoring of 36 railroad bridges over 3 years.[43] Using the Paris law-like relationship between AE count rate and stress intensity factor range,

they were able to classify known cracks into five levels of severity. Noise emissions were eliminated through spatial discrimination and the use of filters based on AE parameter windows determined from laboratory tests on bridge steels.

In 1993, Prine demonstrated the effectiveness of combined AE and strain gage monitoring on tests of three bridges in Wisconsin and California.[44] In a departure from the usual crack characterization function of AE testing, a bascule bridge was monitored to determine the cause of loud impact noises that accompanied the lifting and lowering of the bridge. AE source location was employed to trace the origin of the noises.

Other recent studies on the application of AE to bridge monitoring were performed by Maji and Kratochvil, who field tested an interstate plate girder bridge, and Holford et al., who fatigue tested slender web girders in the laboratory.[45,46]

Physical Acoustics Corporation prepared a report entitled *Acoustic Emission for Bridge Inspection: Application Guidelines,* which was submitted to FHWA in June 1995. In addition, FHWA has posted on the World Wide Web information related to AE monitoring of steel bridge structures (http://www.dot.gov/dotinfo/fhwa/hta/hta-nde.html). Videotapes, one for program managers and another for bridge inspectors, are reportedly in preparation.

Last, a direct outgrowth of this program is a formal cooperative agreement between Physical Acoustics Corporation, FHWA, and the Virginia Transportation Research Council (VTRC) to build a commercially available AE system for remote monitoring of bridges. VTRC is involved in developing AE/parametric function specifications for the system and evaluating and demonstrating the prototype system.

EXPERIMENTAL PROCEDURES

Instrumentation

Data Acquisition System and Transient Digitizer

The AE tests were performed using an 8-channel Spartan ATAE data acquisition system manufactured by Physical Acoustics Corporation (PAC). The system consists of the Spartan unit and a 386 personal computer shown in Figure 1. System setup and data acquisition are controlled by the software program SA-LOC running in a DOS environment. A block diagram of the system is shown in Figure 2.

Of the 8 channels available, 6 were used for performing signal measurements. These channels hold the circuitry that output the time domain parameters of an AE event such as counts, rise time, energy, peak amplitude, RMS, and duration. The two remaining channels were used to digitize and store AE waveforms using the PAC TRA212 Transient Recorder Analyzer system.

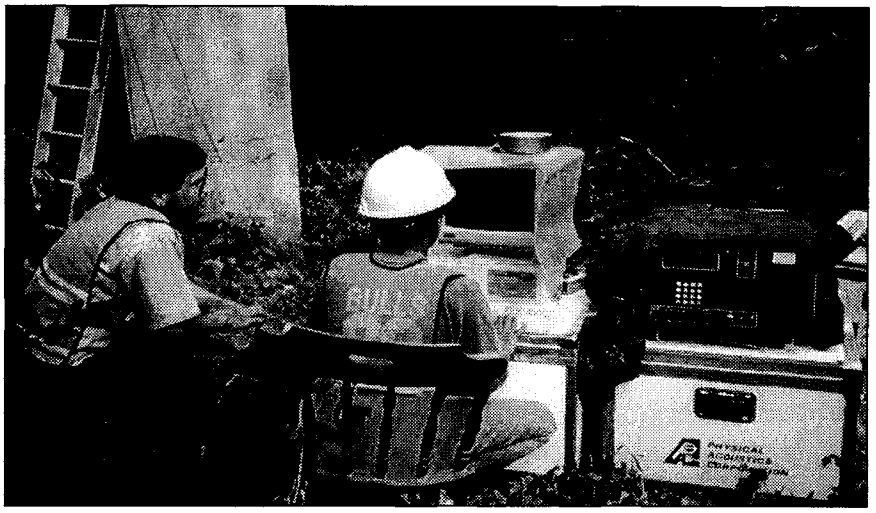

Figure 1. Spartan AT data acquisition system

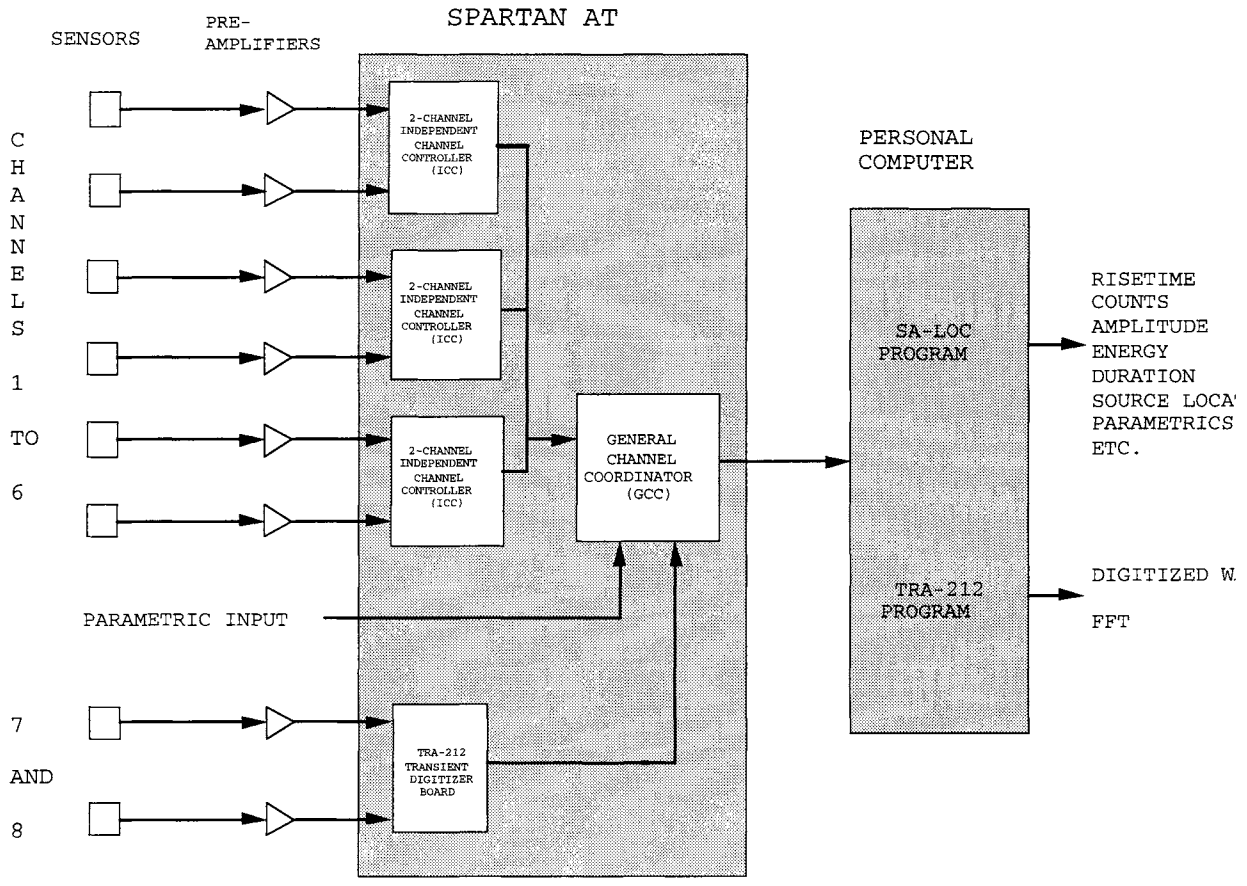

Figure 2. Bridge instrumentation

The SA-LOC program is a menu driven software that sets up the Spartan hardware unit and is capable of real time display and post-test graphical replay of data. This last feature is a powerful data analysis tool that enables the user to display plots of the various measured signal parameters, parametric inputs, and source location results in more than 150 combinations.

Filters can be set up with SA-LOC to accept or reject signals before the main processor board is reached. Up to four filters of user-chosen AE parameters can be configured. Only signals that fall between the specified low and high levels are processed and stored as data.

The source location function of the Spartan system is configured from the location setup menu of SA-LOC. Four types of algorithms are available: zonal, linear, triangular, and rectangular. Since source location is implemented only in software, the system can analyze a set of data using different location configurations. In this study, linear location was used during the bridge tests and zonal location was used during data analysis for implementing guard sensor configurations.

The transient digitizer is controlled by the DOS-based program, TRA212. Features include a maximum digitization rate of 10 MHz and the capability to store samples up to 2 Mb long in memory. The software sets up the digitizing boards, records and stores the measured waveforms on disk files, and performs various display and analysis functions. The frequency spectra of signals are calculated using a FFT algorithm and can be displayed in real time or during post-test analysis. Three modes of triggering are possible: external threshold triggering was used in all bridge tests. Maximum threshold sensitivity is 0.01 V, and signal input voltages of up to 10 V can be recorded. The TRA212 can be run either separately or simultaneously with SA-LOC. The latter mode is accomplished by running TRA212 in background mode while data acquisition is performed with the SA-LOC.

Sensors and Auxiliary Equipment

Two types of piezoelectric transducers, models R30I and WD, both manufactured by PAC, were used in the bridge tests. Table 1 lists their specifications. The R30I is a resonant transducer with a peak resonant frequency of approximately 350 kHz. This model has an integral preamplifier that provides a gain of 40 dB. The WD is a wideband transducer with a relatively flat frequency response between 100 kHz and 1 MHZ. It is a differential transducer that requires a separate external preamplifier. A pair of PAC model 1220A preamplifiers with highpass frequency filters above 20 kHz were used.

The R30I sensors were attached to the hanger by means of magnetic hold-downs while a cyanoacrylic adhesive was used to mount the WD sensor. For the R30I sensors, a thin layer of vacuum grease couplant was applied on the interface between the transducer and the hanger surface to aid in the transmission of AE signals.

The strain gage used was a Micro Measurements Precision gage type EA-O6-20CBW-120 made by Measurements Group, Inc. A general purpose gage designed for strain averaging

Table 1. Specifications for R30I and WD transducers

SENSOR MODEL	DIA x HT (mm)	WEIGHT (g)	PEAK SENSITIVITY Ref V/(m/s)	OPERATING FREQ RANGE (kHz)	RESONANT FREQ (dB)
R30I	1.13 x 1.23	75	98	125-450	350
WD	0.7 x 0.65	8	55	100-1000	125

measurements on large specimens, it has a matrix length of 62.48 mm (2.46 in) and a width of 8.13 mm (0.32 in). The gage was attached using M-Bond 200, a methyl-2 cyanoacrylic adhesive.

Shielded RG58 coaxial cables 15.24 m (50 ft) long connected the sensors (or the preamplifier of the WD sensor) to the Spartan unit. A portion of each cable close to the sensors was either looped around or taped to a secure part of the bridge to prevent the weight of the cable from pulling on the sensors and affecting the quality of the acoustic coupling between the sensor and hanger surface.

A portable, gasoline fueled generator was used to power all instrumentation. Except for the need to shut down the system periodically to allow for refueling, no problems were encountered with the power source.

The Bridge of Madison County

To understand firsthand the constraints imposed on field monitoring with AE, several bridges in Virginia, representing a variety of situations, were monitored. A description of this preliminary monitoring is included in Appendix B. Subsequent to these experiences, it became clear that to assess the engineering application of AE adequately, monitoring of a single structure for an extended period of time was necessary. A particularly convenient candidate was found in the Robinson River Bridge in Madison County Virginia. The need to perform monitoring for an extended period of time, however, raised concern over which methods were most effective for transducer attachment. Appendix C describes "Tests of Transducer Mounting Adhesives."

The long-term field monitoring study was performed on one hanger connection of the northbound bridge. Built in 1934, this two-lane steel bridge, shown in Figure 3, has four steel girders extending over five spans with an overall length of 58.8 m (193 ft). The sole suspended span is supported by eight pin-and-hanger connectors on the north end and pin joints on the south end. The hangers, 609.6 mm (24 in) high by 165.1 mm (6-1/2 in) wide with a 228.6 by 63.5 mm (9 by 2-1/2 in) slot cut out from the middle, were fabricated from steel plats 15.9 mm (5/8 in) thick. The hanger dimensions are shown in Figure 4. The exact specification to which the plate was manufactured could not be determined from existing records of the bridge.

Cracks were discovered in two of the hangers in October 1992. The east exterior hanger had one crack later measured to be 9.5 mm (3/8 in) long. The west interior hanger, which was monitored for this study, had three cracks, two of which are visible in Figure 5. Crack 1 is a flaw 6.4 mm (3 in) long that originated from a punch mark made during fabrication and is visible on

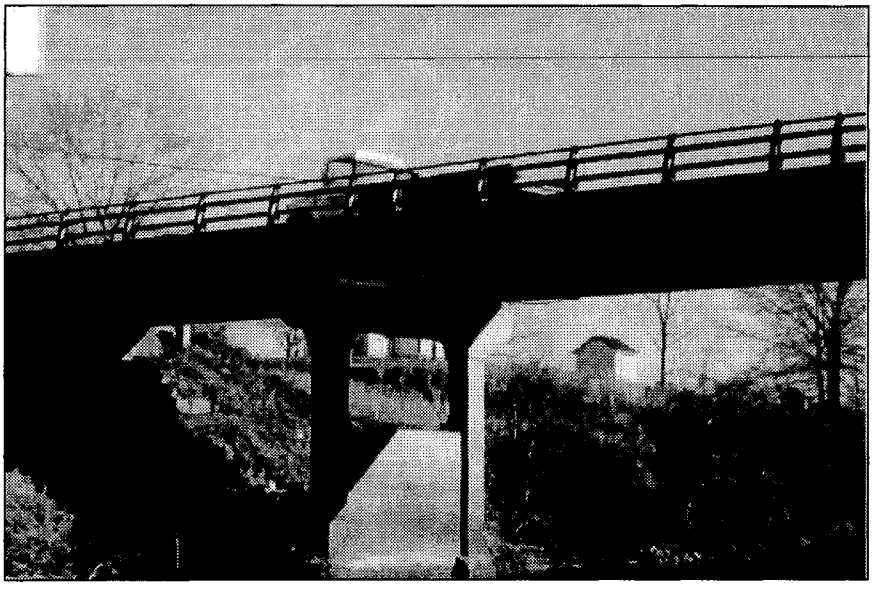

Figure 3. Rte. 29 northbound bridge over Robinson River. Arrow points to monitored hanger.

the exposed hanger face. Crack 2 is on the hidden back face but is partly visible from the inner slot. Crack length for this flaw was not determined during this study. Crack 3 is a conspicuous through crack at the lower part of the hanger and is 36.5 mm (1-7/16 in) long. All three cracks, as well as the crack found on the east exterior hanger, initiated at the internal slot at very similar locations as seen in Figure 4.

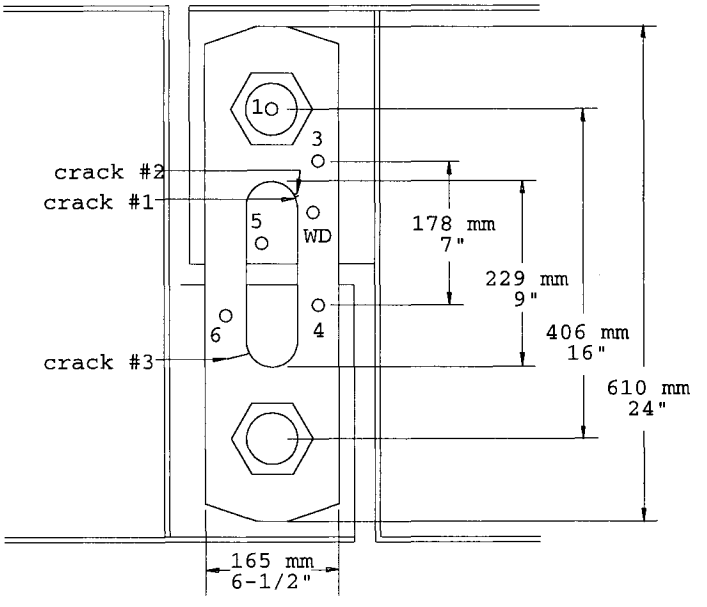

Figure 4. Location of cracks; sensor configuration for Test 1 showing wideband (WD) sensor near cracks 1 and 2; source location sensors 3 and 4; and guard sensors 1, 5, and 6.

Most of the exposed surfaces of the hanger are coated with a sturdy paint layer. This coating was chipped around the cracks to reveal the flaws better. Unpainted surfaces such as the back side of the hanger adjacent to the girder web extension right beneath the cracks had an accumulation of loose and hardened dirt and corrosion products that could enhance transmission of noise from the girder to the hanger. Since such noise would be difficult to isolate from crack-related AE using spatial discrimination, the space between the link and the girder was carefully cleaned prior to the tests. To decrease further the possibility of detecting fretting noise coming from the vicinity of the crack, the area was sprayed with WD-40 lubricant.

Experimental Setup

The scope of the investigation was limited to the monitoring performed on 4 days that are referred to as Tests 1 to 4 corresponding to tests on October 25 and December 8 and 9, 1994, and March 17, 1995, respectively. Since two sensor configurations were used in the December 9 test, they are referred to separately as Tests 3A and 3B. During Test 1, access to the hanger was provided by a bucket truck parked on the slow lane of the bridge. The bridge was later cleared, and both lanes were opened to traffic for the actual test. For Tests 2 to 4, a platform installed beneath the bridge made it possible not to interfere with normal traffic patterns during the entire course of the tests. Cracks 1 and 2 were monitored during Tests 1 to 3A, and crack 3 was monitored during Tests 3B and 4 (see Figure 5).

In Test 1, R30I sensors 3 and 4 were attached 177.8 mm (7 in) apart on both sides of cracks 1 and 2 as shown in Figure 4. The WD sensor was mounted close to the tip of crack 1, and the other three R30I sensors were used as guard sensors to detect noise coming outside the crack zone. Guard sensor 1 was positioned to eliminate rubbing noise from the top pin, and sensor 6 was used to eliminate noise from the lower pin and crack-related AE that might propagate from crack 3. Sensor 5 was mounted on the girder connector plate to filter out noise from the girder itself.

A similar sensor configuration was employed in Test 2 except that another R30I sensor, sensor 2, was attached close to the lower pin so that source location could also be determined for crack 3. This sensor also doubled as a guard sensor for the source location array of cracks 1 and 2 by eliminating noise from the lower pin. Sensor placement is shown in Figure 6. Sensor 5 had to be disabled since the maximum number of operating channels had been reached. Results of Test 1 indicated that very few emissions detected from the girder plate hit this sensor first, making its role as a guard sensor unnecessary. Though unintentional, the distance between sensors 3 and 4 was increased from 177.8 mm (7.0 in) in Test 1 to 184.2 mm (7.25 in) in Test 2. A strain gage was installed on the left side of the hanger during Test 2 and is indicated in Figure 6.

In Test 3, monitoring time was split between the setup of Test 2 and another sensor configuration designed to monitor crack 3 alone. In this second setup, designated Test 3B, the WD sensor was moved close to the tip of crack 3. Guard sensor 1 was mounted on the end of the lower pin, and guard sensor 3 was positioned to eliminate noise from the upper pin. Sensors 2 and 6 were maintained in the same position to determine the linear source location of crack 3.

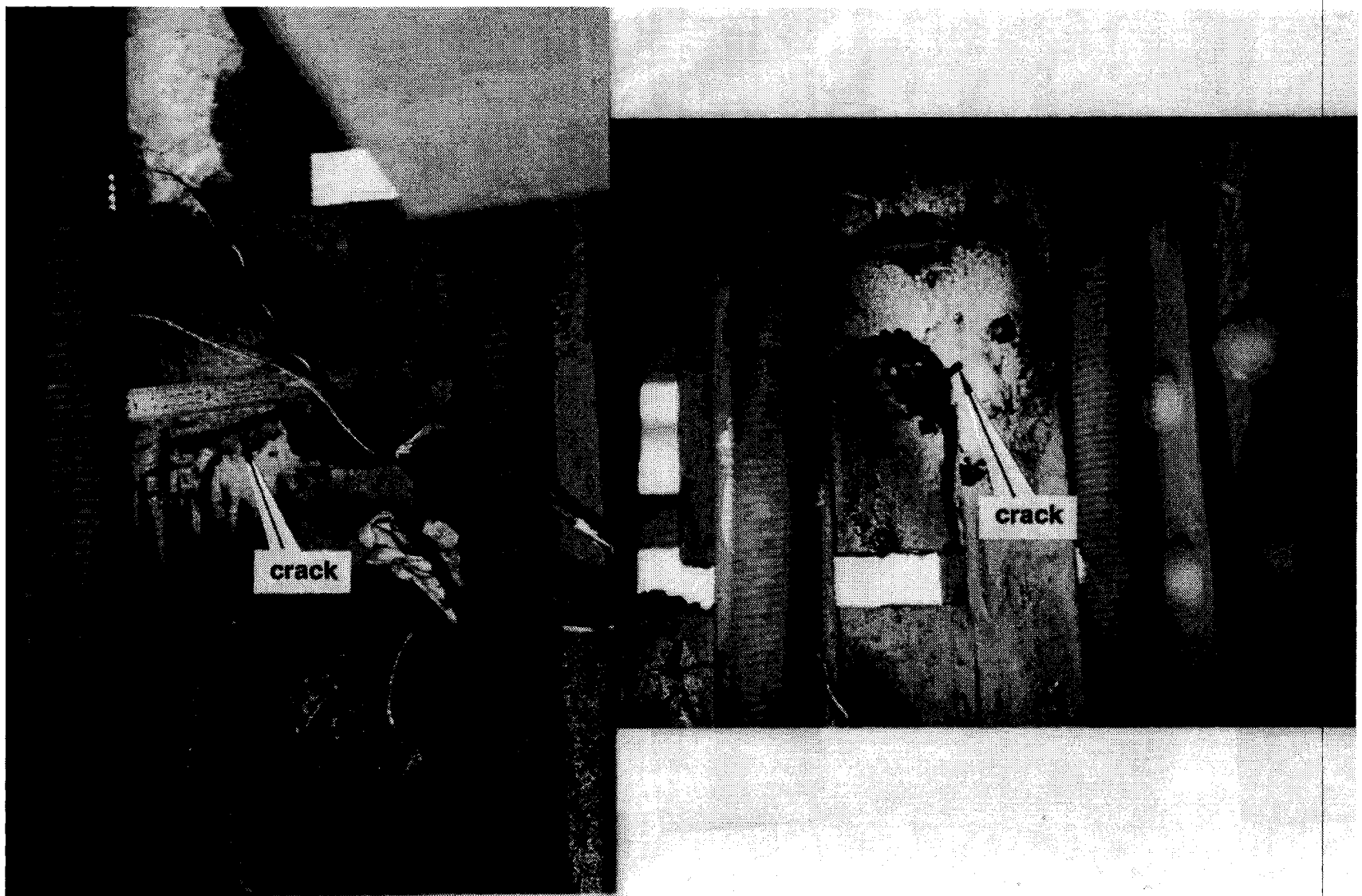

Figure 5. Bridge hanger after dye penetrant test revealing cracks 1 and 3

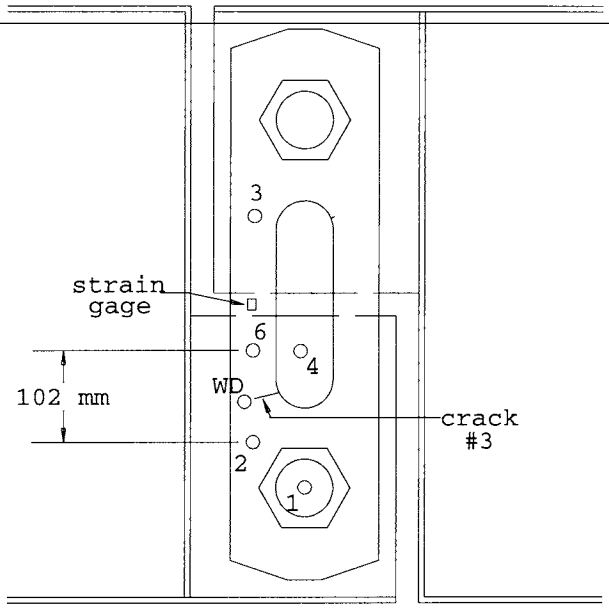

Figure 6. Sensor configuration for Tests 2 and 3A. Shows wideband (WB) sensor near cracks 1 and 2, source location sensors 3 and 4, and guard sensors 1, 2, and 6 (sensors 2 and 6 were also used to locate crack 3 emissions).

Figure 7 illustrates this configuration. This last sensor placement scheme was again used in Test 4, with the exception that the distance between sensors 2 and 6 was increased to 108.0 mm (4.25 in).

The resonant sensors were connected to five channels of the Spartan, and output from the wideband sensor was connected to a Spartan channel and a TRA-212 channel. The Spartan system data consisted of time of arrival and simple AE parameters of the detected signals. In addition, by routing the conditional output of the strain gage to the Spartan and recording such as parametric input 1, each collected signal had a record of the strain level at the time of detection. Strain was sampled at a rate of 10 Hz, and waveforms were collected by the TRA212 at a sampling rate of 5 MHz. The digitizer collected individual waveforms in records 1.17 ms long.

Before each test was begun, pencil lead break calibration checks were performed on all sensors and source location sensor arrays. The test involves fracturing a pencil lead 0.5 mm (0.02 in) in diameter approximately 1.6 mm (1/16 in) from its tip by pressing it against the hanger surface. This generates an intense acoustic signal detected by the sensors as a strong burst of AE. The purpose of the calibration tests is twofold. First, the test ensures that the transducers are in satisfactory acoustic contact with the hanger. The lead breaks were required to register amplitudes of at least 80 dB for a reference voltage of 1 mV and a total system gain of 80 dB for a sensor mounting to be considered acceptable. The second purpose is to check the accuracy of the source location setup. This involves indirectly determining the actual value of the acoustic wave speed on the hanger.

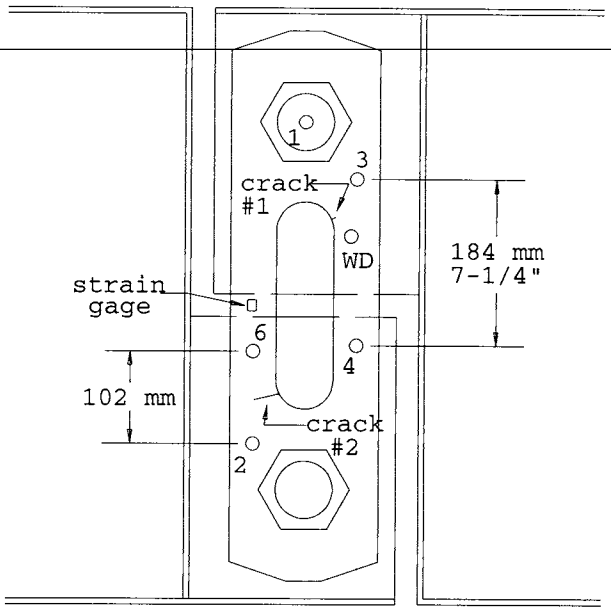

Figure 7. Sensor configuration for Test 3B. Shows wideband (WD) sensor near crack 3, source location sensors 2 and 6, and guard sensors 1, 3, and 4.

The SA-LOC requires the user to input a value for the acoustic wave speed of the material being tested. In AE testing, this could be anywhere between the velocity of longitudinal bulk waves and that of surface waves. The actual wave speed, however, may vary from test to test as influenced by the geometry and condition of the part being tested. An approximate value of this wave speed can be determined using the differences in the time of arrival of lead break signals at two transducers separated by a known distance.

With the actual wave speed entered into the computer, further lead break tests were done to check the accuracy of the source location setup. The lead was broken close to the areas of interest, such as the tips of the cracks, while the location of the detected signal on an event-position graph was checked. A consistently correct location reading indicated the sensors were ready. It should be noted that source location algorithms are implemented completely in software. Location results can be fine tuned during post-test analysis by using different wave speed values or different sensor combinations without having to change the original data or sacrificing the loss of information during data collection. Guard sensor analysis was implemented completely by software.

The final step involved setting the threshold levels of the SA-LOC and the TRA212. Maximum sensitivity was always desired, but the choice was constrained by the level of background noise. A practical and obvious basis for selecting the optimum threshold level was that no AE should be detected when no vehicles were passing over the bridge. Thus noted, a total system gain of 80 dB and a floating threshold of 30 dB, later lowered to 25 dB, were used with the SA-LOC, and the TRA was operated at a total system gain of 80 dB. The digitizer was also threshold triggered at a level that corresponded approximately to that of the Spartan system.

Data Acquisition

Continuous data acquisition and storage can be accomplished with the Spartan system but not with the TRA212. The waveforms recorded by the digitizer are initially stored in computer memory until this is filled. At this point, data collection must be interrupted so that the waveforms can be saved as disk files. At the TRA212 settings used during monitoring, this meant stopping a test after 128 to 170 waveforms were collected. This many waveforms were often recorded from the crack 3 sensor configuration for the few seconds it took a tractor-trailer truck to cross the bridge. It was, therefore, necessary to be selective in determining which batch of collected waveforms were to be stored permanently since the resulting files took up considerable disk space on the computer. For Tests 1 to 3, data acquisition was initiated as soon as the system was ready after the preceding acquisition period. All detected AE activity during these periods was stored for later analysis without regard to actual strain levels that corresponded to the AE data. Results from Test 3 indicated the possible range of live strain levels. Based on this, only the TRA212 files that included waveforms detected at the upper limit of this range were stored during Test 4 for later analysis. These strains were produced by only a few tractor-trailer trucks that crossed the bridge on the fast lane (beneath which the hanger was located) simultaneously with other vehicles. In the 2-1/2 hours the bridge was watched during Test 4, these highest strain levels occurred only on three occasions, corresponding to files N05, N09, and N20, of six high-strain files. For Test 3B, the highest strains were recorded in one file, M33, of nine recorded waveform files.

RESULTS

Results from monitoring the hanger are presented here. Results from the laboratory tests on CT specimens performed to help clarify the AE signal characterization are presented in Appendix D.

As described earlier, waveforms were stored using the TRA212 software, and the Spartan software, SA-LOC, was used to record strain gage output and determine source location results. Because of different timing parameters, the two programs did not always collect the same signals. Also, not all detected signals were located by the Spartan software either because the source was outside the location array or the signals were too weak to trigger both location sensors.

Data presented under "Source Location" are results gathered using the SA-LOC program alone. In the two succeeding sections, "Strain Gage Monitoring" and "Waveforms," only waveforms with corresponding source location and strain data are presented. Table 2 shows the total number of waveforms and the reduced set after pairing the Spartan and waveform data. Another source of discrepancy between recorded waveforms and event waveforms was the very-long-duration signals that took up more than one waveform record.

Table 2. Waveform files recorded with TRA212 transient digitizer

TEST NO.	NO. OF TRA212 FILES	NO. OF RECORDED WAVEFORMS	NO. OF EVENT WAVEFORMS
1	9	882	42
2	7	192	67
3A	6	125	37
3B	9	1212	465
4	6	837	333

Source Location

The results of linear source location for Test 1 are shown in Figure 8. The data were combined from multiple testing periods that totaled 1 hour 35 minutes. Sensor designations and placement are indicated below the abscissa. Figure 8(a) shows 83 events that were located in Test 1. Later analysis revealed that most event signals were too weak to trigger both location sensors at the threshold level used. However, even with this dearth of activity, a clustering of events is evident at $x = 40.6$ mm (1.6 in), which corresponds to the location of crack 1. This is observed more clearly in Figure 8(b) where signals that hit the guard sensors first had been eliminated from the plot.

Although source location was designed to be performed by sensors 3 and 4, the WD sensor close to the crack in conjunction with one or both of the R30I sensors can also perform this function. This would be useful if a crack-related event detected by the WD sensor was detected by either sensor 3 or 4 but not by both. Analysis of the time of arrival data showed this to be the case. Thus, 7 more crack-related events were identified using WD as a locator.

Figure 9(a) shows the location of the 157 events detected during Test 2. The threshold setting in this test was lower by 5 dB than in Test 1, which partly explains why more events were detected during the 44 minutes that cracks 1 and 2 were monitored in Test 2 than the longer monitoring period of Test 1. The observed cluster of events centered around 43.2 mm (1.7 in) corresponds to the location of crack 1. Figure 9(b) shows results after implementing guard sensors that eliminated 70 noise events. No other concentration of activity, particularly from the crack 2 location that was also straddled by the location sensor array of 3 and 4, can be seen from the graphs.

The same sensor arrangement used in Test 2 was used in Test 3A after the sensors were left in place overnight. The expected cluster of events from crack 1 is visibly absent from the source location plot of Figure 10(a) that shows 840 events detected over a cumulative monitoring time of 1 hour 40 minutes. Instead, events were concentrated around 15.2 mm (0.6 in) from sensor 3. These signals are believed to have been generated by crack 2, which was apparently

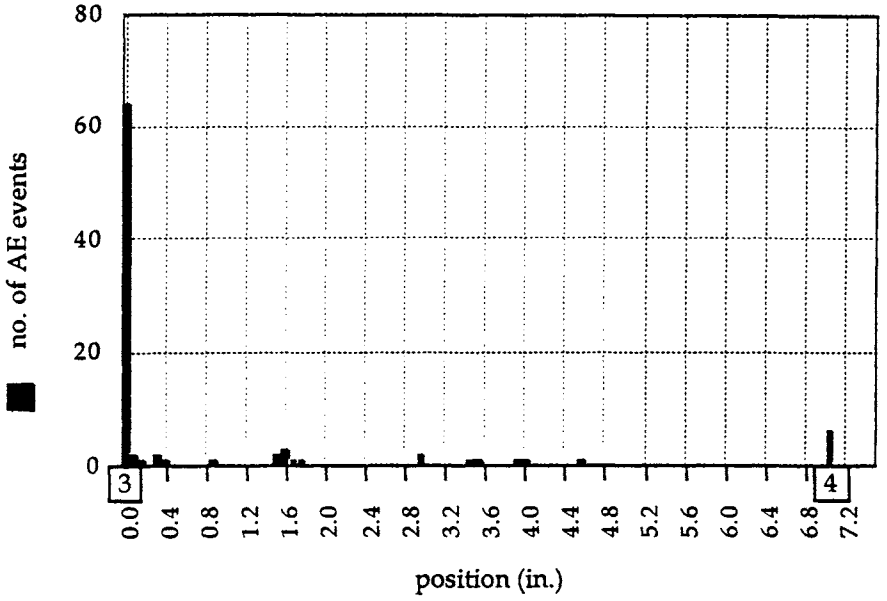

(a)

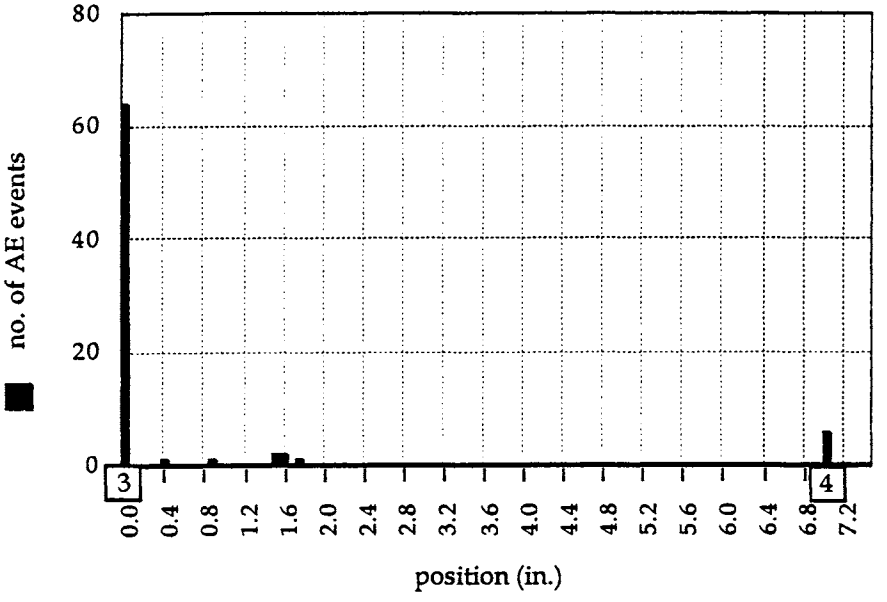

(b)

Figure 8. Source location results for Test 1: (a) without guard sensors, (b) with guard sensors.

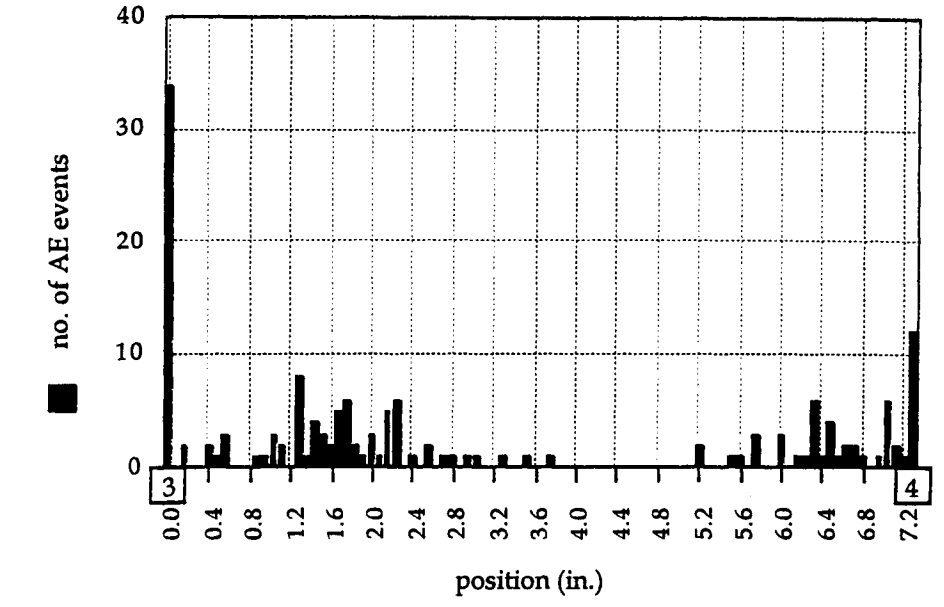

(a)

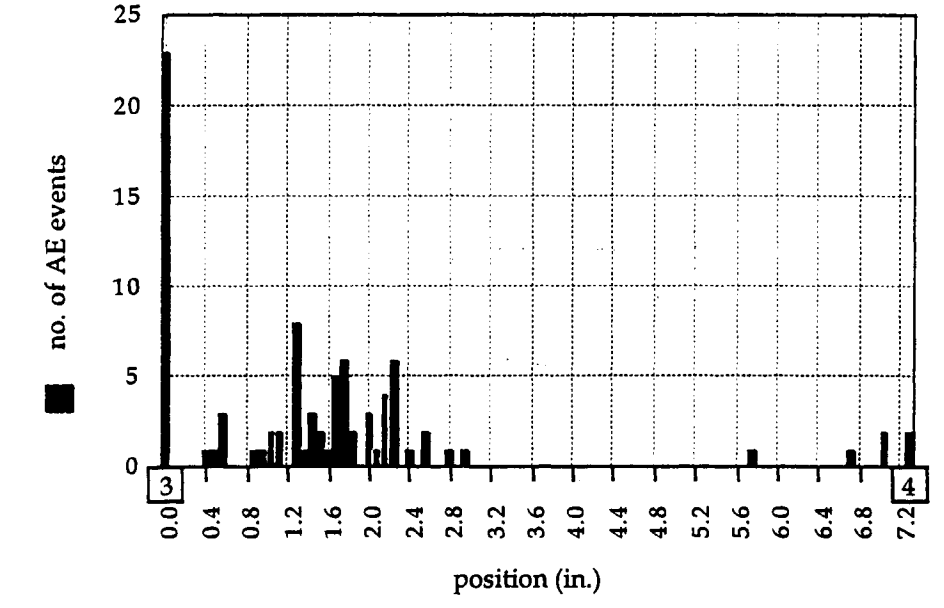

(b)

Figure 9. Source location results for Test 2: (a) without guard sensors, (b) with guard sensors

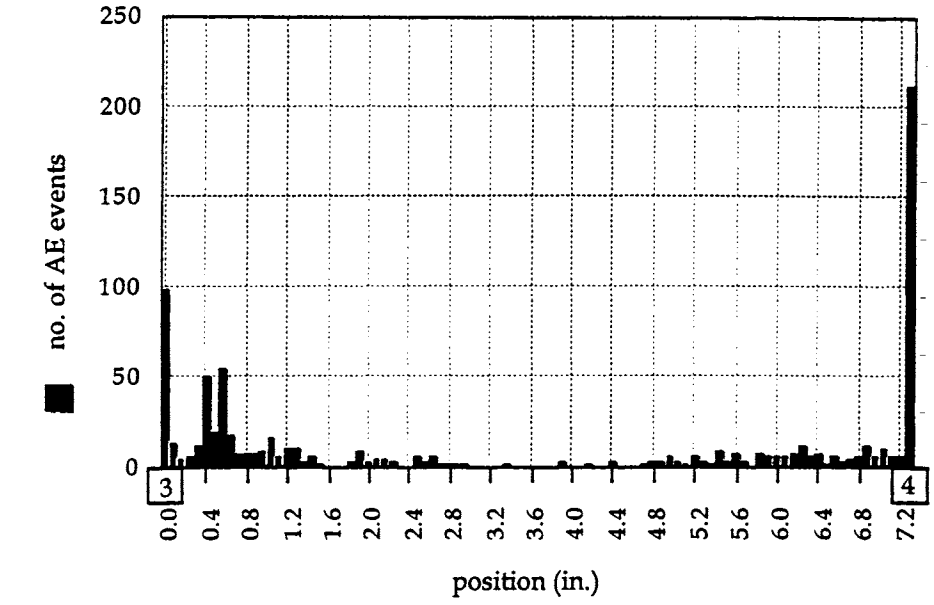

(a)

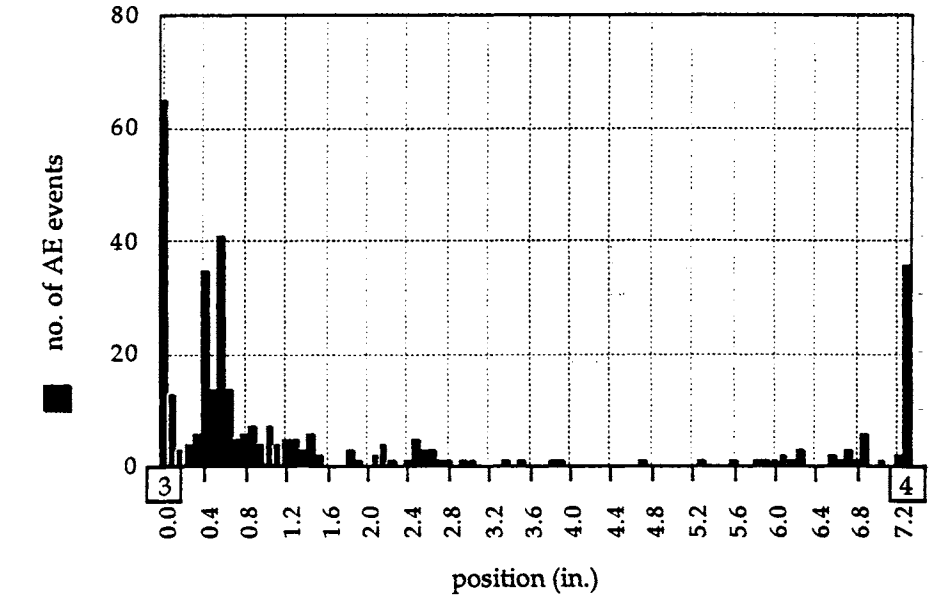

(b)

Figure 10. Source location results for Test 3A: (a) without guard sensors, (b) with guard sensors

quiet in previous tests. A plot of the events that passed the guard sensors is shown in Figure 10(b) wherein events from crack 2 become even more evident. As in Figure 9(b), most of the 496 events eliminated by the guard sensors came from a source closest to sensors 2 and 6. Both plots demonstrate the benefit of implementing guard sensors in monitoring cracks 1 and 2.

Figure 11(a) shows the source location results from monitoring crack 3 during Test 3B. A total of 2,534 events were located in 22 minutes of monitoring. Of these, only 39 were eliminated by the guard sensors. The similar plot of Figure 11(b) shows results from monitoring the same crack in Test 4: 489 events were located in only 2.02 minutes of testing, of which 67 did not pass the guard sensors. As expected, the AE event rate from crack 3 was very much higher than from crack 1 or 2. As many as 247 locatable emissions were detected by the Spartan for a single tractor-trailer truck crossing the bridge. The higher number of events per unit time of monitoring in Test 4 compared to Test 3B was due to the more selective recording of high-strain events in Test 4.

Strain Gage Monitoring

Because of the placement of the strain gage, all collected strain data were representative of the live stress conditions at crack 3 only but not at crack 1 or 2. A study on a similar hanger configuration showed that the presence of bending loads resulting from any seizure of the pins will cause the strain-time profile between the two sides of the hanger to act in opposite directions; i.e., as one side experiences positive loading, the other side undergoes unloading.[48] Figure 12 shows a typical strain-time curve with multiple loading events and highlights the variability in strain magnitudes produced by different vehicles crossing the bridge. In general, the strain level dips before rising sharply for both small and large events. The larger events undergo multiple cycling before returning to baseline strain. Light vehicles produced peak strains of less than 11 microstrains. Most larger vehicles such as buses and trucks produced peak strain increments around 17 to 20 microstrains. In the very occasional instances that heavily loaded tractor-trailer trucks crossed the bridge on the fast lane simultaneously in combination with other vehicles, strain increments of 60 to 90 microstrains were sometimes recorded.

Plots of the three largest strain events from Tests 3B and 4 are given in Figure 13. Located AE events are plotted on the curve to indicate the times during the live load cycle that crack-related emissions were detected. The plot shows that emissions were recorded at various strain levels ranging from minimum live strain to the maximum strain level. Also, signals were detected during both rising and falling live loads. Event waveforms for the plot of Figure 13(a) stopped shortly after peak strain because the memory buffer for the TRA212 program was filled before the loading event was completed. However, for the other test files that contained the highest strain readings, most emissions were detected during decreasing load after attaining peak levels. This can be seen in Figure 13(b) and (c). In general, event rates were the highest at these portions of the live load cycle.

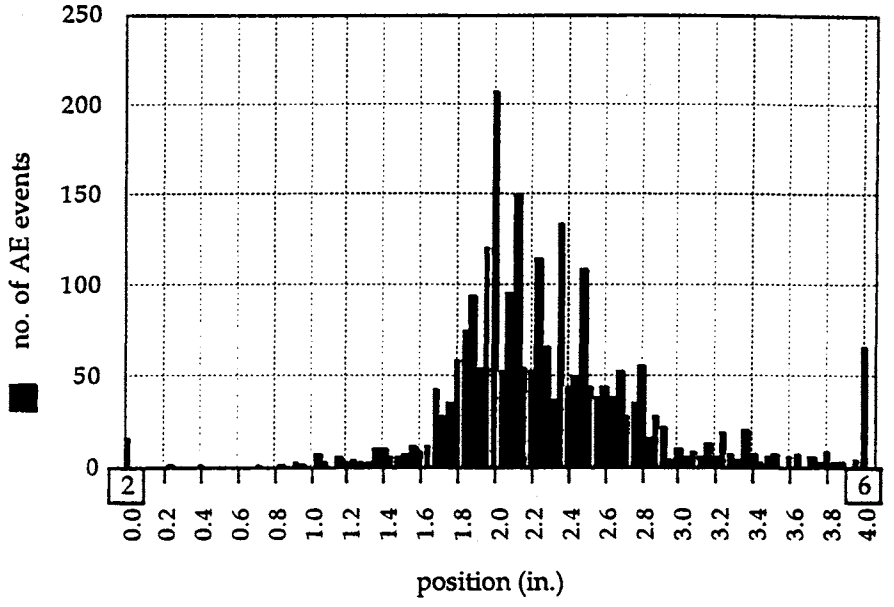

(a)

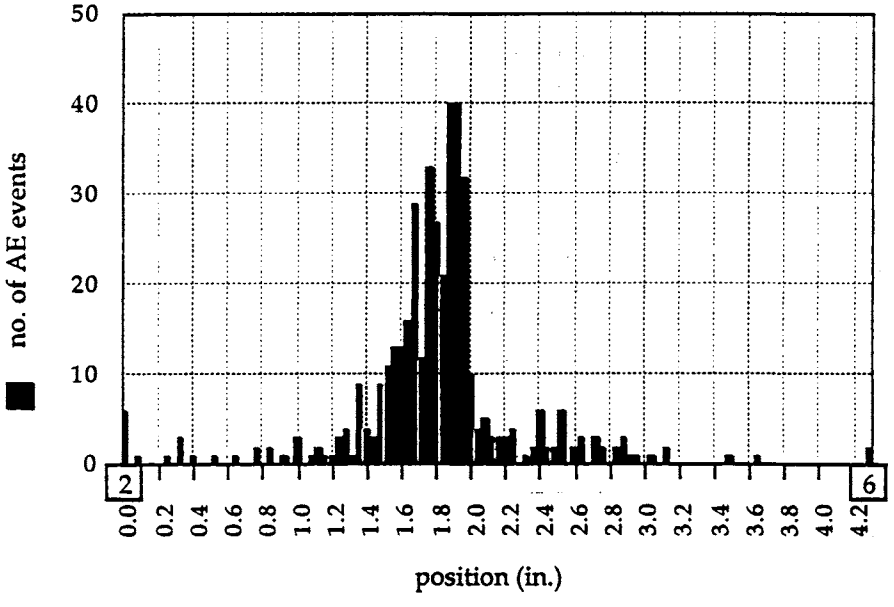

(b)

Figure 11. Source location results for (a) Test 3B and (b) Test 4, both with guard sensors

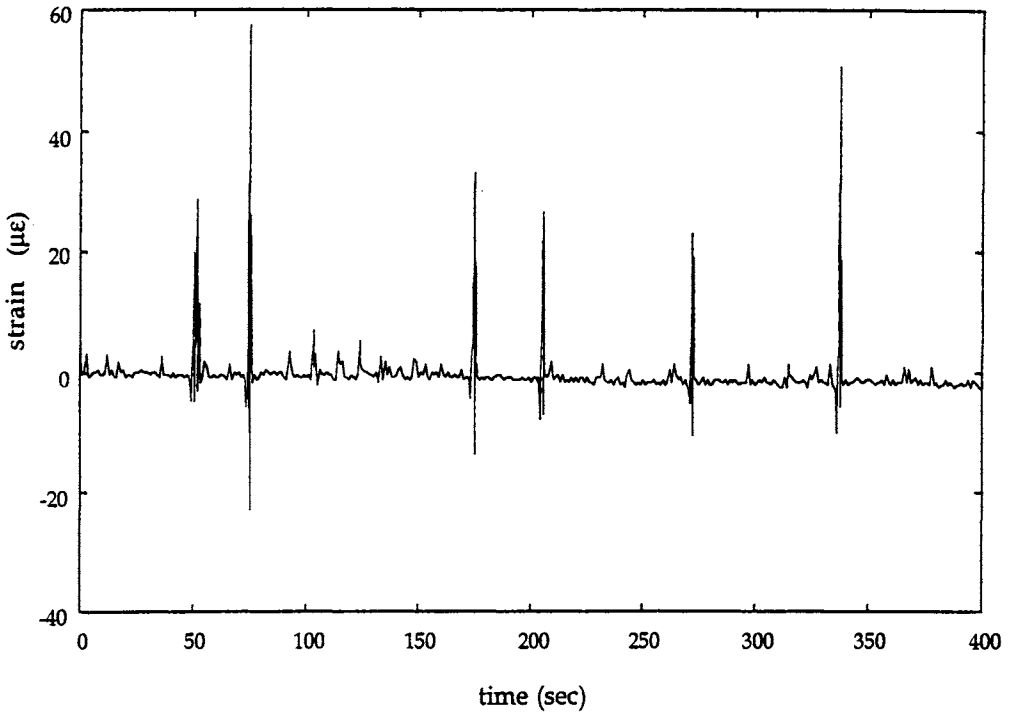

Figure 12. Strain vs. time plot showing multiple loading events

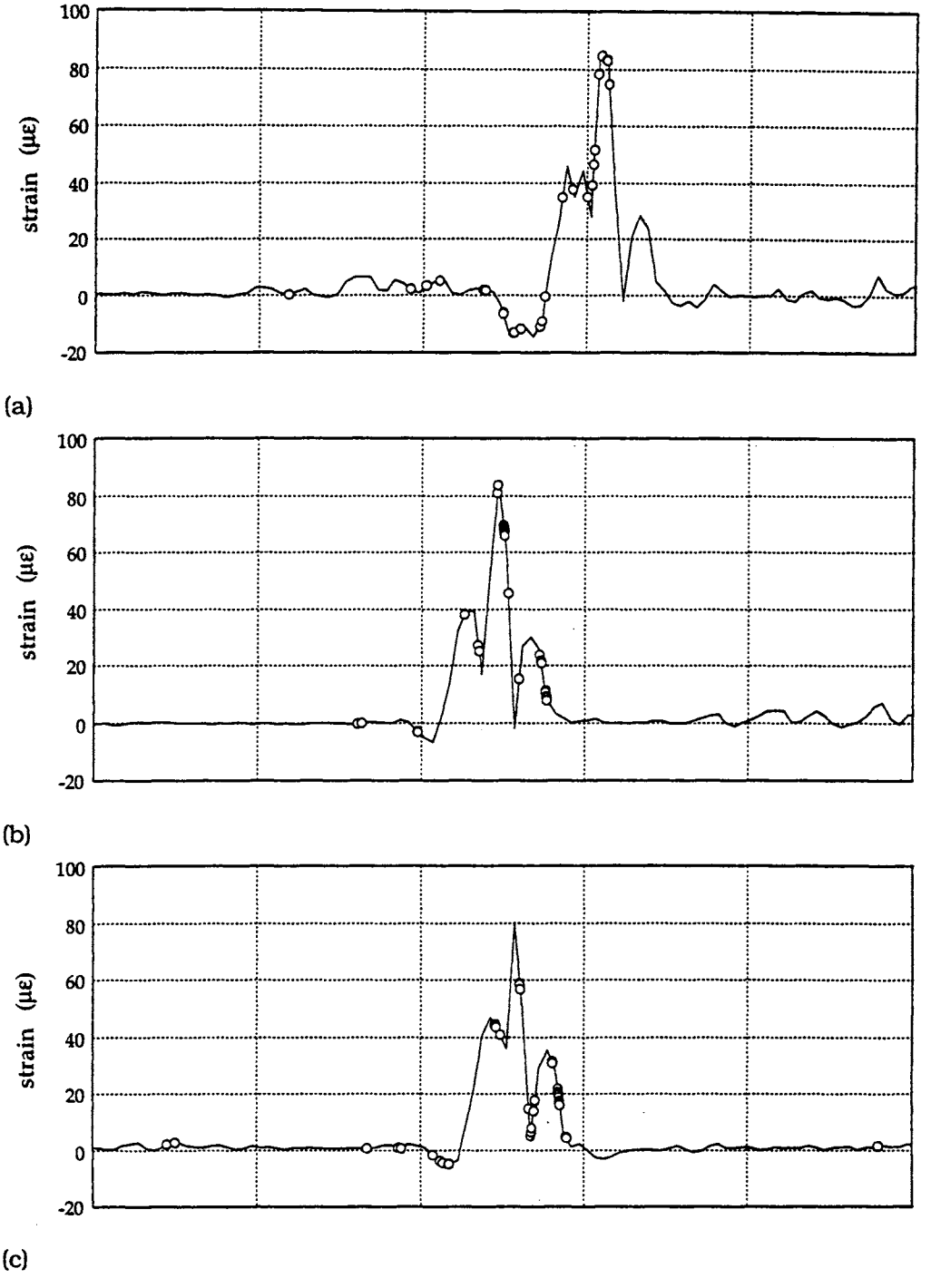

Figure 13. Strain vs. time plots of files from Tests 3B and 4. Three (a,b,c) highest recorded strain levels showing location of AE events on strain cycle (horizontal scale: 2 sec/division).

Waveforms

The 4 waveforms from Test 1 that appeared to have originated from crack 1 based on time of arrival data at the two source location sensors had nearly identical appearances and frequency spectra. A review of the other waveforms revealed 7 more of this type. A check of the time of arrival of these signals at one location sensor and the wideband sensor confirmed that the waveforms originated from crack 1. The signal strength of these 7 emissions were too low to trigger both location sensors at the threshold level used. This level was, therefore, lowered by 5 to 25 dB for the remaining tests. The repeating waveform from crack 1 is shown in Figure 14. This same waveform was again detected during Test 2, nearly 1-1/2 months after Test 1. Of the 67 located waveforms, 39 were of this type, which have peak frequencies of 275 kHz and amplitudes from 46 to 57 dB. Only 3 other waveforms peaked higher than 200 kHz; the rest had peak frequencies lower than 100 kHz. Only 18 percent of the waveforms were nonrepetitive. Other repetitive signals were low-frequency AE not coming from crack 1 but mostly from a location closer to sensor 4 as shown in Figure 9. Some of these waveforms in fact originated from crack 3. An example of these is shown in Figure 15. The repetitive waveforms varied mainly in magnitude such that if each waveform of a particular type was scaled relative to its peak amplitude, all waveforms of that type would, with minimum variation, appear the same.

Of the 37 located waveforms in Test 3A, only 1 was found to be unique: 34 emissions were of one kind and the remaining 2 were similar in appearance to the predominant waveform. The unique waveform was ruled out as a noise waveform because of the absence of a distinct start. The repetitive signals, an example of which is shown in Figure 16, have peak frequencies close to 100 kHz and peak signal amplitudes ranging from 35 to 58 dB.

The large number of waveforms recorded from crack 3 during Test 3B and Test 4 made manual classification impractical. Cluster analysis using the SAS statistical software package was, therefore, used to classify the waveforms. Waveform features used in this analysis were the autocorrelation at 50 different lags between 1 and 100, normalized by dividing by the autocorrelation at lag 1. After trying various time and frequency domain features, we found that the normalized autocorrelation of the waveforms performed best in grouping similar waveforms together. Results of the cluster analysis were then manually verified by visual inspection of each waveform.

Of the 465 located waveforms from crack 3 during Test 3B, 86 percent were found to be repeating waveforms. The largest group had 92 waveforms with an amplitude of 38 to 51 dB. Representative waveforms from two groups are shown in Figure 17. These signals had strong frequency components in the 100 to 300 kHz range but also significant low-frequency components that were evident on the waveforms after the first 0.1-msec segment. Decay times were also characteristically long. Obvious non-crack related waveforms such as that shown in Figure 18 had very limited high-frequency components and very long rise and decay times.

Results from classification of Test 4 waveforms showed that 48 percent of the 333 located signals were only one type of repetitive signal, and another 14 percent were various other repeating signals. The repeating waveform shown in Figure 19.1(a) was detected 160 times during

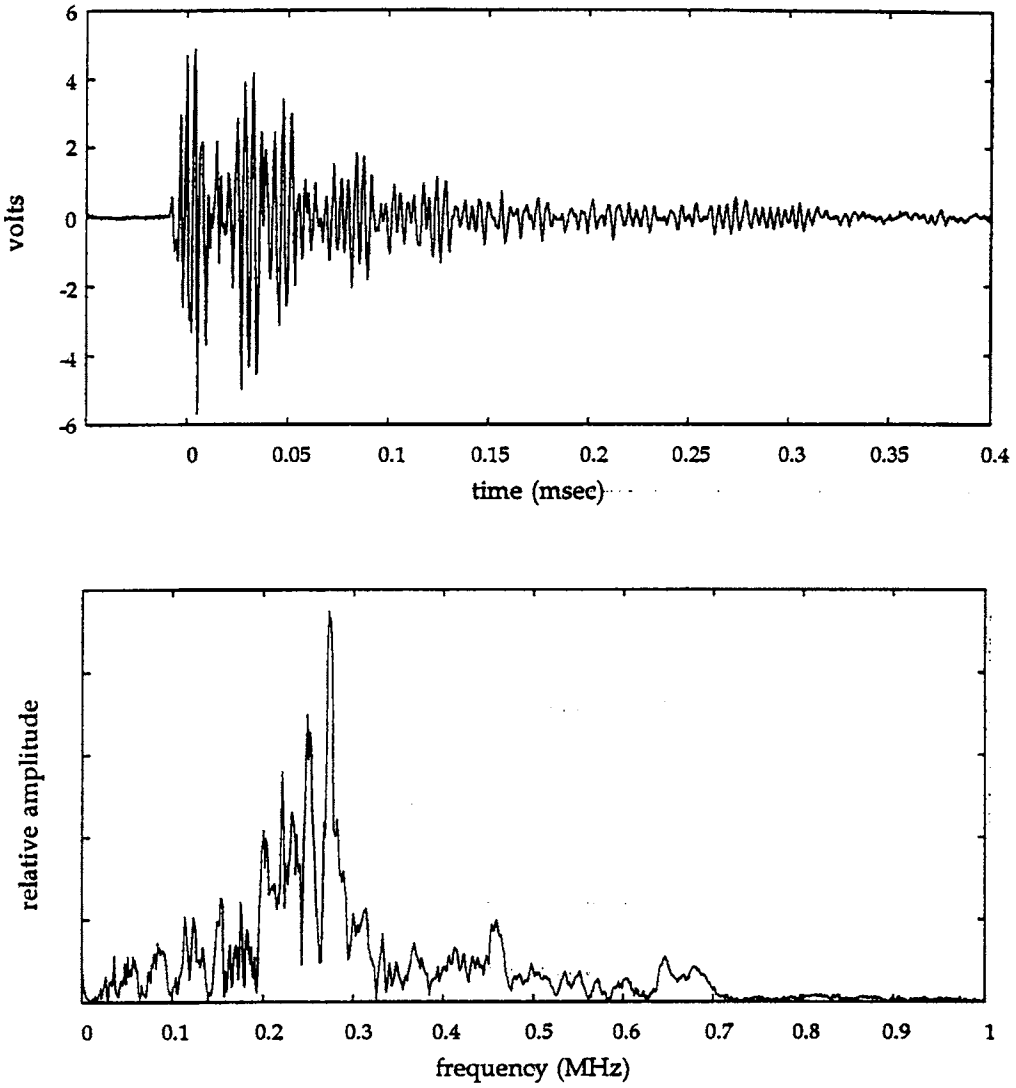

Figure 14. Repetitive waveform from crack 1

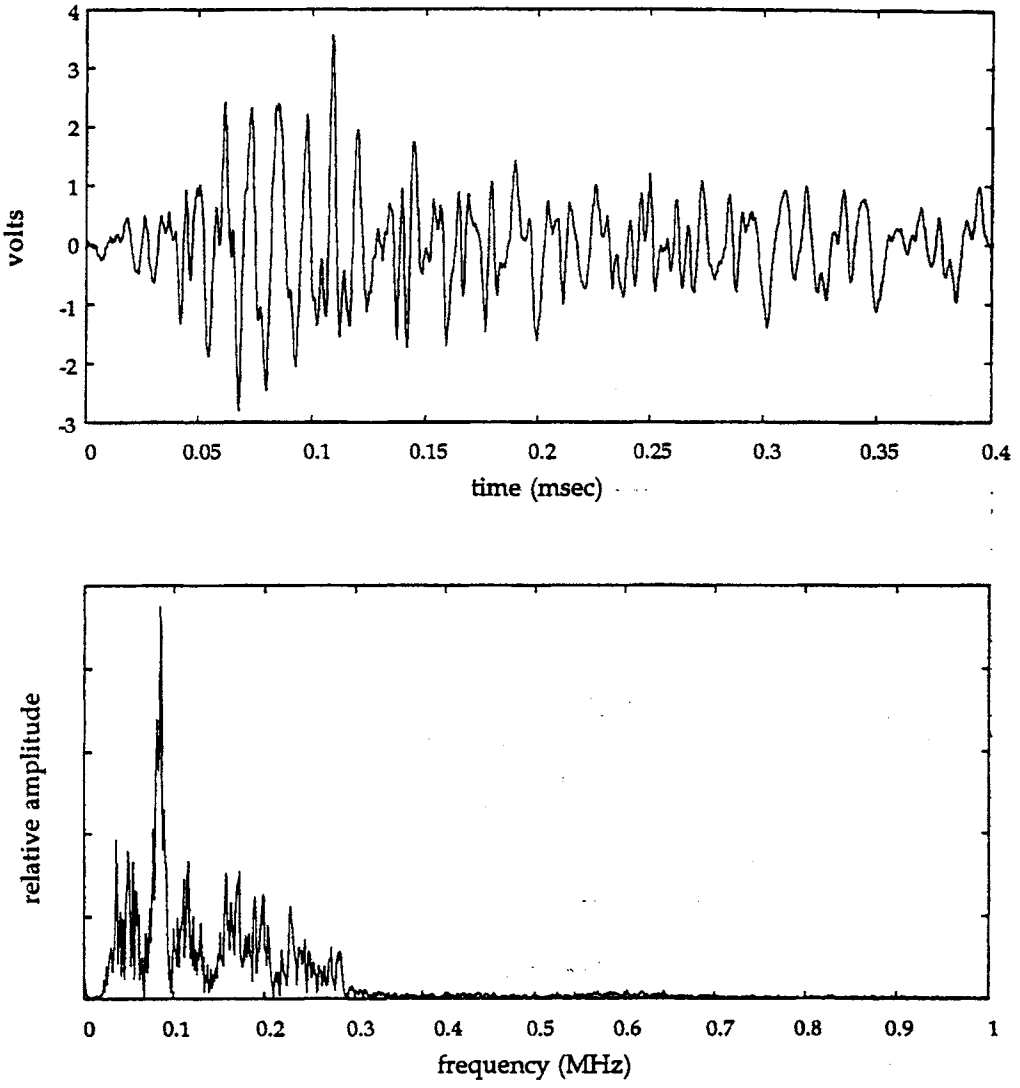

Figure 15. Repetitive waveform from crack 3 detected by sensor near crack 1 (Test 2)

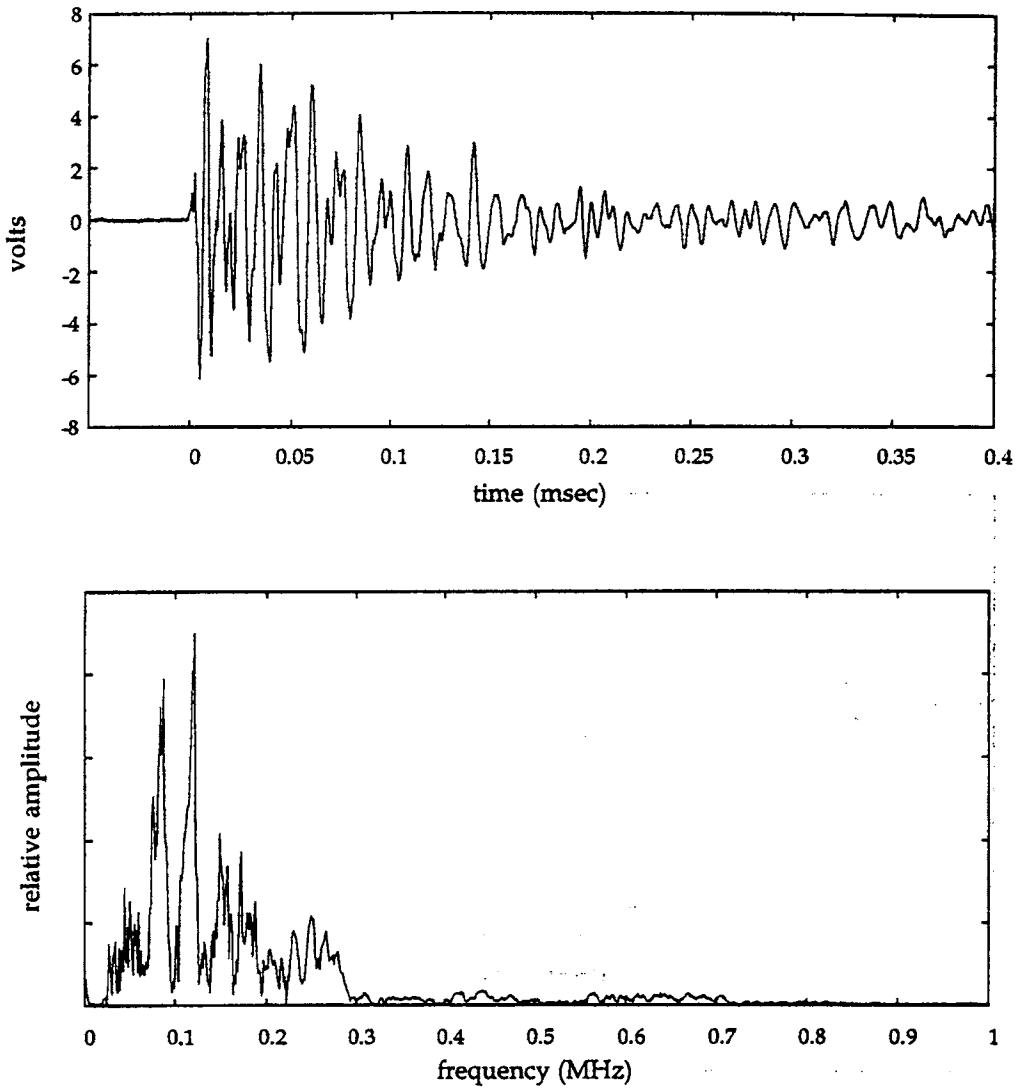

Figure 16. Repetitive waveform from crack 2 (Test 3A)

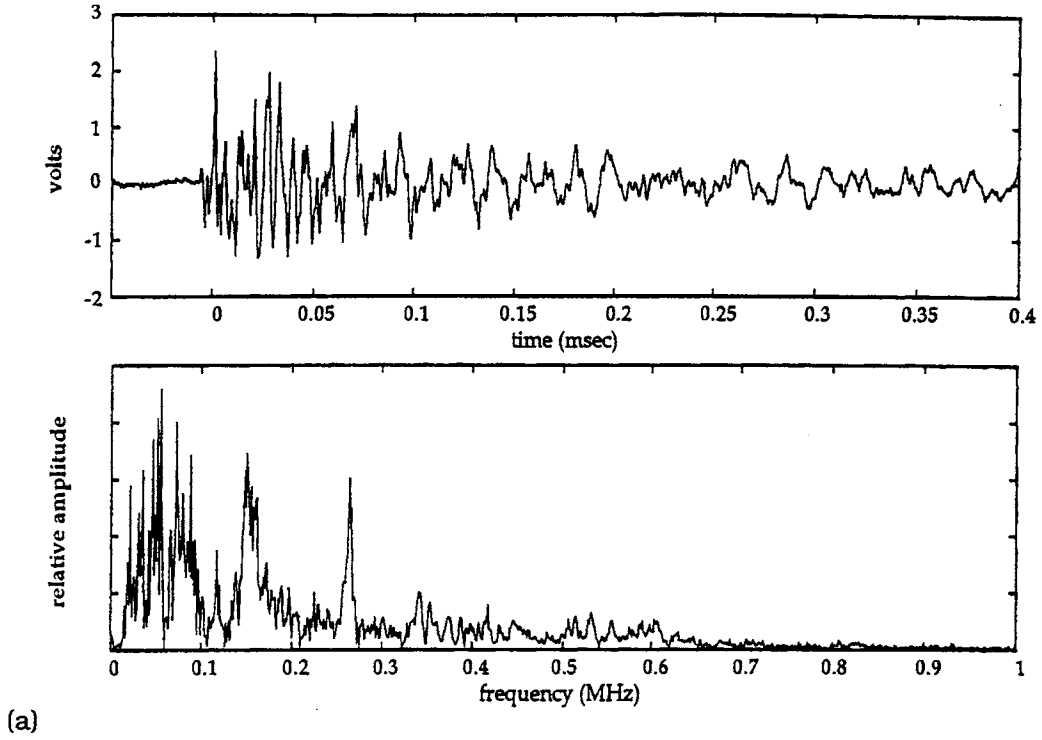

(a)

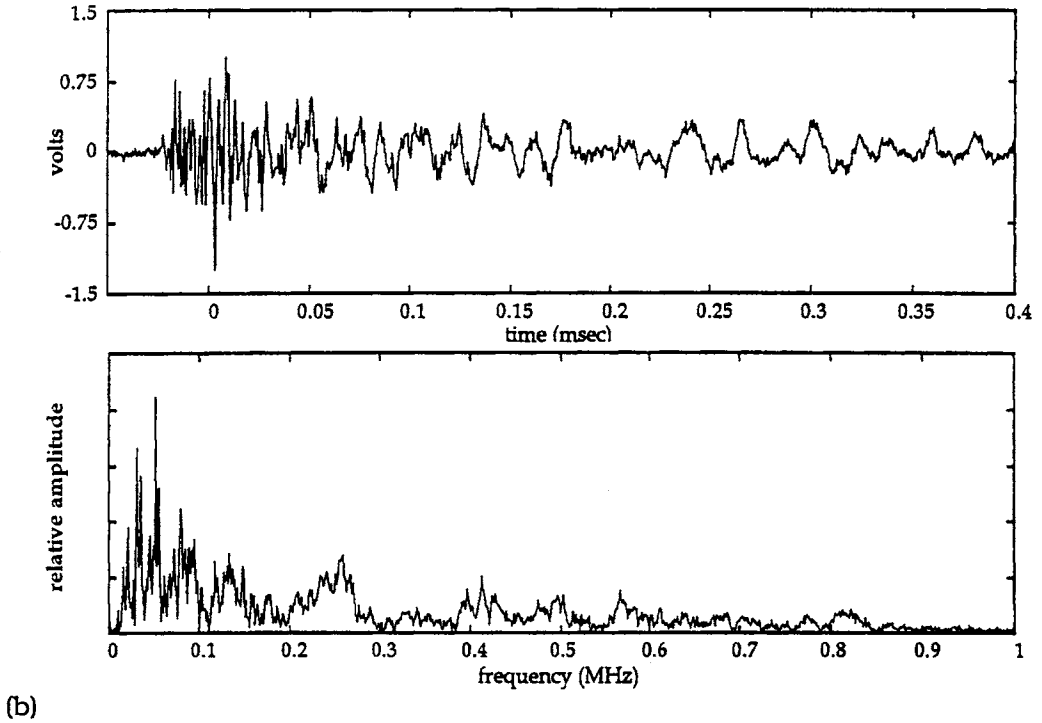

(b)

Figure 17. Two repetitive waveforms from crack 3 (Test 3B)

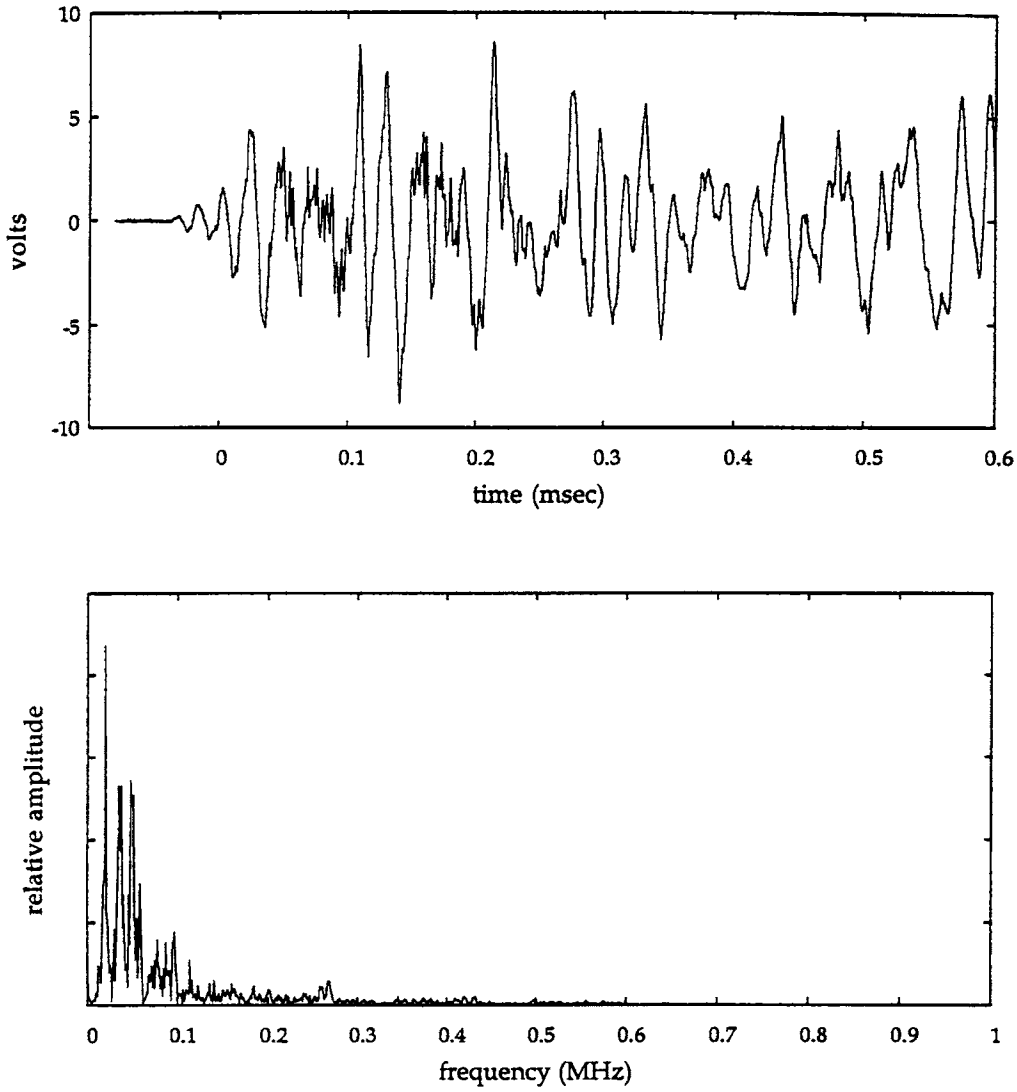

Figure 18. Non-crack related waveform (Test 3B)

rising and falling loads at live strain levels ranging from -12 to 46 microstrains. Figure 20 shows the occurrence of these repetitive emissions during one loading event. Peak signal amplitudes ranged from 42 dB to the maximum digitizer output of 60 dB. Ten of the waveforms had peak oscillations that were cut off by the digitizer limit. Other repetitive waveforms are shown in Figures 19.1(b) and (c). Although most detected waveforms in Test 4 had strong frequency components between 100 and 300 kHz, some, such as the waveform of Figure 19.2(b), had more pronounced components above 500 kHz. These high-frequency waveforms in general were of lower magnitude than the lower frequency emissions (see Figure 19.2).

The predominant repeating waveform in Test 4 was different from the predominant waveform of Test 3B. In fact, no waveforms collected from Test 3B were again detected in Test 4. Conversely, no Test 4 waveforms were detected during Test 3B.

DISCUSSION

A series of criteria were applied to the AE waveforms to determine their most probable source mechanism. These were used to establish whether a detected waveform is a primary emission, a secondary crack related emission, or spurious structural noise. These guidelines include (1) location of the source, (2) magnitude of strain and position in strain cycle, and (3) uniqueness of the waveform.

Source Location Analysis

Source location results clearly indicated the presence of AE activity at all three crack sites. It was successfully demonstrated that noise signals from extraneous sources can be effectively screened out by means of a simple two-sensor linear array in conjunction with properly positioned guard sensors. The effectiveness of and need for guard sensors would necessarily vary from case to case. For the sensor array used to monitor cracks 1 and 2, the effects of guard sensors are more evident than for the array monitoring crack 3. Some of the emissions from crack 3 were falsely located by the crack 1 and 2 sensor array to have originated between sensors 3 and 4 (see Figure 11). This was due to the multiplicity of wave propagation paths on the hanger and the high rate of AE activity from crack 3. The use of guard sensors to augment the location sensors made it possible to correct the false indications.

An AE system employing linear locators and guard sensors would work well in monitoring defects that can be isolated spatially from other sources of noise. Many defects found on steel bridge structures such as cracks on welded girders and beams would fall under this category. Other defects, such as cracks on hanger pins or riveted joints, would require more sophisticated source characterization techniques to identify crack-related emissions from structural noise attributable to fretting.

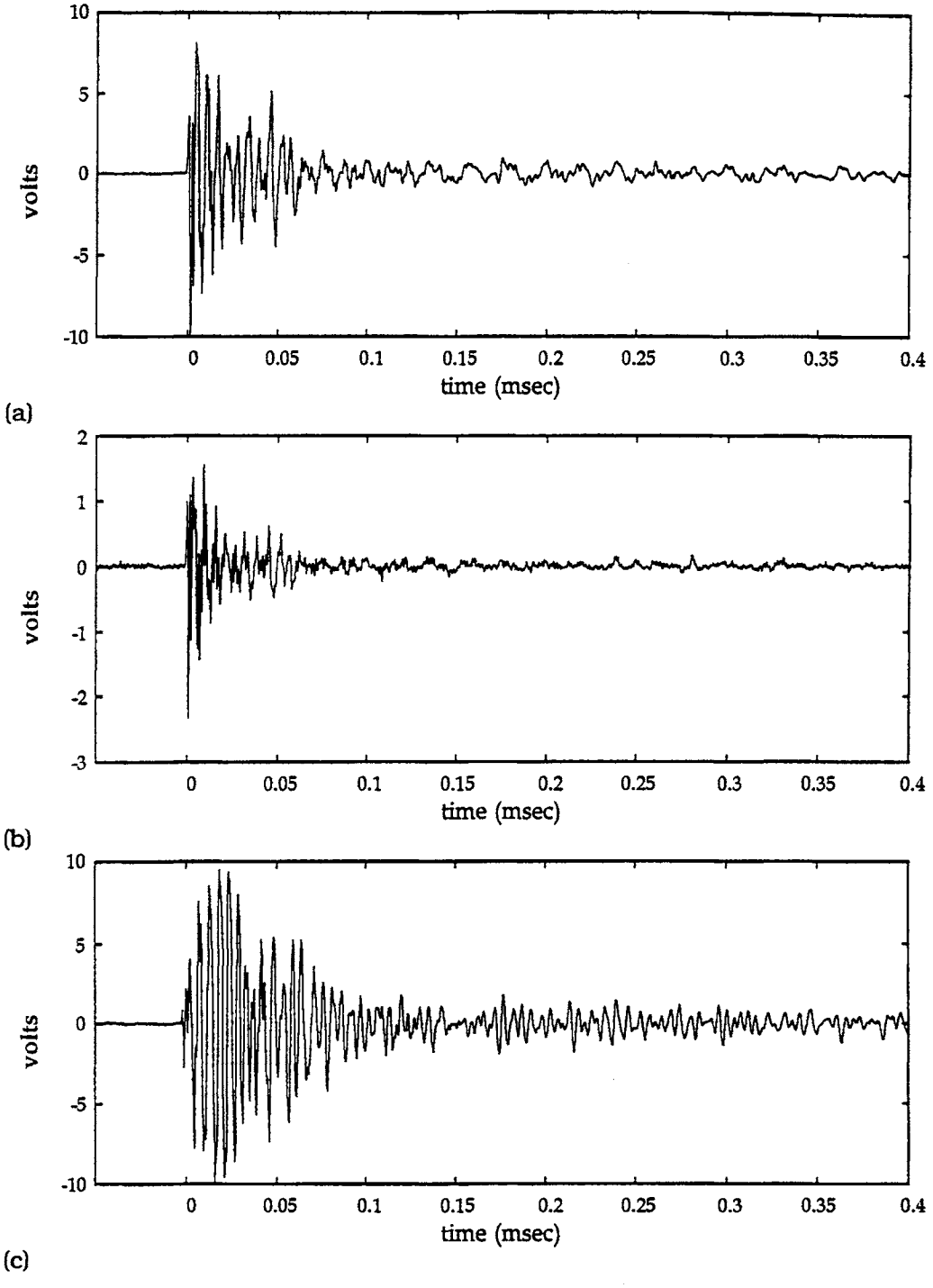

Figure 19.1. Three repetitive waveforms from Crack 3 (Test 4)

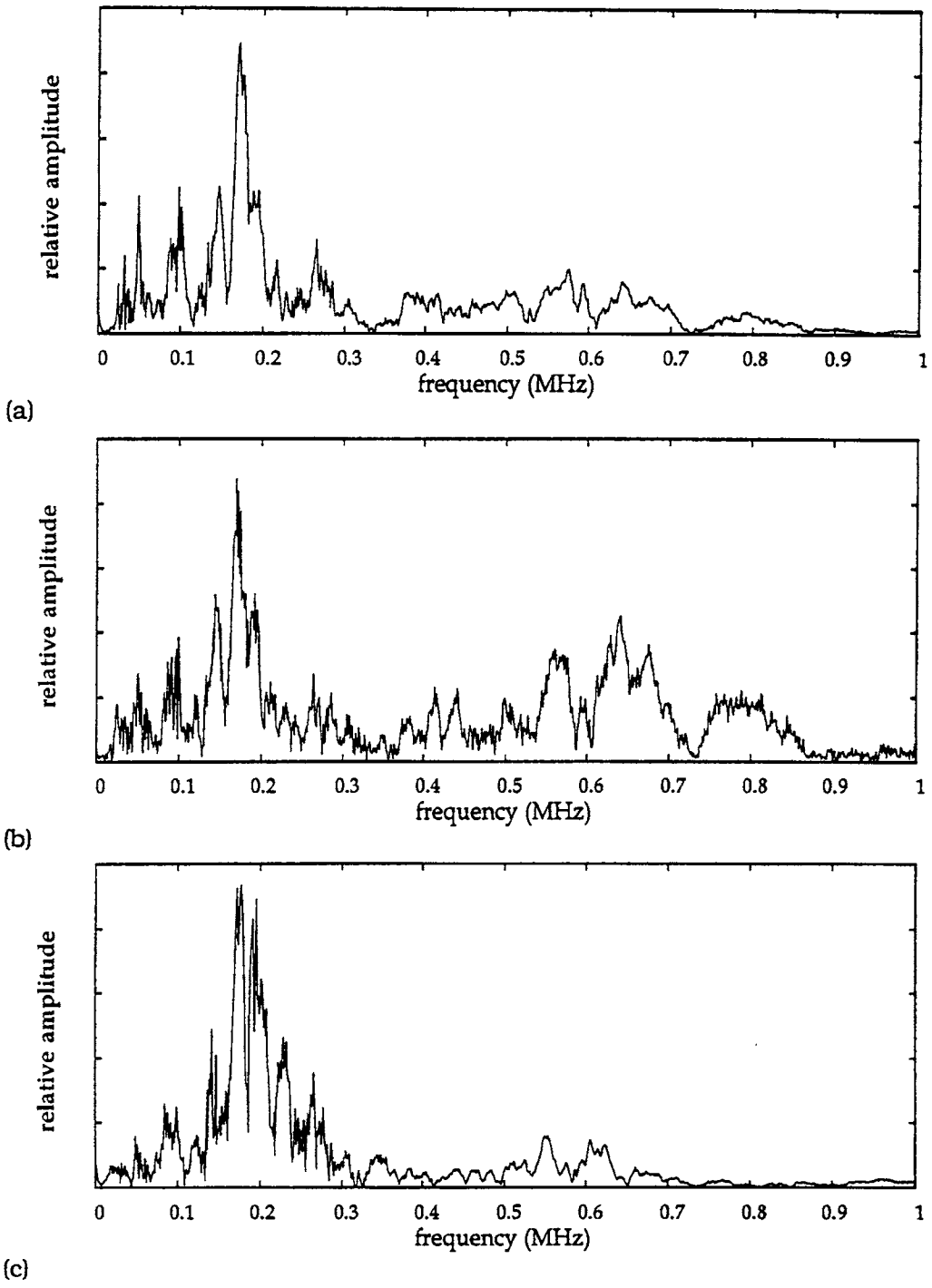

Figure 19.2. FFT from crack 3 (Test 4)

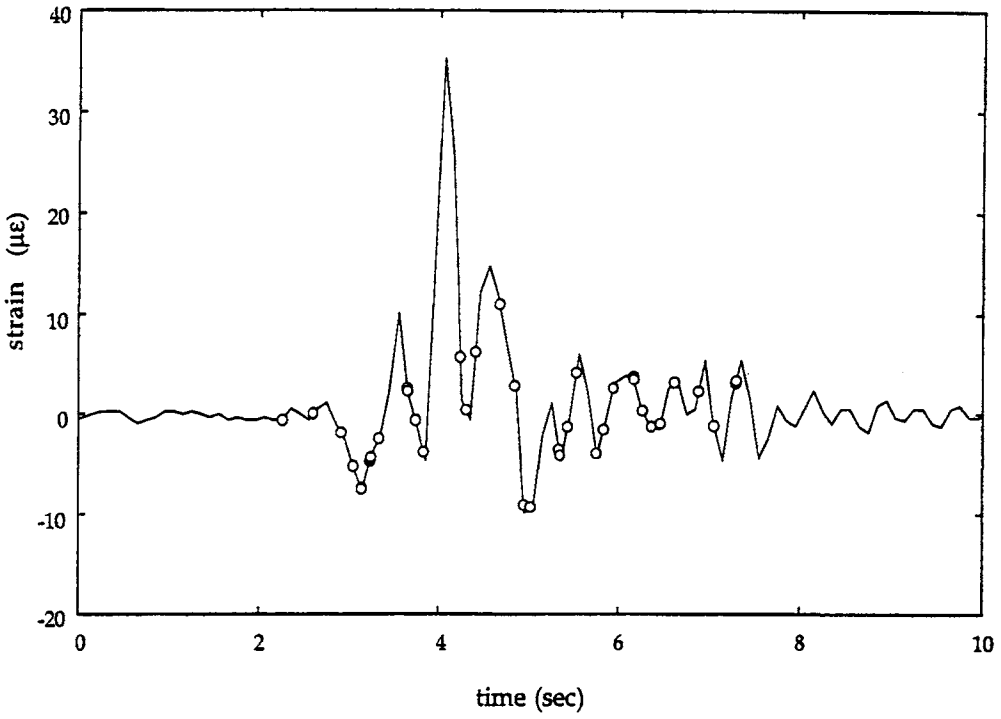

Figure 20. Strain cycle plot of repetitive waveform from crack 3

As mentioned previously, Tests 2 and 3A were performed 1 day apart using the same sensor setup. It was observed that AE activity shifted from crack 1 to crack 2 in the period between the tests. These results indicate that crack activity varies from time to time, with "quiet" periods occurring between periods of AE activity. Other studies have shown that even under constant amplitude cyclic loading wherein crack progression is also constant, AE attributable to crack growth occurs intermittently at random intervals. In addition, changes in AE activity on a real structure such as a bridge part may be attributable to actual shifts in loading conditions brought about by external forces or changes in environmental conditions. The observed irregularity in activity points out the necessity for known defects to be monitored over extended periods of time rather than by short-term survey testing. Since no strain gage data were available for the tests on cracks 1 and 2, it could not be established whether changes in loading patterns were responsible for the shift in AE activity. If they were, then a longer term strain gage monitoring should precede a shorter term AE test to ascertain whether all significant loading patterns have been covered during an AE test.

Since source location is one of the main criteria used to distinguish between primary and noise emissions, a comment on the accuracy of the commercial AE system used is warranted. Aided by the relative absence of other emission activity close to the crack locations, Figures 8 to 11 clearly show the clusters of events coming from the crack locations. Even then, an obvious spread in the location of the emissions can be observed. The extent of spread or error was verified using the location of the predominant repeating waveforms that theoretically should have originated from a single spot. With crack 1, the position of a waveform varied from 31.5 mm (1.24 in) to 60.2 mm (2.37 in). For crack 2, it varied from 0.0 mm (0.0 in) to 34.8 mm (1.37 in),

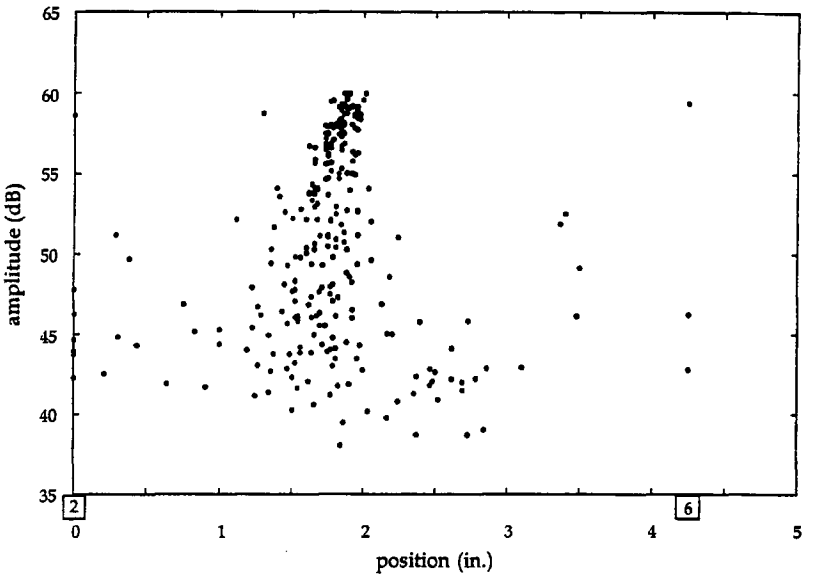

Figure 21. Amplitude vs. position plot of Test 4 AE events

and for crack 3, from 0.0 mm (0.0 in) to 68.3 mm (2.69 in). The errors for cracks 1 and 2 are comparable since only one sensor setup was used to monitor both cracks, whereas the error for crack 3 was twice that of the other cracks.

The accuracy of signal location based on time of arrival data is influenced by the rise time, amplitude, shape, and frequency of the signal as well as sensor location with respect to emission source. The effect of amplitude is illustrated in Figure 21. The plot shows the strongest emissions accurately located close to the center where the crack is supposed to be. Progressively weaker signals tend to be smeared over wider distances from their true locations. To eliminate the possibility that the close proximity of the two location sensors affected the accuracy of the results, source location was also calculated using the time of arrivals at location sensor 2 and guard sensor 3 (refer to Figure 7), which were 267.0 mm (10.51 in) apart. Similar results were obtained. Thus, in order not to eliminate valid emissions from further analysis prematurely and erroneously, all to have emanated from crack 3. Waveform and frequency analyses were then later used to distinguish between crack-related and spurious emissions.

Strain Analysis

The most probable sources of crack-related emissions from the hanger flaws in this study are crack face interaction, crack growth, and crushing of corrosion products trapped between crack faces. The behavior and characteristics of AE from the first two sources under constant amplitude cyclic fatigue loading have been thoroughly investigated. A more limited knowledge base exists on AE from complex fatigue cycles or AE from overload cycles.[10,15,49,50] The laboratory tests on the compact tension specimens (Appendix D) were designed to produce information that would aid in interpreting results from the bridge tests as well as confirm the validity of the analysis procedures used.

Results from the tests on the CT specimens showed that crack growth AE is detected only on the overload cycles despite minor cycles that are above the constant amplitude cyclic fatigue threshold levels. However, the detected crack-growth AE does not fully account for the observed increase in crack length. This is easily evident from the minimal number of crack-growth AE detected in both specimens over the entire tests. In several segments of the tests, crack progression was observed without detecting corresponding AE activity from the crack at all. This occurred more often at the regions of lower DK and in specimen CT3, which had more minor cycles between overloads than CT2. It is, therefore, likely that more than one type of AE is produced by crack growth in A588 steel. In addition to the emissions detected close to the maximum overload levels, weaker emissions could have occurred at lower loads, including the minor cycles. Other studies have shown that even load cycles below threshold levels contribute to fatigue damage if they are part of a variable amplitude load cycle.[51,52] A crack growth mechanism that yields very weak or no emissions must, therefore, be present. It is apparent from the CT tests that this mechanism, which accounts for most of the observed crack growth, occurred at lower stress intensity ranges than the mechanism that produced detectable AE. The high likelihood that weaker emissions were not identified is demonstrated by the crack growth waveform shown in Figure D6(a) in Appendix D. Like many other primary as well as secondary emissions, this waveform is just barely recognizable from the background noise. Emissions with even smaller amplitudes would have been masked by the continuous background noise signals.

The tests on the CT specimens agree with results from constant amplitude cyclic fatigue AE tests that emissions attributable to crack face rubbing occur over the entire load range during falling or rising loads. However, with regard to the occurrence of repetitive AE sources, two types of load cycle behavior were observed. Persistent, repetitive emissions of the type shown in Figure D4 in Appendix D commonly occurred every cycle at the same load level and location on the cycle within experimental error. Another kind repeated less often, at times more than 100 cycles between successive occurrences, and at varying load levels. Repetitive AE from the crushing of corrosion products had the most variability in terms of occurrence in the load cycle. These appeared during both overload and minor cycles, on positive and negative load gradients and on widely varying load levels.

AE attributable to crack advance is expected to occur only on rising load and only above a certain threshold level. For the hanger studied, there was no direct means for determining this fatigue threshold load, and it was beyond the scope of this investigation to determine analytically the actual stresses on the hanger. In this study, the static load on the hanger was essentially unknown. The maximum live strain levels of less than 90 microstrains attained during the tests were much lower than the normal fatigue strain limit of steels. However, crack length measurements have increased about 0.8 mm (1/32 in) between October 1994 and April 1995. The crack is definitely growing. What needs to be determined is whether incremental crack growth occurred during the periods that waveforms were collected from the hanger. Because of the relatively limited duration of the actual monitoring periods, it would be difficult to gauge the probability of crack growth occurrence. However, the following information does support the likelihood that some increment of crack growth may have taken place. High-strain events included in the analyses occurred only five times during the 2-1/2 hours the bridge was monitored in Test 4 and once during the 2.9 hours it was tested in Test 3. Maximum detected peak strain levels in

these tests were consistently between 80 and 90 microstrains, giving the impression that these are among the highest strains attainable.

Another factor to consider in gauging the likelihood that crack growth occurred is the effect of overloads. The typical hanger loading is such that a multiple overload cycle is sandwiched between numerous smaller load cycles. A tensile overload has the effect of blunting a fatigue crack, temporarily halting or slowing down crack advance until the cumulative effect of smaller load cycles or another overload causes the crack tip to grow through the plastic zone created by the initial overload.[52] However, if the overloads are too few or too many, these would have no effect on the rate of crack growth.[53] No actual count of vehicles was made during Tests 3B and 4. A conservative estimate of four light vehicles a minute translates to 120 smaller loading events for each major loading event in Test 4. Whether the spacing between overloads is sufficient for crack growth attributable to a recorded overload condition not to be affected by a preceding overload could not be ascertained. If the major overloads are of the same magnitude, however, it is reasonable to assume that crack growth would occur at all load levels close to maximum even if the overloads are closely spaced. The CT test results indicated that crack growth AE is detected only on the overload cycles close to maximum loads. Taken together, this information leads to the conclusion that AE from crack growth is unlikely to be detected during low-load events. AE would most likely be detected at load levels above the predominant low-load cycles produced by cars and other small vehicles. A threshold level of 20 microstrains was, therefore, established. All events that occurred above this threshold and on a positive load gradient were considered candidate crack growth AE.

Since strain was sampled at 10 Hz and detected emissions occurred at higher rates, it was necessary to interpolate the actual strain levels of closely spaced signals to determine whether these occurred on rising or falling loads. It was observed that repetitive secondary emissions were detected during both rising and falling loads, at various strain levels several times a cycle. Results from the CT tests suggest that these emissions were more likely attributable to crushing of corrosion particles rather than crack face rubbing whose repetitive predominant waveforms occurred at similar locations on the load cycle. However, the relative complexity of the load cycle to which the hanger was subject may also explain why the repeating waveforms occurred at varying load levels rather than at fixed locations on the cycles. The predominant secondary emissions shown in Figures 17 and 19 occurred mostly at low strains (< 12 microstrains), whereas the majority of secondary emissions that occurred at high strains and negative load gradients were generally unique. Since the higher strains were rarely attained, the mechanisms producing these unique secondary waveforms may not have been triggered often enough to become as manifest as the low-strain waveforms. An explanation for the higher event rate on unloading after reaching peak strain levels can be given if these emissions are assumed to be attributable to the action of the crack faces, whether rubbing or crushing of corrosion particles. Higher loads would cause a longer segment of the crack faces to displace a larger amount. More rubbing and crushing would thus be expected when these faces close down on unloading. Crack 3 appears to have enough length and tightness for such a mechanism to occur.

Waveform and Frequency Analysis

Using the criteria of source location, strain level, and position on the strain curve, only 10 waveforms from crack 3 were determined to be the most probable crack growth emissions. Of these, 3 were found to be repetitive and were further eliminated. The remaining 7 waveforms, 4 of which are shown in Figure 22, had no obvious common time or frequency domain characteristics that set them apart from the rest of the emissions that originated from crack 3. Like most signals, the frequency spectra have a large component below 100 kHz. Many of the secondary emissions that occurred at high strains also had frequency components above 500 kHz similar to the waveform of Figure 22(a). Other known distinguishing characteristics of crack growth AE such as short rise times and long durations are also displayed by the secondary emissions. It would be noted from the 4 waveforms in Figure 22 that rise time and duration varied considerably between these probable crack growth emissions. Statistical pattern recognition techniques were initially used to classify and distinguish the waveforms, but because of the very small number of candidate crack growth signals, results were inconclusive. The possibility that some or even all of these 7 emissions were in fact secondary emissions cannot be ruled out. It can only be speculated that the hanger material has sufficient toughness such that brittle cracking, which produces higher amplitude AE, is not the main mechanism of flaw growth. Concern that AE from crack growth on base metal would be difficult to detect was voiced by Vannoy and Azmi based on laboratory tests of bridge beams.[41] AE from cracks propagating on welds stand a better chance of being detected, especially if regions of low toughness resulting from unsatisfactory welding or heat treatment procedures are present.

A common phenomenon observed concerning AE from all three cracks was the presence of a predominant, repetitive waveform, as well as other repetitive waveforms. These emissions were attributable to mechanisms associated with crack closure: either crack face rubbing or the crushing of corrosion and dirt particles between crack faces. Even in the absence of actual crack growth AE, secondary emissions are important in that they enhance the prospect of a crack being detected and located. In the case of crack 3, many of the secondary emissions were high amplitude, exceeding the 60 dB maximum signal input of the TRA212 used in the tests. At the very least, the presence of secondary emissions is proof that crack face movement, an obvious prerequisite to crack growth, exists. Other NDE methods are not capable of even such a general assessment of a flaw. If the purpose of monitoring a bridge is strictly flaw detection, an AE system having adequate source location capability would suffice as a monitoring unit with no need for complex waveform collection and analysis features. If source location could be performed with a high degree of precision, the actual advance of a crack front could even be determined by locating the source of secondary emissions. Further developments in instrumentation in the near future could produce the necessary AE systems and transducers.

Secondary AE can also indirectly reveal the nature of crack growth. The waveforms detected from crack 1 were later detected during Test 2, 1-1/2 months later. If these signals were attributable to rubbing surfaces, this means that the condition and relative position of the interacting surfaces producing the emissions did not change between the time the two tests were conducted. This suggests that the crack may not have grown significantly longer or was not subject to a significant number of loading cycles during that period. It was observed from the CT speci-

mens that AE from crack face rubbing is not always present. Persistent rubbing emissions such as those plotted in Figure D4 would show up irregularly and later die down after a number of cycles. The most repeated emission was detected for 129 complex cycles during which the crack had grown less than 0.05 mm (0.002 in). This supports the contention that crack 1 on the hanger could not have grown significantly in the period between Test 1 and 2.

The absence of waveforms from Test 3B identical with the waveforms in Test 4 may be attributable to several causes. If the emissions had been attributable to rubbing, then the number and severity of load cycles between the tests might have been enough to wear out the rubbing surfaces or displace them with respect to each other. If the emissions were attributable to the crushing of corrosion particles, then they would not be expected to retain their characteristics for very long. Results from the CT tests support this idea. The reason for the more rapid evolution of the rust-crushing waveforms is because they are loose particles that get displaced in position as the crack is cycled. The small shifts in location result in a change in waveform characteristics. The locations of rubbing surfaces, on the other hand, are relatively fixed on the crack surface. AE from this mechanism would, therefore, be able to retain its features for a greater number of load cycles. Another factor to consider is the change in thermal conditions between AE tests that could significantly affect the tightness of a crack and, consequently, the relative position of contacting surfaces. Moisture from rain or snow that gets into a crack would also result in rubbing surfaces being altered by corrosion, resulting in a change in the features of secondary emissions. Since multiple factors may contribute to the nonappearance of common waveforms between AE tests, it is less plausible to link the absence of these waveforms to crack growth than it is to speculate that their presence indicates the absence of crack growth.

Two other signal characteristics were found to be distinctly different for rubbing and crushing emissions: frequency content and range of signal amplitudes. It is shown in Appendix D that emissions from crushing of rust have significantly lower frequency content than emissions from crack face rubbing. It should be noted from Table D1 that the frequency content of emissions from CT2 before the application of WD-40 is also low. These signals were in fact attributable to crushing of pencil lead particles. A number of broken lead pieces were stuck on the wedged opening of CT2 with vacuum grease couplant after the initial calibration tests. It was later discovered that load cycling of the crack resulted in the lead being drawn in and pulverized between the crack faces. Not unexpectedly, emissions attributable to the lead particles had characteristics similar to the emissions from the simulated rust crushing. In terms of signal amplitudes, it was found that repetitive AE from rust crushing have a much larger range of peak amplitudes than repetitive emissions from crack face rubbing.

In comparing the predominant repeating waveforms of the different cracks, it can be noted that the crack 1 waveforms have higher frequency content than the predominant waveforms of cracks 2 and 3. Moreover crack 1 waveforms have an amplitude range of 11 dB compared to those of crack 2, which have a 22 dB range. These data suggest that the enduring emissions from crack 1 were most likely attributable to crack face rubbing and AE detected from crack 2 were most likely attributable to corrosion and dirt particles being crushed by the crack faces. It is also conjectured that the predominant emissions of crack 3, especially those detected during Test 4, were also attributable to trapped corrosion particles. In addition to having rela-

tively low-frequency content and an amplitude range of more than 18 dB, the Test 4 waveforms exhibit the slight variability in waveform appearance between otherwise nearly identical waveforms that was observed from the simulated rust crushing emissions of specimen CT3. This would, therefore, partly explain why emissions from crack 3 detected during Test 3B and 4 were different from each other.

If there was difficulty in attempting to discriminate between the different sources of crack-related emissions, no such problem was encountered in distinguishing spurious, structural noise. It was observed that waveforms that originated from outside the source location sensor arrays, i.e., outside noise, were distinctly different from waveforms that emanated from cracks. An example is shown in Figure 18. These signals have much lower frequencies and are of longer duration, sometimes several 1.17 ms-long waveform records, than the primary or secondary emissions. These characteristics may be attributable to fundamental differences in source mechanisms, or the signals may actually be strong fretting noise whose higher frequency components have been damped by the longer propagation path to the detecting sensor. In any case, these distinct differences can be used to design frequency or duration filters to block out extraneous noise as an alternative to using source location with multiple sensors.

As noted before, the repeating waveforms showed up with different signal strengths. For an AE system that collects only simple time domain parameters such as counts or duration, these changes in amplitude could easily be misinterpreted as being attributable to differences in source mechanisms. If such a system would have difficulty identifying repetitive emissions, it is not unreasonable to expect that it would not be capable of discriminating between different types of emissions. Further, it has been a common practice in AE monitoring of structures to employ resonant transducers. The reason given for this convention is twofold. First, such transducers are more sensitive. Second, by choosing an appropriate sensor resonant frequency, detection of known sources of noise, frequently low-frequency mechanical noise, could be avoided. However, characterizing and discriminating emissions using such sensors would be anomalous because of the high degree of distortion that resonant sensors impart on detected signals. Assuming that spurious structural or traffic noise, because of its obvious differences with crack-related AE, could be distinguished by a simple-parameter-only system or a system using resonant sensors, it is unlikely that these would be able to tell the difference between the various crack emissions.

Background noise was not a major concern during testing. Most detected signals had amplitudes much larger than the background noise threshold. The main difficulty encountered in discerning emissions occurred during instances where the event rate was so high that smaller signals following large, long-duration signals were effectively merged into the preceding emission. In such a case, determining source location is nearly impossible. However, the relatively clear detection of waveforms from the hanger, much better in fact than from laboratory specimens mounted on test machines, is very encouraging. It shows that the expected high-noise environment of a bridge is not a serious obstacle to effective AE monitoring.

A limitation to the test setup used in this study was the inability to perform source location of all recorded waveforms. As explained earlier, not all waveforms recorded by the transient digitizer were in turn recorded by the SA-LOC used for source location. A better setup would

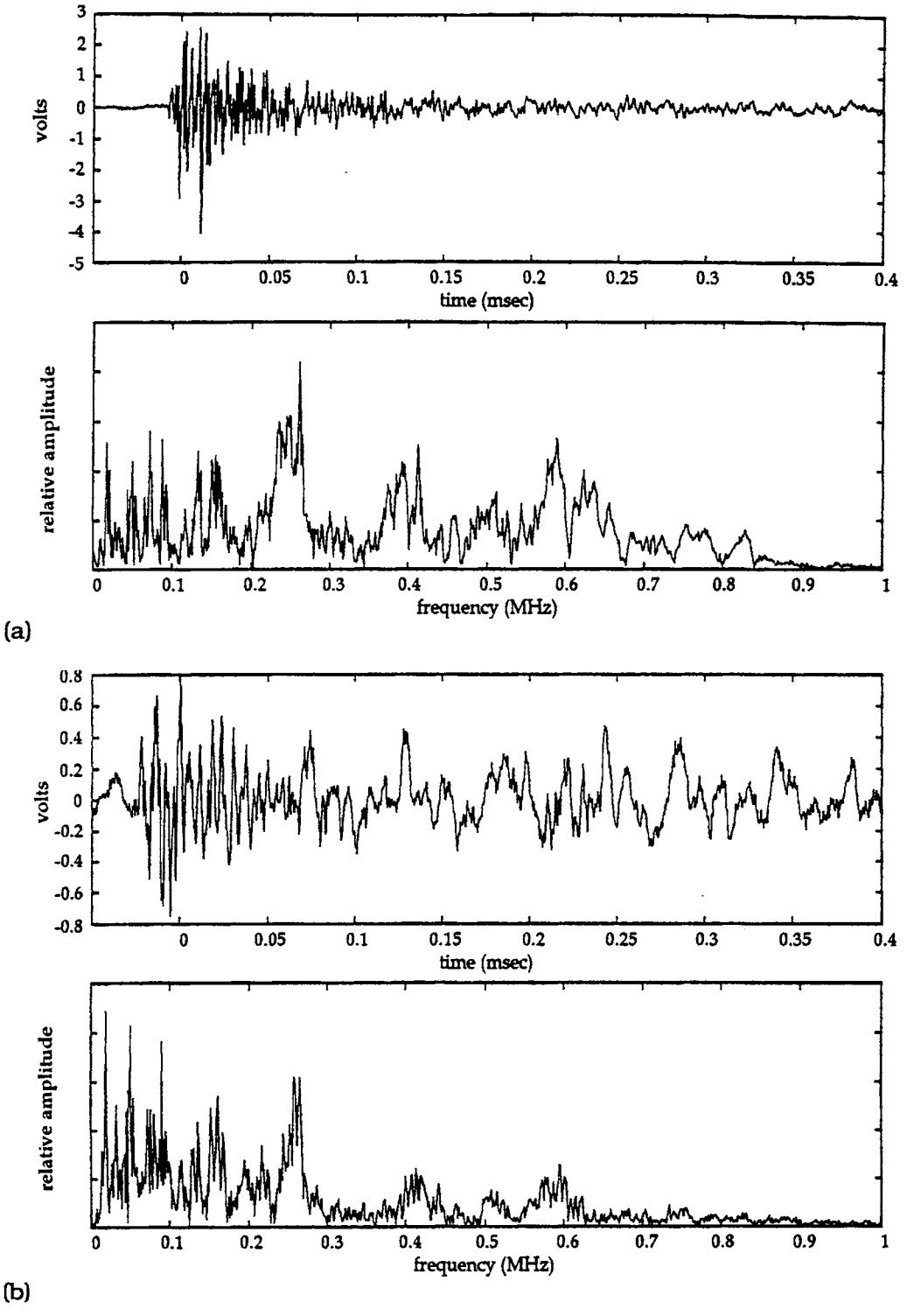

Figure 22.1. Probable crack growth AE (4 waveforms and FFT) from crack 3

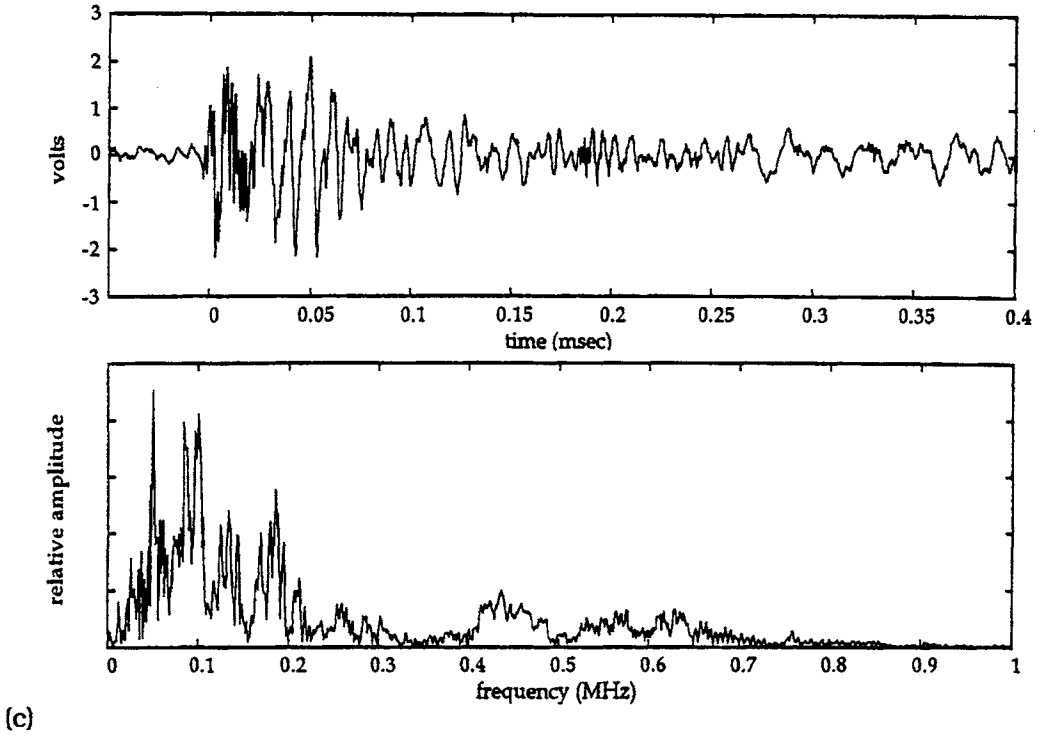

(c)

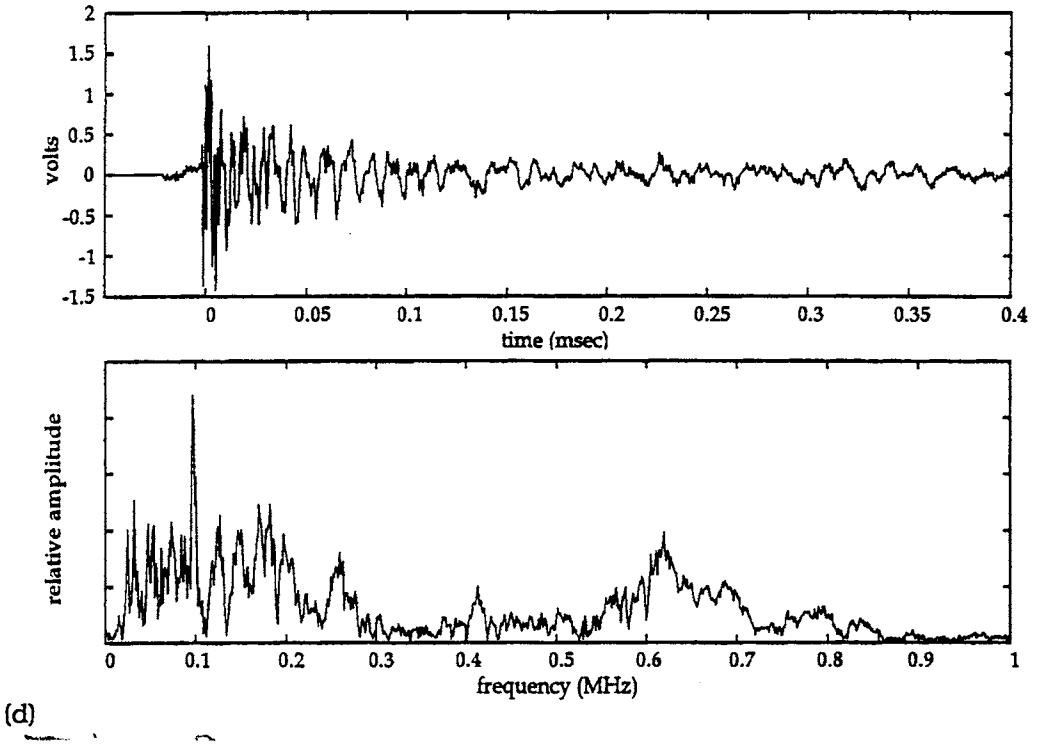

(d)

Figure 22.2. Figure 22.1 continued

involve at least two channels collecting waveforms, similar to the setup used in the CT specimen tests. Visual inspection of each waveform pair to determine actual sensor arrival times or the use of cross correlation would not only yield more accurate source location results but would also provide location information for every single waveform pair recorded. It was not uncommon during high-strain events for several waveforms to be recorded in one individual waveform file. Since crack-growth AE are expected to occur during these high-rate periods, the use of multiple sensors collecting waveforms would preclude the possibility of not getting location information on an all-important crack growth emission.

REMOTE AE FIELD MONITORING

As a result of the extensive AE signal characterization work based on the long-term monitoring of the Robinson River Bridge, as supplemented by the laboratory testing, a strategy for distinguishing crack growth related AE from all other AE from a bridge was developed. To establish the validity of this strategy it was determined that continuous monitoring was necessary in order to assure that monitoring was taking place during the period of crack growth. To accomplish this continuous monitoring an AE monitoring system that could remain at the bridge location for extended periods of time was necessary. It also seemed desirable to be able to remotely reprogram the system monitoring configuration; such a capability could easily include remote reporting of collected data. Appendix E briefly describes a companion program that successfully developed such a remote AE bridge monitoring system.

A prototype system was configured and installed on the Robinson River Bridge in order to monitor the AE associated with crack 3. In order to establish whether crack growth had occurred during the corresponding monitoring period surface replicas, as well as photographs of liquid penetrant examination were made.

It is important to remember that the crack front for this crack (typical of any "real" crack) did not advance uniformly and all crack front advance is not evident at the surface. (This is due in part to geometry of the component, the complex state of stress that results from as built structural configurations, and a variety of cyclic loading patterns that result from trucks and cars of different numbers, loads, speeds, and spacing intervals.) Consequently, in some respects it is at best fortuitous if a one-to-one correspondence is seen between crack growth related AE and crack front advance manifest at the surface of the hanger.

For the specific circumstance considered during the continuous monitoring two wideband AE transducers with integral preamplifiers were positioned above and below the crack of interest, the location of the strain gage has been described above. The strain gage and AE signals were digitally sampled at 6.25 MHZ when the strain signal was surpassed a level achieved only by large tractor-trailer trucks, and the AE signals exceeded an amplitude threshold set just above

the background noise level; both conditions had to be satisfied before data acquisition was triggered. 16 microseconds of data were stored for each of the AE signals (waveforms) and the strain gage output each time the system satisfied the trigger conditions.

Although all AE monitoring situations are unique in some ways the following specifics regarding the remote field monitoring performed in this study. These details depend on the hardware and software, so they are meant only to serve as an indication of the "magnitude" of data acquisition that must be contemplated.

It is estimated that using the monitoring system with no restriction on the acquisition except establishing a threshold for the AE signal channels just above the background noise level that the maximum quantity of data that could be acquired was 2 gigabytes/24 hours. Should the subject of the monitoring be active the amount of data requiring analysis could be daunting. Some form of automated analysis is necessary in that no department of transportation will want to devote personnel exclusively to analyzing such massive amounts of data. The experience developed in this study, as a result of laboratory and field tests, suggested that AE due to cracking under cyclic loading conditions, typically occurs during high points in the strain cycles.

To restrict the AE acquired in our study, while retaining the opportunity to "capture" AE due to cracking, a threshold was set for the strain monitoring channel; to trigger the system all threshold conditions had to be meet. The effects of this "restriction" can be seen in the following statistics. The system used in this study was capable of being reconfigured from the laboratory without revisiting the structure.

The overall system gain for the AE channels was 80 dB; the system used did not have the capability of changing the gain remotely. Such a feature is possible, but some investigators believe that a preferred approach is to use 16 bit waveform digitization.

From 8/11/95-8/14/95, using only AE threshold triggering (>0.086 V) for both channels, 64.8 megabytes of data per day were acquired, 8/18/95-8/22/95 threshold >0.105 V, 4.6 megabytes/day acquired, 8/23/95-10/16/95 threshold >0.117 V, 3.0 megabytes/day.

Using thresholds on both AE and strain, >0.008 V for AE, > 0.047 V for strain (change in strain is reflected by this measure since the structure was under load when the strain gage was attached) from 4/4/96-5/1/96 1.0 megabytes of data/day were acquired. This suggests that such a procedure has the effect of reducing the data to be further analyzed by approximately a factor of 65.

A note of caution: the precise values should not be seen as typical, but rather indicative of the potential magnitude of data to be processed and how appropriate threshold selection might reduce this task. Alternative approaches that utilize on-board real time processing can also reduce the amount of data stored. However, the overhead associated with this analysis will reduce the rate at which incoming signals can be considered.

As indicated in the appendix, the system used could remotely report the data collected, however, in order to avoid interrupting the monitoring during the reporting period all of the data was stored on board the system. Periodic visits to the bridge were used to allow for measuring the crack length. This made it possible to assure that for the period of time monitored that any crack length change must have occurred during the period of monitoring, and vice versa for any crack AE (identified, based on laboratory testing, as a crack growth related AE) detected.

The crack length was determined using both surface replicas, that could be examined microscopically upon return to the laboratory, and visible dye penetrants. Of course it is important to emphasize that the measurements only reflect the crack length as indicative of the intersection of the crack front and the hanger surface.

Unfortunately, the presence of the crack is responsible for surface corrosion due to moisture being retained in the crack. This feature frustrated efforts to fully clean the surface since the corrosion caused pitting near the crack. Such surface pitting retains penetrant, and along with "pumping" of penetrant resulting from passing vehicles made it impossible to photographically record the crack indications near the crack tip. This pitting also made it difficult to form the surface replica because of the pitted surface topography. The surface replicas formed, however, were examined microscopically and suggest that the crack did not advance during the period monitored continuously.

Ultimately, continuous monitoring of the subject crack was terminated because the project ended. In the future, similar monitoring should prove to be more routine as a result of the joint PAC/FHWA/VTRC portable AE monitoring system development program. A definitive answer to this question can only be obtained if cracking occurs during the period of AE monitoring under a variety of typical traffic conditions in order to establish that cracking does not typically occur without detectable AE.

CONCLUSIONS

- A pattern recognition process involving source location, strain magnitude, location on strain cycle and uniqueness of waveforms could be used to effectively distinguish between primary and secondary AE and spurious noise.

- A large majority of detected emissions from the cracks were repetitive, with near identical AE waveforms. These were due to crack face rubbing and the crushing of dirt and corrosion products between the crack faces.

- Very few probable crack growth AE were recorded.

- Secondary AE, especially repetitive emissions, were high amplitude, readily detectable signals. In the absence of actual crack growth AE, secondary emissions can aid in identifying and locating flaws in steel bridge structures.

- Crack activity varies from time to time with quiet intervals occurring between periods of discernible activity. It is therefore necessary that continuous monitoring be performed over a significant length of time to ensure that all loading and environmental conditions which could affect crack activity are covered during the period of testing.

- The progress of a crack can be assessed qualitatively using the apparent longevity of repetitive AE due to crack face rubbing. The presence, for example, of AE waveforms that appear unchanged from one monitoring period to another are an indication that significant flaw growth could not have taken place between the tests.

- The nature of repetitive emissions, wherein a single type of near identical waveforms had signal strengths that varied in magnitude by as much as 22 dB, make it unlikely that time domain analysis of AE from bridge members by itself can accurately distinguish between noise and crack growth emissions.

- Wideband sensors should be used in conducting preliminary AE tests on bridges since these are more capable of distinguishing between different AE source types than resonant sensors.

- AE waveforms not originating from the cracks such as traffic, mechanical and fretting noise are distinguishable from crack related AE due to their lower frequency contents and much longer rise times and durations.

- Variable amplitude fatigue tests on A588 compact tension specimens showed that crack growth AE is detected only on overload cycles and generally above 92 percent of maximum load. AE from crack face rubbing occurred at all load levels and on positive or negative load gradients.

- Predominant repetitive AE from crack face rubbing occurred at successive load cycles at the same locations in the cycle. Repetitive AE due to crushing of corrosion particles between the crack faces were shown through the CT tests to have no load dependence at all. These were also found to contain lower frequencies and greater variability in magnitude than crack face rubbing AE.

RECOMMENDATIONS

1. *Studies on the following related areas should be conducted:*

    - Known active fatigue cracks on a steel bridge should be monitored for waveforms over an extended period of time. An attempt should be made to correlate changes in waveform characteristics, both for primary and for secondary emissions, to actual progress of the

flaw. Although an effort was made to accomplish this task, the period of time available for monitoring proved to be insufficient. This task was also complicated by the nature of the crack growth of the crack selected for consideration. Because of its unpredictability, it is difficult to "plan" the period of monitoring. Efforts directed at accomplishing this objective should be open ended regards the monitoring period.

- More laboratory tests should be conducted to characterize AE from flaw growth and fatigue damage under variable amplitude load cycles using waveform analysis and possibly statistical pattern recognition. The precise load cycle and load level dependence of primary and secondary emissions should be studied. It is important to note that the results of this study suggest that servo-hydraulic loading systems typically used for laboratory work create significant amounts of noise not present in the field environment, consequently consideration of different means for cyclically loading test specimens might improve the potential for detecting all crack growth related AE.

- Since it has been demonstrated that secondary emissions are far easier to detect, it should be studied whether such could be used as indirect yet reliable indicators of crack severity. A particular challenge with regard to this issue is the difficulties associated with accurately simulating the causes for such emission in the laboratory, or systematically studying these effects in the field environment.

2. *Bridge management should use AE monitoring in accordance with the procedural guide for applying AE monitoring to steel bridge components provided as Appendix F.*

ACKNOWLEDGMENTS

The authors thank D. B. Sprinkel and R. Truxell of the Culpeper District, W. L. Sellars of the Lynchburg District, and J. W. Lillard of the Northern Virginia District of VDOT for their cooperation and assistance; A. R. Zadeh of VPI & SU and C. Apusen and A. French of VTRC for their technical support; and R. Combs and E. Deasy for their great assistance with the graphics and photographs. C. S. Napier, Jr., and P. Fuchs of the Federal Highway Administration, H. L. Reis of University of Illinois at Urbana-Champaign, M. Carlos of Physical Acoustics Co., R. Truxell of the Culpeper District, and M. M. Sprinkel of VTRC reviewed the report and suggested helpful improvements. Linda Evans edited the report. In addition, the authors express their gratitude to G. R. Allen for his continuous support of advanced NDE research at VTRC.

REFERENCES

1. Gorman, M.R., New Technology for Wave Based Acoustic Emission and Acousto-Ultrasonics, *Wave Propagation and Emerging Technologies,* AMD-Vol. 188, ASME, 1994, 47-59.

2. Graham, L.J., and Alers, G.A., Spectrum Analysis of Acoustic Emission in A533-B Steel, *Materials Evaluation,* 1974, Vol. 32, No. 2, 31-37.

3. Graham, L.J., and Alers, G.A., Acoustic Emission in the Frequency Domain, *Monitoring Structural Integrity by Acoustic Emission,* ASTM STP 571 , ASTM, 1975, 11-39.

4. Hartman, W.F., and Kline, R.A., Variations in Frequency Content of Acoustic Emission During Extension of HF-1 Steel, *Materials Evaluation,* 1977, Vol. 35, No. 7, 47-51.

5. Crostack, H.A., Basic Aspects of the Application of Frequency Analysis, *Ultrasonics,* 1977, Vol. 15, No. 6, 253-263.

6. Morton, T.M., Harrington, R.M., and Bjeletich, J.G., Acoustic Emissions of Fatigue Crack Growth, *Engineering Fracture Mechanics,* 1973, Vol. 5, 691-697.

7. Morton, T.M., Smith, S., and Harrington, R.M., Effect of Loading Variables on the Acoustic Emissions of Fatigue-Crack Growth, *Experimental Mechanics,* 1974, Vol. 14, No. 5, 208-213.

8. Harris, D.O., and Dunegan, H.L., Continuous Monitoring of Fatigue-Crack Growth by Acoustic Emission Techniques, *Experimental Mechanics,* 1974, Vol. 14, No. 2, 71-81.

9. Lindley, T.C., Palmer, I.G., and Richards, C.E., Acoustic Emission Monitoring of Fatigue Crack Growth, *Materials Science and Engineering,* 1978, Vol. 32, 1-15.

10. Sinclair, A.C.E., Connors, D.C., and Formby, C.L., Acoustic Emission Analysis During Fatigue Crack Growth in Steel, *Materials Science and Engineering,* 1977, Vol. 28, 263-273.

11. Kim, C.J., Lu, G., and Weertman, J., Fatigue Crack Advance Presumably Detected by Acoustic Emission Signals, *Scripta Metallurgica,* 1983, Vol. 17, 359-364.

12. Cherfaoui, M., Chretien, J.F., Spieldener, J.P., and Roget, J., Study of Acoustic Emission Associated with Fatigue Damage to Aluminum Alloys, *Acoustic Emission Monitoring and Analysis in Manufacturing,* ASME, NY, 1984, 35-53.

13. Weatherly, G., Titchmarsh, J.M., and Scruby, C.B., Acoustic Emission Monitoring of Fatigue in 7010 Aluminum Alloys, *Materials Science and Technology,* 1986, Vol. 2, 374-385.

14. Bowles, S.J., Acoustic Emission Load-Cycle Dependence Applied to Monitoring Fatigue Crack Growth Under Complex Loading Conditions, *NDT International,* 1989, Vol. 22, 7-13.

15. Nakamura, Y., Acoustic Emission Monitoring System for Detection of Cracks in a Complex Structure, *Materials Evaluation,* 1971, Vol. 29, No. 1, 8-12.

16. Horak, C.R., and Weyhreter, A.F., Acoustic Emission System for Monitoring Components and Structures in a Severe Fatigue Noise Environment, *Materials Evaluation,* 1977, Vol. 35, No. 5, 59-68.

17. McBride, S.L., and Maclachlan, J.W., Acoustic Emission Due to Crack Growth, Crack Face Rubbing and Structural Noise in the CC-130 Hercules Aircract, *Review of Progress in Quantitative NDE,* 1984, Vol. 3b, 717-727.

18. Friesel, M.A., Application of Signal Analysis to Acoustic Emission from a Cyclically Loaded Aluminum Joint Specimen, *Materials Evaluation,* 1989, Vol. 47, No. 7, 843-849.

19. Scala, C.M., and Coyle, R.A., Acoustic Emission Waveform Analysis to Identify Crack Propagation in a Mirage Aircraft, *Journal of Acoustic Emission,* 1987, Vol. 6, No. 4, 249-256.

20. Deuster, G., Cklarczyk, C., and Waschkies, E., Detection and Analysis of Defects in Reactor Pressure Components by Location and Interpretation of Acoustic Emission Sources, *Nuclear Engineering Design,* 1991, Vol. 129, 185-190.

21. Buttle, D.J., and Scruby, C.B., Characterization of Fatigue in Aluminum Alloys by Acoustic Emission, Part I: Identification of Source Mechanism, *Journal of Acoustic Emission,* 1990, Vol. 9, No. 4, 243-254.

22. Buttle, D.J., and Scruby, C.B., Characterization of Fatigue in Aluminum Alloys by Acoustic Emission, Part II: Discrimination Between Primary and Other Emissions, *Journal of Acoustic Emission,* 1990, Vol. 9, No. 4, 255-269.

23. Scruby, C.B., Beesley, M.J., Stacey, K.A., Bentley, P.G., Daniels, W., and Buttle, D.J., Acoustic Emission Measurements During Hydrotest and Cyclic Fatigue of a 1/5 Scale PWR Vessel, *Nuclear Energy,* 1990, Vol. 29, No. 4, 247-266.

24. Harrington, T.P., and Doctor, P.G., Acoustic Emission Analysis Using Pattern Recognition, *Proceedings of the Fifth International Conference on Pattern Recognition,* Vol. 2, 1980, 1204-1207.

25. Scala, C.M., and Coyle, R.A., Pattern Recognition and Acoustic Emission, *NDT International,* 1983, Vol. 16, No. 6, 339-343.

26. Hutton, P.H., and Lemon, D.K., Development of Acoustic Emission Methods for Inflight Monitoring of Aircraft Structures, *Review of Progress in Quantitative NDE,* 1983, Vol. 2A, 459-470.

27. Graham, L.J., and Elsley, R.K., Acoustic Emission Source Identification by Frequency Spectral Analysis for An Aircracft Monitoring Application, *Journal of Acoustic Emission,* 1993, Vol. 2, No. 1/2, 47-55.

28. Horvath, P., and Cook, F.J., Establishing Signal Processing and Pattern Recognition Techniques for Inflight Discrimination Between Crack-Growth Acoustic Emission and Other Acoustic Waveforms, *Review of Progress in Quantitative NDE,* 1981, Vol. 1, 436-437.

29. Melton, R.B., Doctor, P.G., and Daly, D.S., Pattern Recognition Analysis of Acoustic Emission from 7075-T651 Aluminum Simulated Joint Specimens, *Review of Progress in Quantitative NDE,* 1983, Vol. 2a, 489-501.

30. Pollock, A.A., and Smith, B., Stress-Wave Emission Monitoring of a Military Bridge, *Non-Destructive Testing,* 1972, Vol. 5, No. 6, 348-353.

31. Hutton, P.H., and Skorpik, J.R., Acoustic Emission Monitoring Simplified Using Digital Memory Storage and Source Location, *Materials Evaluation,* 1977, Vol. 35, No. 11, 55-60.

32. Hopwood, T., and Havens, J.H., Acoustic Emission and Fatigue Characteristics of Typical Bridge Steels, *Transportation Research Record 664,* 1978, 129-135.

33. Salane, H.J., Baldwin, J.W., and Duffield, R.C., Dynamics Approach for Monitoring Bridge Deterioration, *Transportation Research Record 832,* 1981, 21-28.

34. Hartman, W.F., *Acoustic Emission Monitoring of Electroslag and Butt Welds on Dunbar Bridge, West Virginia*, Report No. FHWA-WV-83-001. Dunegan Corporation, San Juan Capistrano, California, 1983.

35. Noyes, L.M., Wood., B.R.A., and Harris, R.W., Acoustic Emission Testing of a Rivetted Open Braced Bridge Girder Span, *4th Pan Pacific Conference on Nondestructive Testing,* Sydney, 1983, 1-5.

36. Miller, R.K., Ringermacher, H.I., Williams, R.S., and Zwicke, P.E., *Characterization of Acoustic Emission Signals*, Report No. R83-996043-2. United Technologies Research Center, East Hartford, Connecticut, 1983.

37. Prine, D.W., and Hopwood, T., Improved Structural Monitoring with Acoustic Emission Pattern Recognition, *Proceedings of the 14th Symposium on NDE, Southwest Research Institute,* San Antonio, Texas, 1985.

38. Hopwood, T., Acoustic Emission Inspection of Steel Bridges, *Public Works,* 1988, Vol. 5, 66-69.

39. Vannoy, D.W., Azmi, M., and Liu, J., *Acoustic Emission Monitoring of the Woodrow Wilson Bridge*, Report No. FHWA-MD-87-06. University of Maryland, College Park, 1987.

40. Vannoy, D.W., and Azmi, M., *Acoustic Emission Detection and Monitoring of Highway Bridge Components,* Report No. FHWA-MD-89-10. University of Maryland, College Park, 1991.

41. Hariri, R., *Acoustic Emission Investigation and Signal Discrimination in Steel Highway Bridge Applications*, Ph.D. Dissertation, University of Maryland, College Park, 1990.

42. Carlyle, J.H., Leaird, J.D., and Ely, T.M., *Acoustic Emission Monitoring of the I-95 Woodrow Wilson Bridge, I-10 Mississippi River Bridge and I-80 Bryte Bend Bridge*, Phase Report No. R90-259. Physical Acoustics Corporation, Lawrenceville, New Jersey, 1992.

43. Gong, Z., Nyborg, E.O., and Oommen, G., *Acoustic Emission Monitoring of Steel Railroad Bridges, Materials Evaluation,* Vol. 50, No. 7, 1992, 883-887.

44. Prine, D.W., Application of Acoustic Emission and Strain Gage Monitoring to Steel Highway Bridges, *Proceedings of the ASNT 1994 Spring Conference,* New Orleans, Louisiana, 1994, 90-92.

45. Maji, A.K., and Kratochvil, T., Acoustic Emission Monitoring of Steel Bridges, *Structures Congress XII,* 1994, 1322-1327.

46. Holford, K.M., Davies, H.W, and Sammarco, A., Analysis of Fatigue Crack Growth in Structural Steels by Classification of Acoustic Emission Signals, *Engineering Systems Design and Analysis,* 1994, Vol. 8, 349-353.

47. *Acoustic Emission Sensors*, Physical Acoustics Corporation, Princeton, New Jersey, 1992.

48. Fisher, J.W., *Fatigue and Fracture in Steel Bridges: Case Studies*, John Wylie and Sons, New York, 1984.

49. Zhou, Z., and Zwerneman, F.J., Fatigue Damage Due to Sub-Threshold Load Cycles Between Periodic Overloads, *Advances in Fatigue Lifetime Predictive Techniques: Second Volume,* ASTM STP 1211, ASTM, Philadelphia, 1993, 45-53.

50. Scala, C.M., and Cousland, S.McK., Acoustic Emission During Fatigue of Aluminium Alloy 2024: The Effect of an Overload, *Materials Science and Engineering,* 1985, Vol. 76, 83-88.

51. Zwerneman, F.J., and Frank, K.H., Fatigue Damage Under Variable Amplitude Loading, *Journal of Structural Engineering,* 1988, Vol. 114, No. 1, 67-83.

52. Dowling, N.E., *Mechanical Behavior of Materials: Engineering Methods for Deformation, Fracture and Fatigue*, Prentice Hall, Englewood Cliffs, New Jersey, 1993.

53. Tilly, G.P., and Nunn, D.E., Variable Amplitude Fatigue in Relation to Highway Bridges, *Proceedings of the Institute of Mechanical Engineers,* 1980, Vol. 194, 259-267.

54. Barsom, J.M., and Novak, S.R., *Subcritical Crack Growth and Fracture of Bridge Steels*, NCHRP Report 181, 1977.

55. Alawi, H., and Shaban, M., Fatigue Crack Growth Under Random Loading, *Engineering Fracture Mechanics,* 1989, Vol.3 2, No. 5, 845-854.

56. Beattie, A.G., Acoustic Emission Couplants I: The ASTM Survey, *Journal of Acoustic Emission,* Vol. 2 No. 2, 1983, pp. 67-68.

APPENDIX A

BASIC ACOUSTIC EMISSION

AE is defined as a transient elastic wave generated within a material because of the rapid release of energy from a localized source. Damage mechanisms in metals such as plastic deformation or the fracture of brittle inclusions bring about a redistribution of stress and strain that result in the release of stress waves that propagate throughout the material and to the material surface. Other mechanisms that give rise to AE in metals are phase transformation, twinning, corrosion, and friction between contact surfaces.

A general method of classifying AE divides it into two types: burst and continuous. Burst AE are individual emission events with distinct rise and decay segments of the waveform such as would result from fracture of materials. Continuous AE are the result of emission events occurring in rapid succession such that signal level appears sustained. Plastic deformation and fluid leakage on a pressure boundary produce AE of this type.

Frequencies of emissions range from below the audible range of humans, as in the case of earthquakes that are also considered AE, to well above it in the ultrasonic range. AE as an NDE method did not gain wide acceptance or achieve true practicality until instrumentation was developed that enabled detection of signals in the ultrasonic range while ignoring lower frequency noise and vibrations.

AE are detected by means of suitable sensors acoustically coupled to the material surface that are sensitive to mechanical movement or velocity. The most common type used in practical field applications employs a piezoelectric element to convert detected surface oscillations into electrical voltage. Piezoelectric sensors can detect a wide range of signal frequencies. The specific type of sensor used in an application, whether resonant or wideband, would depend on the type of information desired from a test. Resonant sensors have the advantage of being more sensitive and are thus used when detection and quantification of AE activity is the primary objective. Wideband sensors detect a wider range of signal frequencies and are therefore more accurate in reproducing the actual signal. These sensors are advantageous when characterization studies are performed to identify different AE source mechanisms.

An example of an AE waveform is shown in Figure A1 with the simple time-domain parameters indicated. During the first two decades of instrumented AE testing, AE activity was measured mainly by counting the number of times an oscillating signal exceeded a preset threshold. Ringdown counts were correlated to load, strain, fatigue cycles, stress intensity factors, and other measurable parameters to obtain an understanding of how damaged materials emit AE. Other AE parameters such as RMS voltage and amplitude were also used in characterizing material failures.

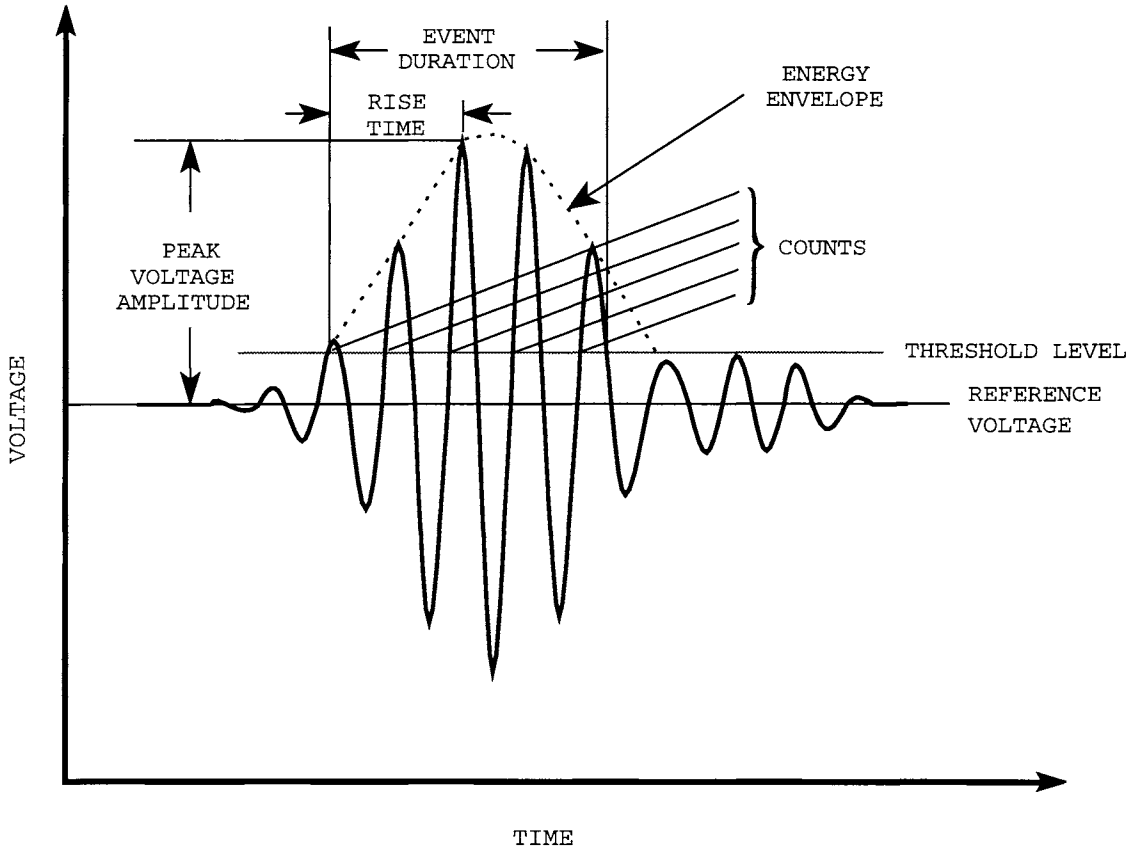

Figure A-1. AE waveform with definition of simple waveform parameters

APPENDIX B

PRELIMINARY AE MONITORING

New River Bridge

AE monitoring was performed on the Rte.460 westbound bridge over the New River in Glenlyn, Virginia, on September 24, 1993. The bridge is a continuous span, multigirder bridge with 16 pin-and-hanger and 8 pin-and-hinge connections. Since 1990, suspected cracks in four pins have been monitored using ultrasonic inspection. It was decided to replace all the pins and hangers, which are made of A588 weathering steel, with A276 stainless steel material. VDOT contractors were in the process of replacing the pins at the time the test was conducted.

Two pin and hanger connections on the western end of the westbound lanes were chosen for monitoring: one had a crack, and the other was newly installed. The monitoring equipment was positioned under the bridge close to the pins that were about 4.6 m (15 ft) above the ground.

The pins are 0.304 m (1 ft) long and 25.4 mm (4 in) in diameter at the widest section. A R30I sensor was attached to each end of the two pins as close as possible to the axial center of the pin. Figure B1 shows one end of the cracked pin where a sensor was placed.

Magnetic hold-downs were used to attach the sensors to the cracked pin while the duct tape was used on the sensors mounted on the stainless steel pin. The Spartan system was configured to perform linear source location, and an old pin that had been removed prior to the test was

Figure B1. Pin and hanger connection, Rte. 460 bridge in Glenlyn, Virginia

used to check the accuracy of the system settings. Since the pins being monitored were not exposed, the actual sensor setup was simulated on the old pin, and pencil lead break tests were performed along the length of this pin

Live loading of the bridge was done exclusively by normal passing traffic, although one lane (passing lane) was closed because of repair work that was then being done on the bridge. Data were collected for 1 hr 52 min at the old pin, and the new pin was monitored for 18 min.

Source location results for the cracked pin and the new pin are plotted in Figure B2. The boxed numbers below the x axis indicate the position and number designation of the sensors. Sensors 1 and 2 were attached to the cracked pin, and the new pin had sensors 3 and 4.

Ultrasonic inspection had indicated a crack about 4 in from sensor 1. However, there was no obvious clustering of events at this location. A concentration of events here would have been a good indication of an active crack. Possible differences were investigated in the AE characteristics of the events that occurred between 3 and 5 in and the rest of the detected AE events that were presumed to be rubbing noise. The ranges of signal characteristics (counts, amplitude, etc.) of the two groups were found to overlap each other completely. Application of the AE method to monitoring pins and similar fasteners presents a special challenge to this NDE method. The presence of fretting noise sources very close to or at the same locations as the defects prevents the use of spatial discrimination as a means of distinguishing flaw-related AE signals from noise signals. Other means of discrimination must be employed. Continuing work on the project using waveform and frequency analysis of AE signals from the other bridges tested is exploring these other means that may prove useful for application to pin-and-hanger components.

The newly installed stainless steel pin was monitored for a different purpose. It has been postulated that the seizing of pins attributable to corrosion contributed to the growth of the cracks since this produces added torsional and bending loads not necessarily accounted for in the design of the pins. A freely rotating pin would surely cause rubbing on the mating pin and hanger surfaces that can be detected as rubbing noise by the AE sensors. AE can thus be used to determine qualitatively if a pin is seized.

The Figure B2 graph for the new pin shows events detected over 18 min. A total of 125 events occurred between the ends compared to only 114 for the cracked pin that was monitored for close to 2 hr. It is natural to expect that the old pin has more limited movement, and this was shown by the results. However, the greater event rate for the new pin may also be attributable to mating surfaces that have yet to be smoothed by constant rubbing.

The use of AE in this manner should be approached with caution as it is entirely qualitative. It is also necessary to compare the results from a particular pin to those for another similarly configured pin known to be moving freely to gauge the extent of seizing.

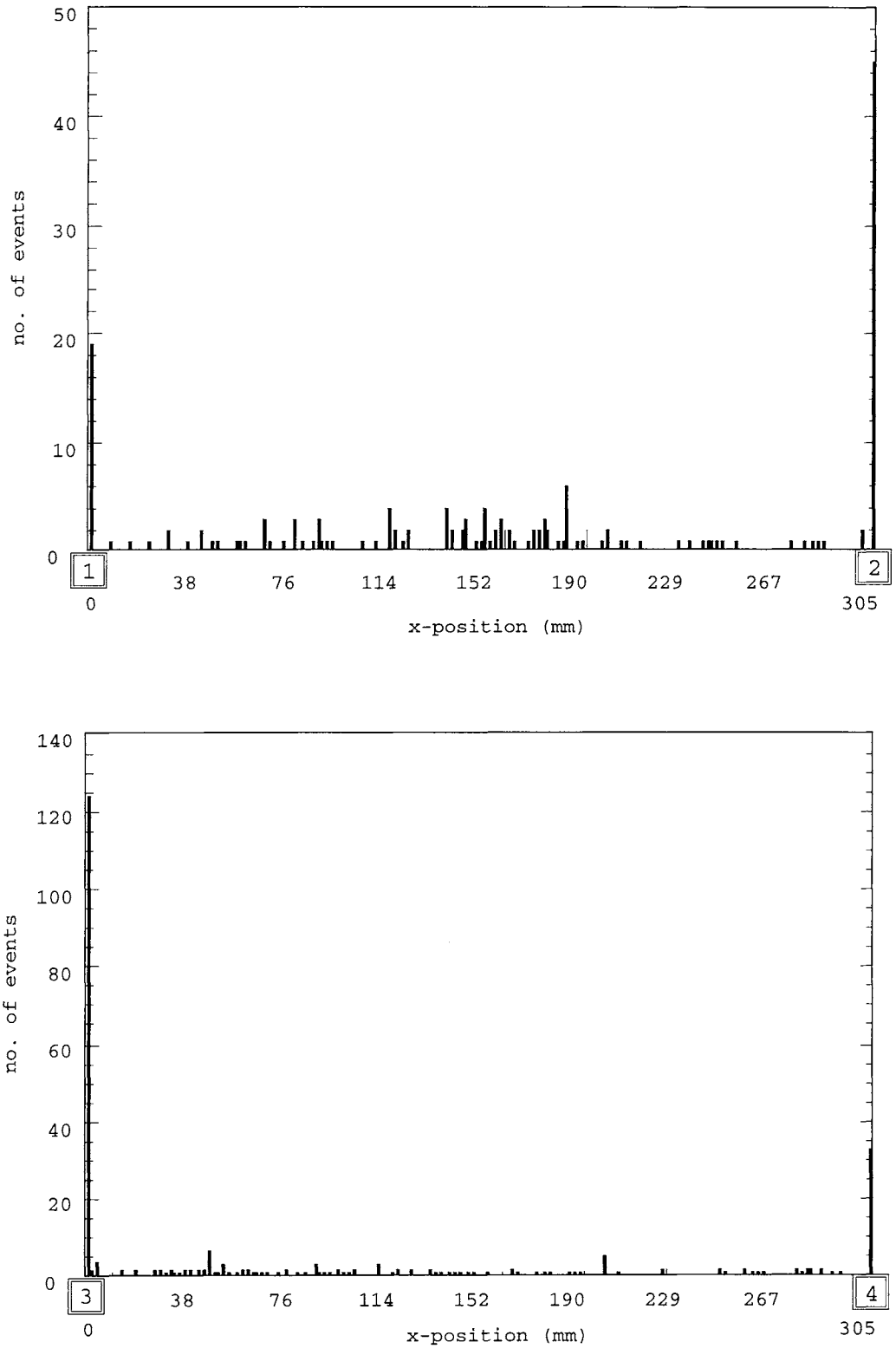

Figure B2. Source location results for (top) *cracked pin, showing no activity, and* (bottom) *new pin*

Staunton River Bridge

The Rte. 29 bridge over the Staunton River in Altavista, Virginia, was monitored on July 19, 1994. VDOT personnel were on hand to assist during the testing identified and suggested the locations to be monitored. Two sites, which were accessed using the Bridgemaster, were chosen for monitoring. The bridge is pictured in Figure B3, showing the outer girder similar to the one that was monitored.

The first location was on the 9.5 mm (3/8 in) thick cracked web of an inner girder that had been retrofitted with a 9.5 mm (3/8 in) thick splice plate bolted to the web as shown in Figure B4.

The crack continued to grow in spite of the retrofit and had progressed passed the splice plate and under the bolted angular connector to the diaphragm. R30I sensors 1 and 2, spaced 155 mm (6-1/8 in) apart, were set up for linear source location to detect activity at the lower exposed end of the crack. A third sensor was attached to the flange to function as a guard sensor against fretting noise that might come from the flange bolts. The second location lies on the same girder with the crack also on the web.

Holes have been drilled at both ends of the crack to arrest further growth. R30I sensors 3, 4, and 5 were positioned for the triangular planar source location, as shown in Figure B5. The aim was to detect the presence of crack activity past the lower stop drill hole that is right above the flange weld.

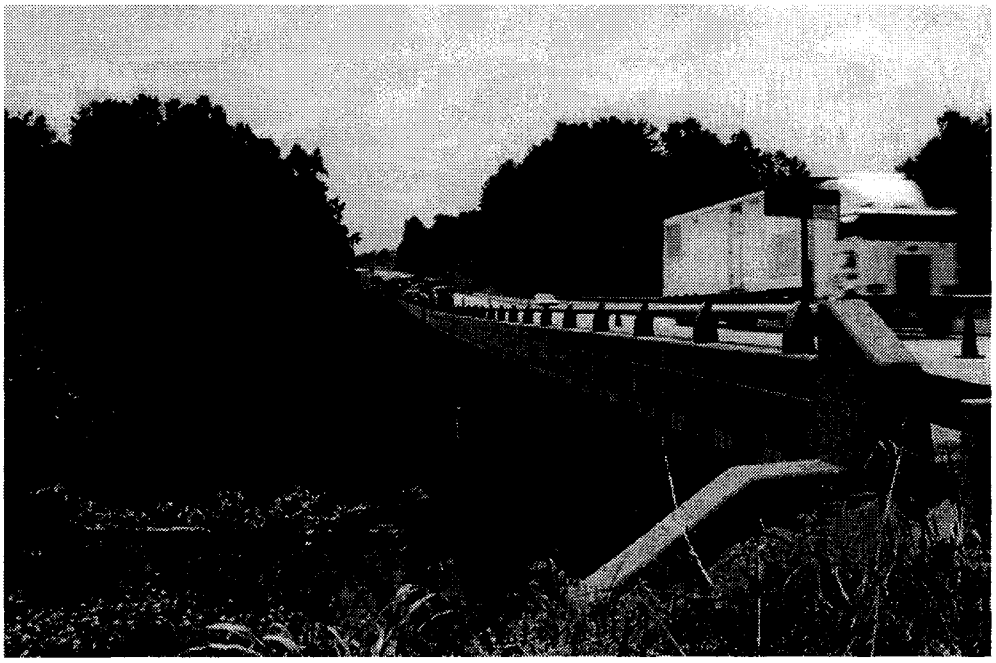

Figure B3. Rte. 29 northbound bridge over Staunton River

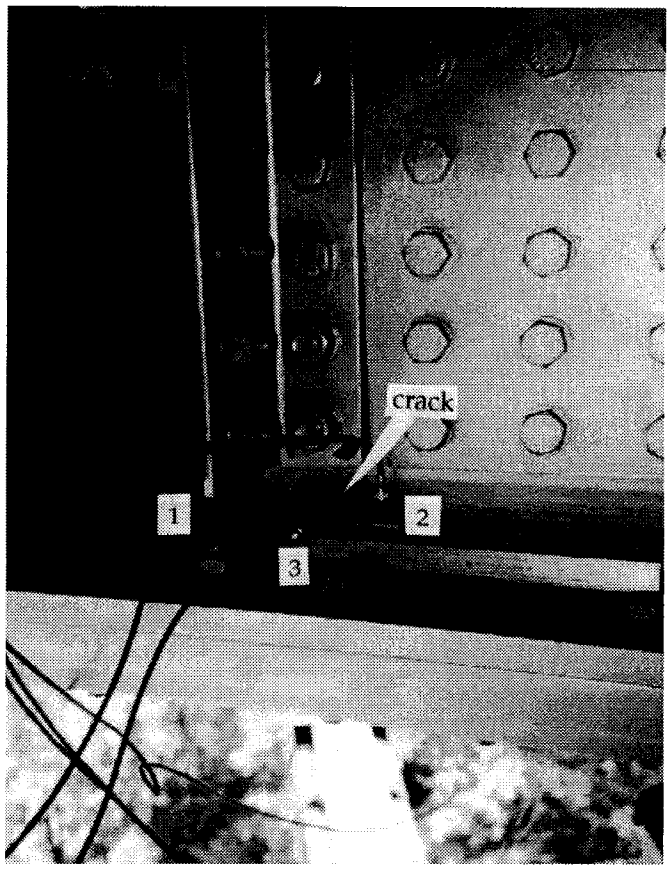

Figure B4. Sensor placement at location 1 showing sensors 1 and 2 positioned for linear source location, guard sensor 3.

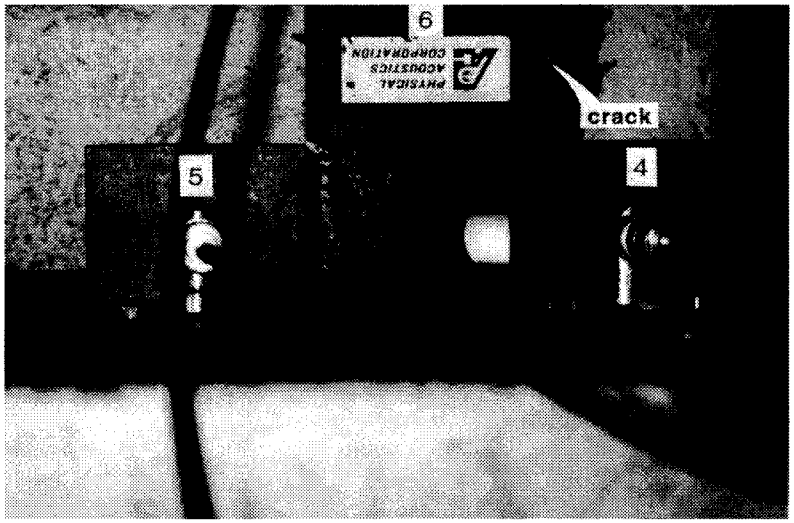

Figure B5. Closeup view of sensor placement at location 2 showing sensors 4, 5, and 6 positioned for triangular source location. Lower stop drill hole of crack is visible.

The Spartan unit and the PC were set up above the bridge, leaving only the inner lane open to traffic. Loading was accomplished via normal bridge traffic. The first location was monitored for approximately 1 hr and the second one for about 45 min.

No events coming from the crack top were detected by the sensor array at location 1. For the triangular array at location 2, no events were detected at all. Figure B6 shows the detected events at location 2 when the pencil lead break tests were performed. The cluster of events at about 3.5,.5 were a series of lead breaks done at the 6 o'clock position of the lower hole where a crack would be expected if one had propagated past the drill hole.

The results show that the crack at location 1 was not active during the time the monitoring was performed. It is also shown that crack growth at location 2 had been successfully arrested by the drill hole. However, since monitoring time was limited, the results may not be fully representative of the general behavior of the cracks, especially since the test was done during a non-rush hour period and the bridge was loaded on only one lane.

The main difficulty encountered in this test was the limited space around the cracks available for sensor placement. The relatively large size of the R301 sensors and the magnetic hold-downs limited the options for positioning the sensors to fewer than what would have been ideal. This affects both source location accuracy and the ability to set up effective guard sensors. This shows the need for adapting the instrumentation, particularly the sensors, to each application.

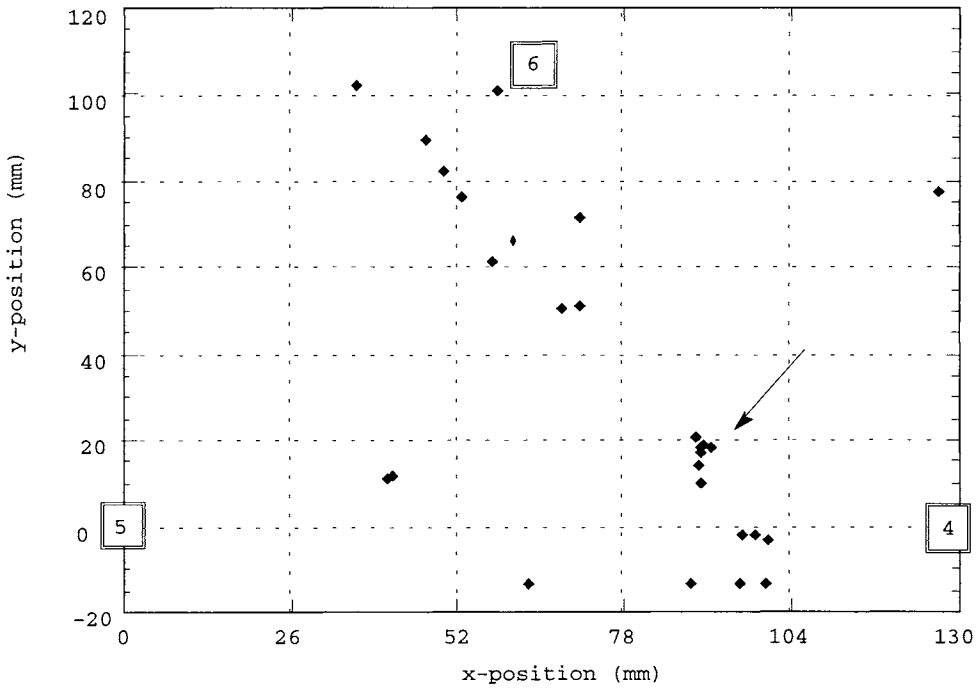

Figure B6. Triangular source location plot of pencil lead breaks at location 2. Arrow points to lead breaks done below lower stop hole.

Moormans River Bridge

The Rte. 671 bridge over the Moormans River in Albemarle County pictured in Figure B7 was monitored on July 27, 1994. A load limit of 3 tons had been posted for the bridge, attributable in part to a crack found on one of the : in square diagonal counters shown in Figure B8. This was the only defect monitored for AE. The part monitored had a simple geometry, and the crack was well separated from possible noise sources that could propagate only from the ends of the bar. Two R30I sensors were attached at either side of the crack a distance of 6 in from each other. These sensors were set up for linear source location. A WD sensor, to be used to record waveforms, was mounted close to the crack on the opposite side of the bar. The AE equipment was set up away from the bridge. Being on a secondary road, the bridge was loaded intermittently. The crack was monitored for about 1.5 hr during a steady rain. Although AE were detected every time a vehicle passed through, only three events were recorded by the source location program for the entire period, none of which came from the location of the crack. The triggering threshold of the TRA had been set at absolute minimum, yet no signals detected were strong enough to trigger it. No waveforms were thus recorded. The results show that the crack is benign and has become inactive. The unbroken appearance of rust covering the crack tends to support this conclusion.

I-66 South Exit Bridge Over Rte. 29

AE monitoring of the I-66 south exit bridge over Rte. 29 in Gainesville, Virginia, was performed on August 16, 1994. A truck passing under the bridge, shown in Figure B9, had accidentally hit the lower flange of the northernmost girder, causing the web and a stiffener to deform and the welds to crack. The girder was repaired by replacing the stiffener, heat straightening the web back, and rewelding the flange weld and damaged cover plate. Repairs had just

Figure B7. Rte. 671 bridge over Moormans River

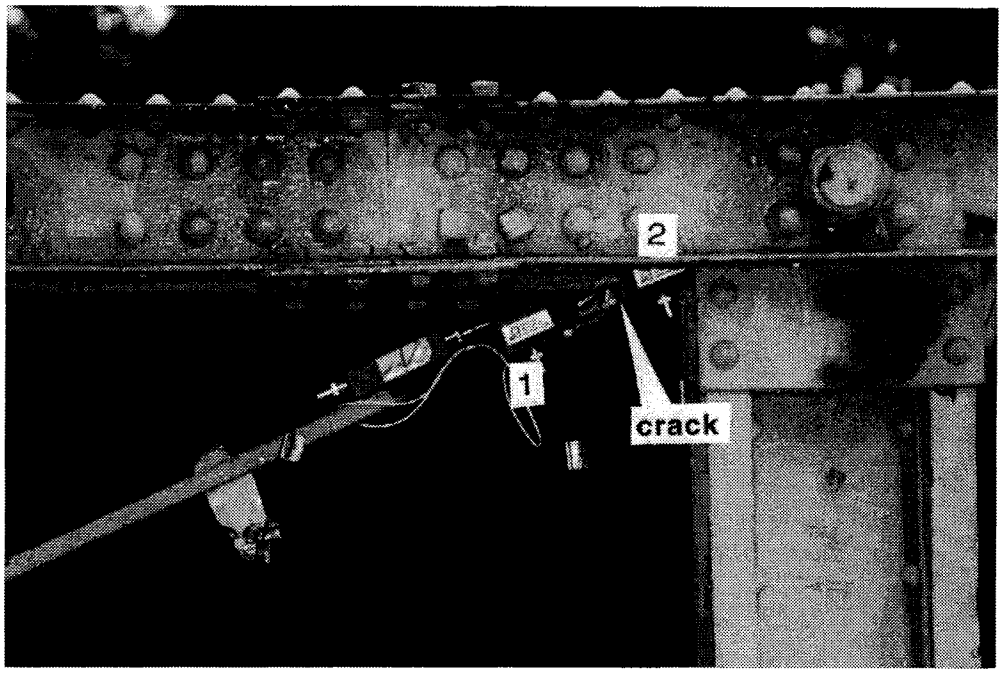

Figure B8. Sensor placement at cracked diagonal counter

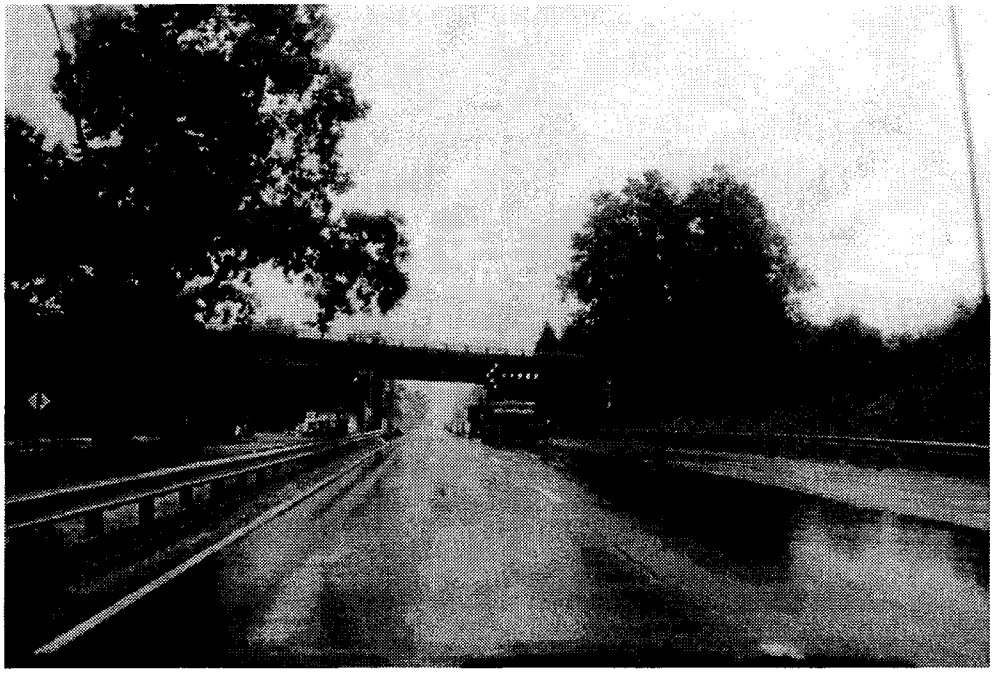

Figure B9. South exit bridge over Rte. 29 in Gainesville

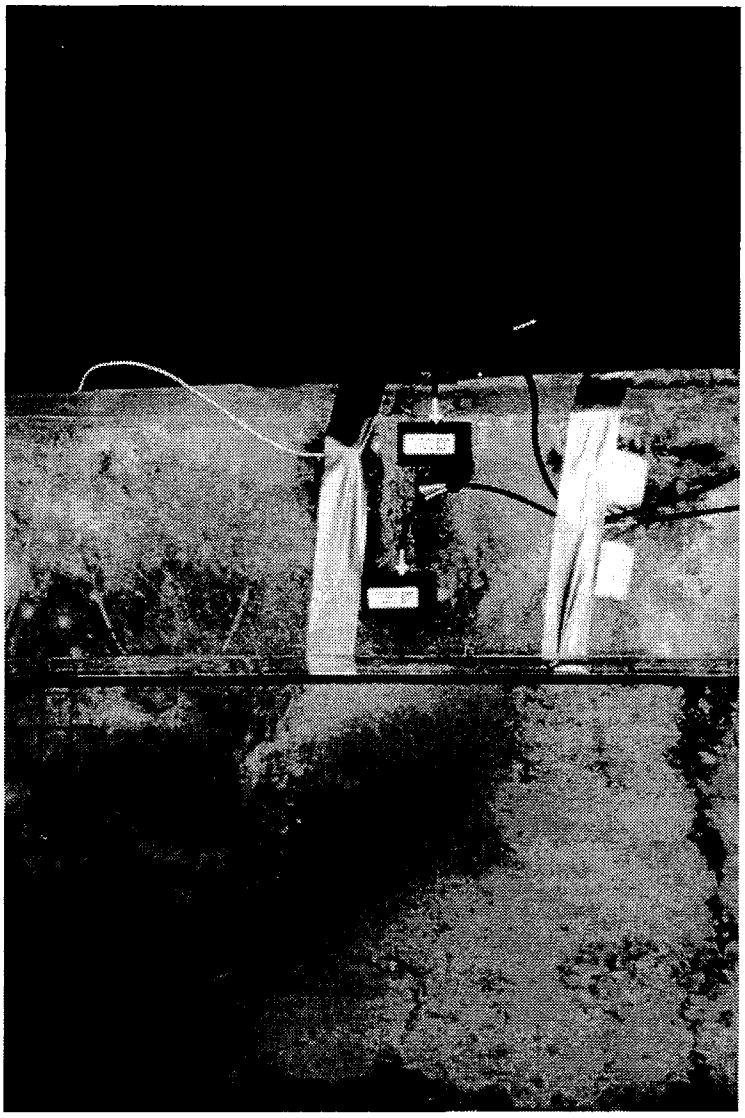

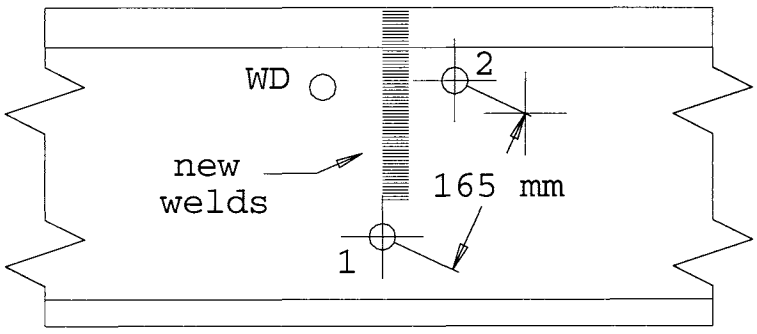

Figure B10. Sensor placement at cover plate showing sensors 1 and 2 positioned for linear source location to monitor new weld

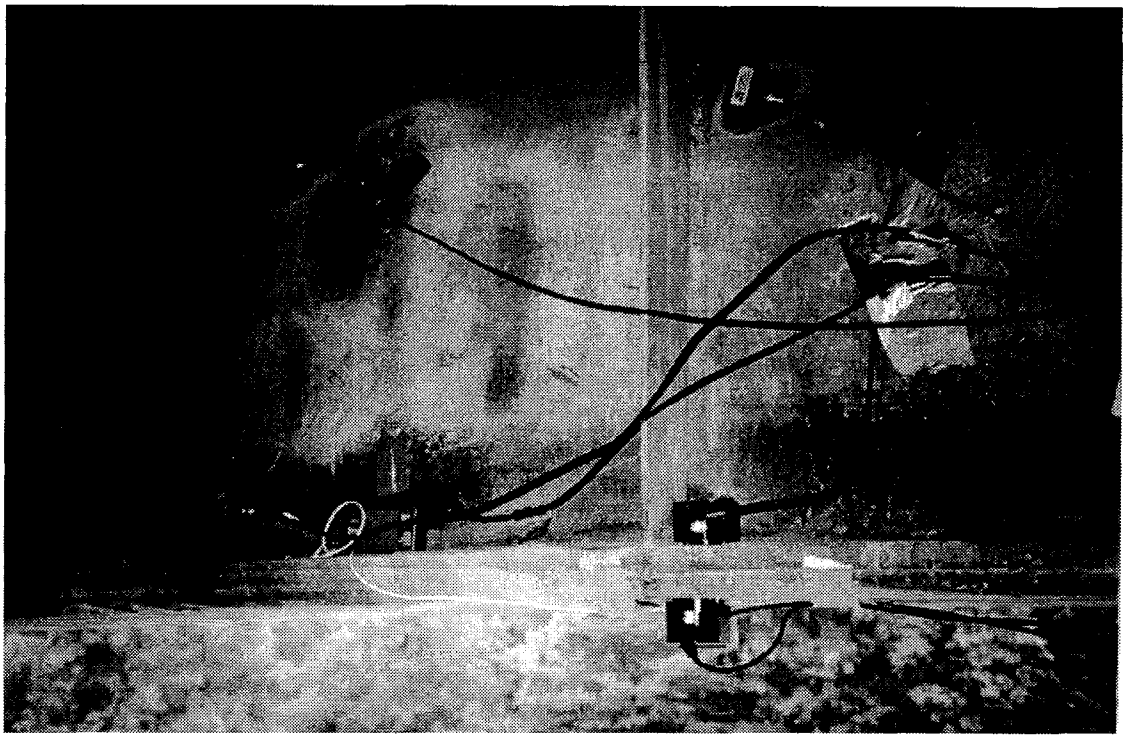

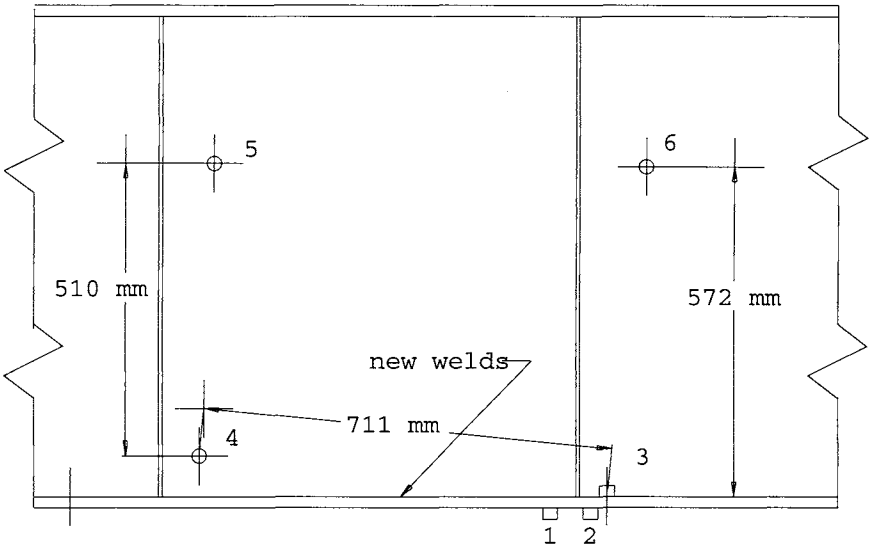

Figure B11. Repaired girder showing location of sensors 3 and 4 positioned for source location to monitor lower flange-to-web weld and guard sensors 5 and 6

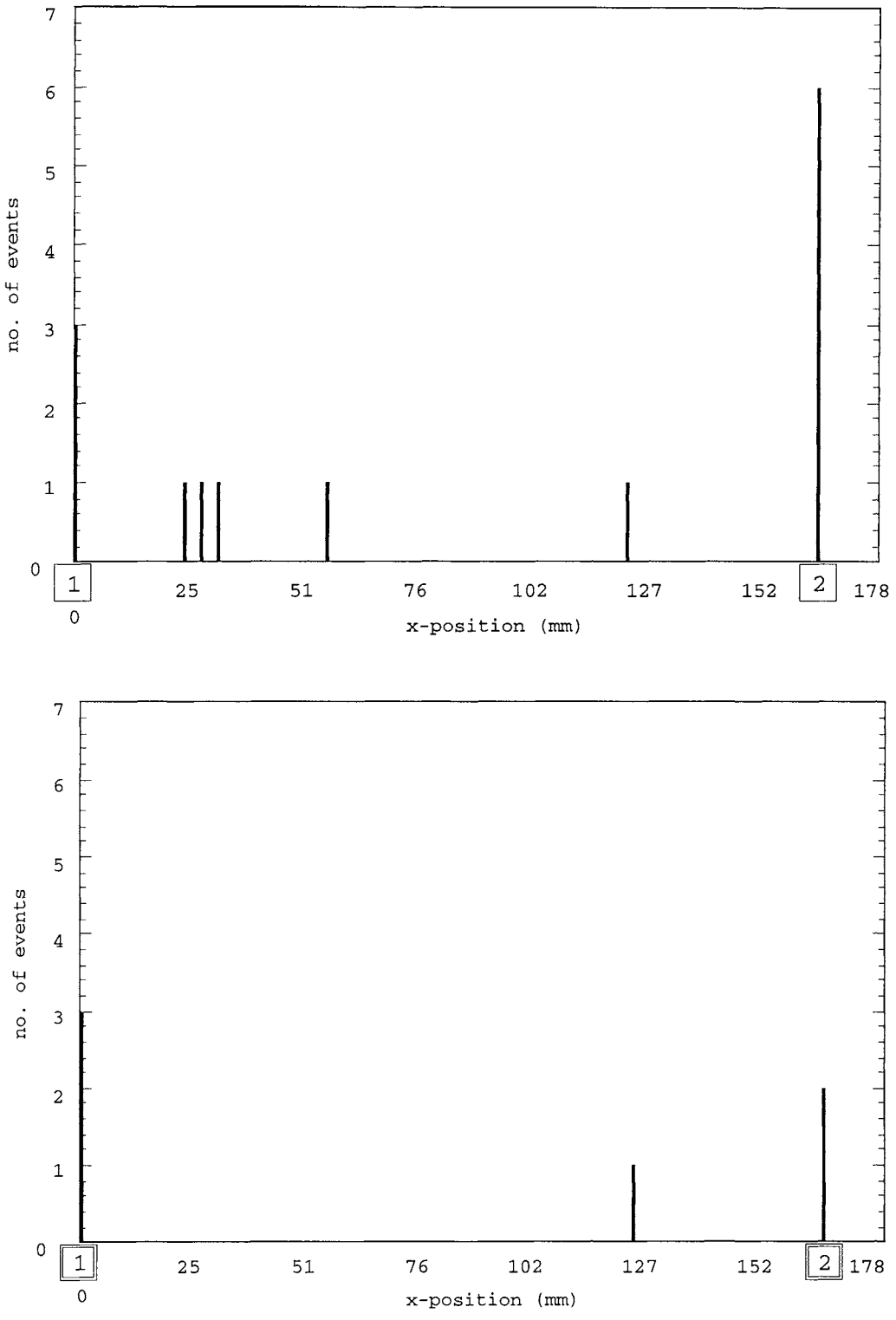

Figure B12. Top: Source location results for cover plate weld (without guard sensors) showing no evident crack activity. Bottom: Same location using guard sensors 3, 4, 5, and 6.

been completed when the AE test was conducted. Two R30I sensors, labeled 1 and 2, were attached on the cover plate for source location on the new weld as shown in Figure B10. The R30I sensor 3 was installed on the flange above the first array. This sensor serves as a guard sensor to sensors 1 and 2 while also doing linear source location with sensor 4. These two sensors were set up to monitor the rewelded web to flange section. The remaining sensors, 5 and 6, were positioned as shown in Figure B11 to act as guard sensors against noise coming from the floor beams. The WD sensor was mounted close to the cover plate weld to record waveforms. The bridge pavement was under repair at the time of the test. Only one lane was open to traffic that had to be slowed down as the bridge was crossed. AE data were collected for 1 hr 25 min. Figure B12 shows the results of source location for the two sensor arrays. In both cases, very few events were detected. The effects of having guard sensors are also shown, although even without these, the location findings clearly indicate that no active cracks were detected. No data were collected by the TRA, because even at minimum threshold settings, no AE detected by the WD sensor were strong enough to trigger the transient digitizer.

Although results from this AE monitoring test were negative for crack activity, such could not be a reliable gauge of whether repair to the damaged girder was successful. The reason was that the bridge was not subjected to normal loading. It was most likely experiencing less dynamic loads during the test than when in service.

APPENDIX C

TESTS OF TRANSDUCER ADHESIVES

In preparation for application to long-term AE monitoring on bridges, tests were done to assess the performance of three adhesives as bonding agents for transducer attachment. The three considered were hot-melt glue, 5-minute epoxy, and a cyanoacrylic adhesive. Hot melt glue had been used with success on metal and fiberglass surfaces by the Monsanto Corporation, Saint Louis, Missouri. It has been used mainly to attach sensors for extended periods to pressure vessels that are periodically hydrotested. Five-minute epoxy gel, an epoxy resin manufactured by Devcon Corporation, is being used by Babcock and Wilcox Nondestructive Systems and Diagnostics Section personnel in their AE tests. Cyanoacrylic adhesive is a popular AE sensor bonding agent, ranking third in a survey conducted by ASTM in 1981.

The same survey showed that the failure of bonding agents is caused mainly by differential expansion between the sensor and the specimen. This can be induced by either strain in the specimen or different thermal expansion rates between the sensor and specimen. This was the main issue studied in the tests described.

Equipment

Transducers: Model AC375L resonant transducers manufactured by Acoustic Emission Technology. These sensors have a nominal resonant frequency of 375 kHz. Six were used for the tests.

Preamplifier: Model 1220A preamplifier with a 100 to 300 kHz bandpass filter manufactured by PAC.

Pulser: AE-CAL 2 acoustic emission simulator manufactured by Physical Acoustics Corporation. Amplitude, rise time, decay time, and frequency of the pulse are user-selected. The pulser itself is a V109 ultrasonic transducer manufactured by Panametrics, Inc.

Experimental Procedure

The sensors were bonded to a 6 mm (3 in) thick piece of steel (shown in Figure C-1) using the different adhesives. The steel surface was sanded to remove dirt and thoroughly cleaned before the sensors were mounted. Initial readings were taken with simulator settings of 10 :s rise time, 10 :s decay time, 300 kHz frequency, and 80 and 70 dB amplitude at high dB setting. The sensor connection ports were taped over with masking tape to prevent ingress of moisture during exposure. The plate was then subjected to thermal cycling between 21.11 C and 9.4 C.

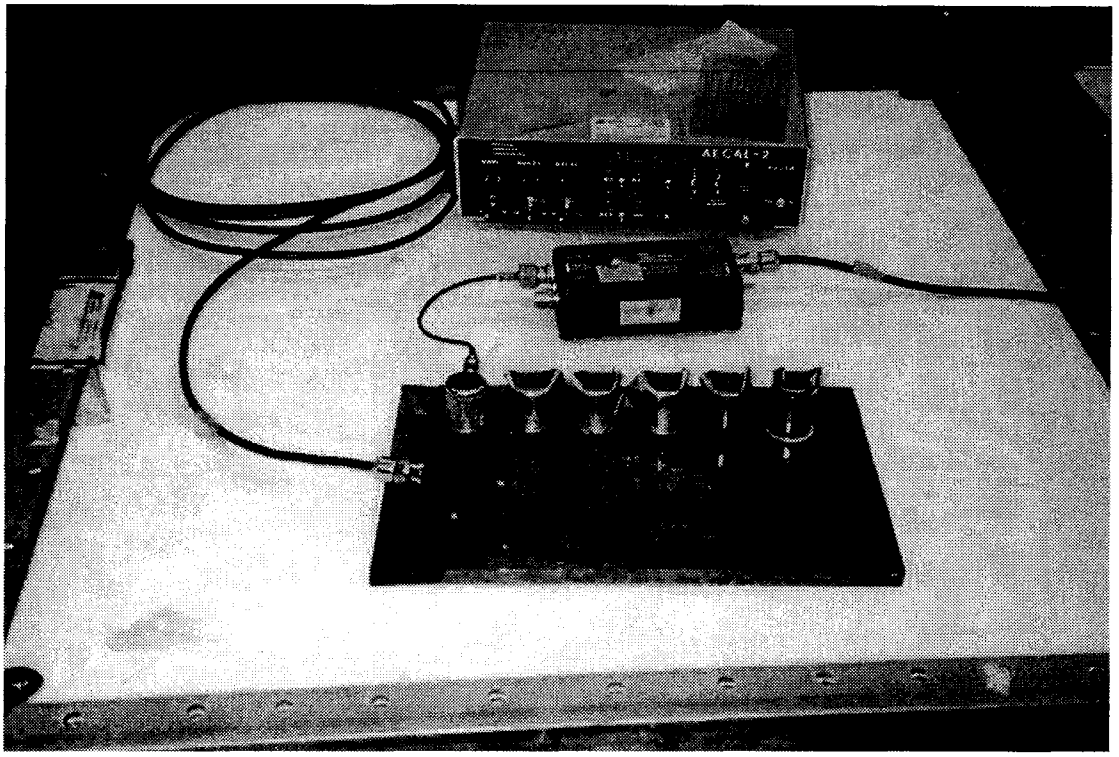

Figure C1. Experimental setup showing test plate, AET transducers, preamplifier, and AE-CAL2 simulator

Results

Hot melt glue: Difficulty in using the hot melt glue was experienced even during mounting of the sensors. The plate had to be heated so that glue applied to the steel surface would not harden before the sensors could be bonded. Rigorous surface preparation was required for the bond to hold adequately. This adhesive was abandoned even before the plate was thermally cycled because bond strength was insufficient unless supplemented by a mounting instrument such as a magnetic hold-down. Though practical for such applications as pressure vessels, a magnetic hold-down on a vibrating structure such as a bridge is not expected to perform well in the long term.

Five-minute epoxy gel: Three sensors were attached using 5-minute epoxy. The bonding agents were tested after 25 cycles by pulsing using the same AE simulator settings as in the initial test. However, one of the sensors detached after 20 cycles, and another was detached as the tape covering was being removed prior to the test at 25 cycles. In both cases, debonding occurred at the sensor side. The one remaining sensor was tested. The amplitude of the detected pulse was more than 10 dB lower than the initial reading. Therefore, the use of this adhesive for long-term monitoring in an exposed environment is not recommended.

Cyanoacrylic adhesive: Initially, three sensors were attached using the cyanoacrylic glue. After the failure of the 5-minute epoxy, the two detached sensors were reattached using cyanoacrylate. Regular cyanoacrylic (True bond super glue was used), which has a watery consistency, was used for the first three. Mounting was easier on the other two because a thicker, more viscous type (Duro Quick Gel made by Loctite Corporation) was used. Amplitude results taken at 25 and 40 cycles are shown in Figure C2. There was practically no deterioration in the signal. The decrease shown by sensor 3 might well be attributable to experimental error. One of the three original sensors was detached after 25 cycles while the masking tape was being removed. The cause appeared to be insufficient adhesive. The regular cyanoacrylic flowed out under the sensor before the bond could set. The sensor was reattached using the viscous type adhesive.

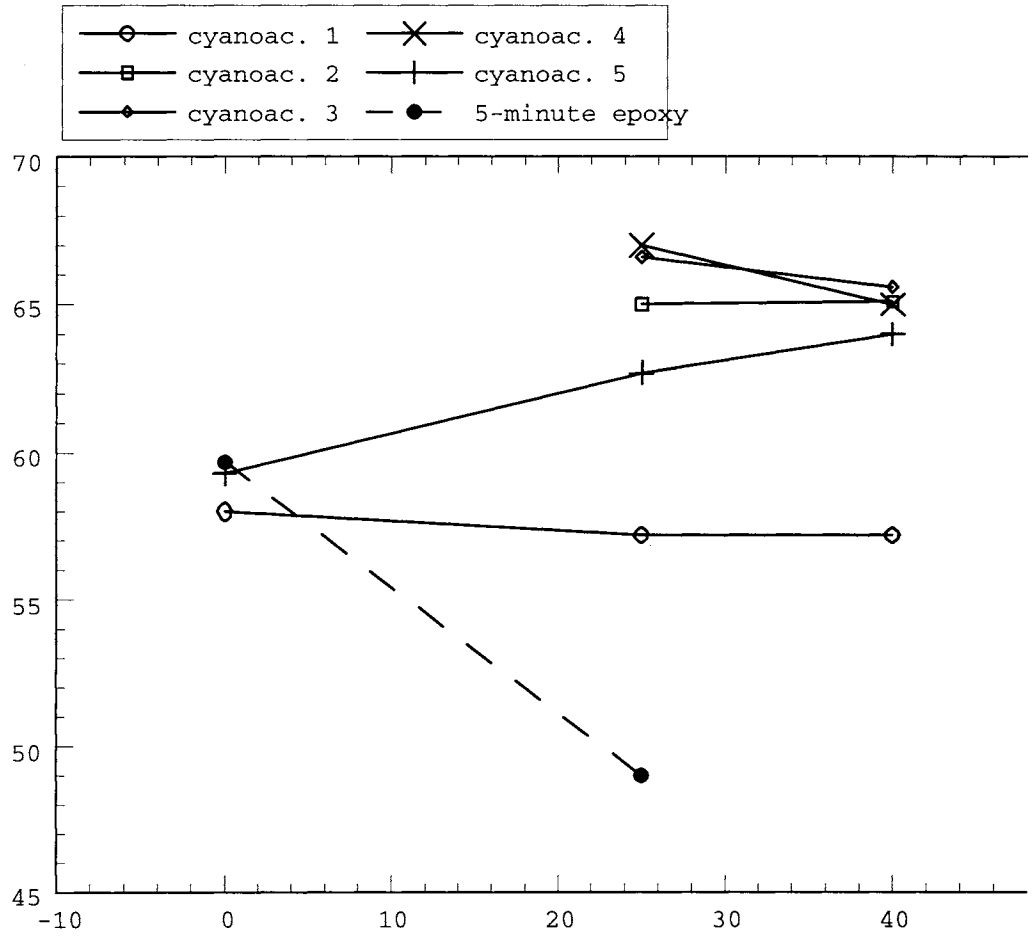

Figure C2. Detected amplitudes of standard simulated AE signal from test sensors at 0, 25, and 40 thermal cycles

Conclusion

Of the three tested bonding agents, the viscous type of cyanoacrylic adhesive performs best under temperature cycling and is recommended for use on long-term monitoring of bridges.

Continuing work on this investigation involves further cycling of the plate with the sensors attached with cyanoacrylic adhesive. Higher cycling temperatures will also be used to determine their effect on the bond. The effect of vibration on the bond will also be explored.

APPENDIX D

LABORATORY FATIGUE TESTS

Experimental Setup

Two standard compact tension (CT) specimens fabricated from A588-70 steel were used in the fatigue tests. A588 is a structural weathering steel widely used in bridge construction. The width of the specimens was 63.5 mm (2-1/2 in) and the thickness was 6.4 mm (3 in) (Figure D1).

Two loading machines were employed. To minimize noise detected from the loading frame, AE data were acquired with the specimens loaded on a belt-driven machine; an Instron 4468 testing system with an 50 kN (11.2 kips) actuator was used for this purpose. However, the limited loading speed of this machine made it necessary between AE measurements to transfer the specimens to an electrohydraulic testing system to grow the cracks to the necessary lengths for AE acquisition. An MTS 808 closed loop system with a maximum dynamic capacity of 89 kN (20 kips) was used.

Crack length was measured using a traveling microscope with a maximum of 7x magnification. This was aided by scribe marks 1.6 mm (1/16 in) apart on the CT specimens.

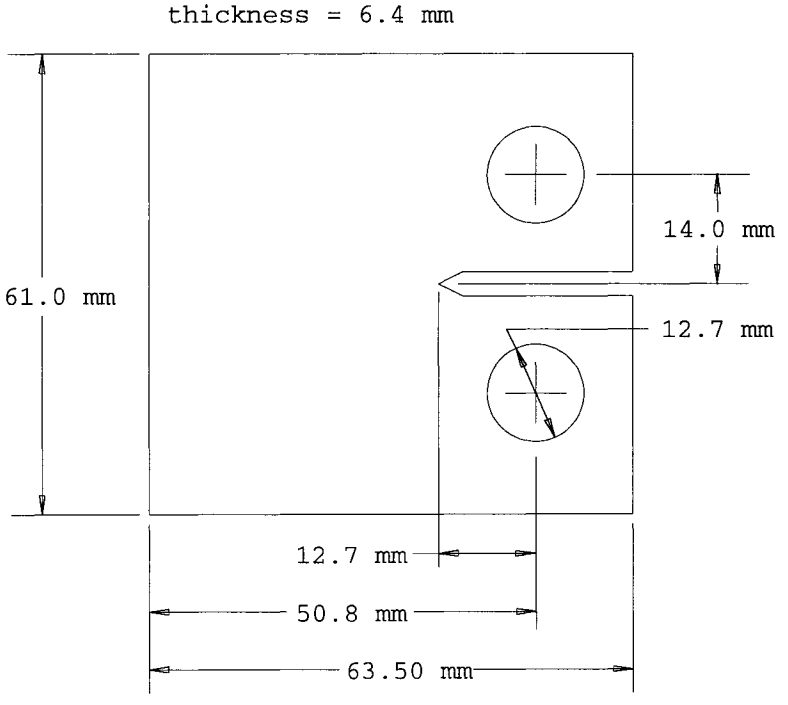

Figure D1. Standard compact tension specimen in accordance with ASTM E647 used in laboratory fatigue tests

AE Instrumentation and Setup

Two wideband sensors, model WDI manufactured by Physical Acoustics Corporation, were used for AE detection. These sensors are similar to the WD model used in the bridge tests, having the same flat frequency response between 100 kHz and 1 MHz, but have preamplifiers that provide 40 dB gain integral to the sensor housing. The two sensors were mounted symmetrically on the lower and upper edges of the CT specimens. A rubber band was used to hold the sensors in place. The sensors were positioned such that any emission coming from anywhere along the crack would arrive at both sensors simultaneously. Noise from the loading frame and grips, as transmitted through the pin, would hit one sensor ahead of the other.

AE waveforms detected by both sensors were monitored and recorded with the TRA transient digitizer program using simultaneous threshold triggering; i.e., any channel that is triggered by a signal above the preset threshold in turn activates the other channel. The computer displays one waveform above the other, making it convenient to distinguish simultaneous wave arrivals at the two channels. The SA-LOC program was used to record the load output from the Instron machine while running the TRA program in the background mode. Data acquisition proceeded in the following manner: (1) SA-LOC was turned on and then stopped after a preset time or after the TRA memory buffer filled up, whichever came first; (2) SA-LOC was closed and the TRA program opened; and (3) each waveform pair was visually inspected and valid waveforms were saved to file. All waveform pairs that were not obviously repetitive judging from the quick visual check during the experiments and which appeared to arrive at both sensors very closely were saved to file. Cross-correlation analysis was used during data processing to identify emissions that did in fact arrive simultaneously at both sensors and eliminate grip and loading frame noise that were nevertheless saved as disk files during the tests.

Threshold trigger levels were set just above the value that resulted in continuous triggering. This was generally at 1 to 2 percent of the maximum signal input of 10 V. An additional 1220A preamplifier with a high pass filter above 20 kHz was used on each TRA channel for a total system gain of 80 dB. Load values were sampled by SA-LOC at a rate of one reading every 0.15 sec.

Loading Program

Each complex load cycle consisted of one overload cycle and several minor cycles. The load cycle for specimen CT2 had 4 minor cycles and CT3 had 19 minor cycles to each overload cycle. Step loading was used since this was conveniently implemented on the available Instron machine. The loading spectrum for CT2 is illustrated in Figure D2.

Both specimens were precracked to a length of 14.3 mm (9/16 in). The first AE measurements were done at this crack length with P_h= 8.50 kN (1.91 kips), P_i = 2.00 kN (0.45 kips) and P_l = 0.50 kN (0.11 kips) corresponding to K_h = 2.10 MPa-m$^{1/2}$ (28.93 ksi-in$^{1/2}$), K_i = 7.48 MPa-m$^{1/2}$ (6.81 ksi-in$^{1/2}$), and K_l =1.87 MPa-m$^{1/2}$ (1.70 ksi-in$^{1/2}$), respectively. P_i and P_l

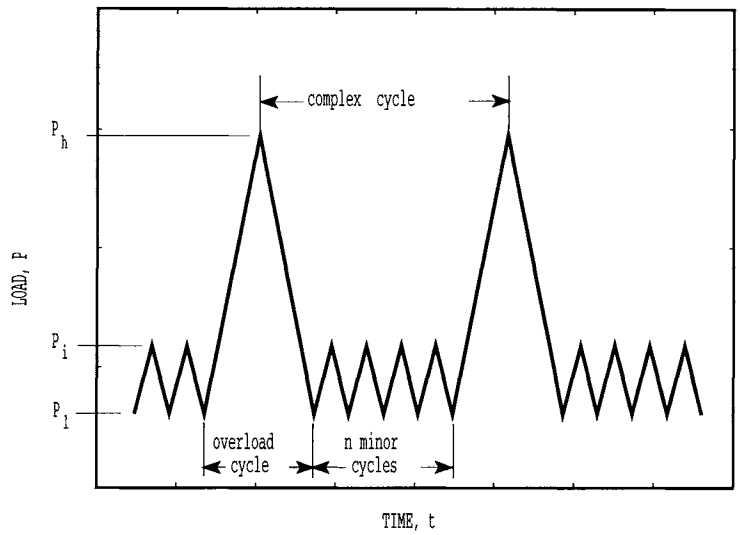

Figure D2. Loading spectrum for CT2

were chosen such that *DK* for the minor cycle at this initial AE measurement was just above the fatigue threshold predicted by the Barsom formula,[54]

$$\Delta K_{th} = 6.4\ (1 - 0.85R)\ \text{ksi}\sqrt{\text{in}} \qquad (R \geq 0.17)$$

This equation provides a conservative estimate of the fatigue crack propagation threshold values for a wide range of steels. The overload level was chosen to give a high stress intensity factor value even at the initial crack length. This enhanced the probability that crack growth would occur over the relatively few number of cycles that AE data acquisition was enabled. The load levels were maintained to the next crack length at which AE were measured, about 15.9 mm (5/8 in). P_h was then decreased to 6.32 kN (1.42 kips) to ensure that the specimens would not fracture before a crack length of 25.4 mm (1 in) was achieved. The crack was propagated another 4.8 mm (3/16 in) before AE were again collected. At this length, the crack tip was beyond the plastic zone formed by the preceding overload of 8.50 kN (1.91 kips). The largest theoretical plastic zone size was calculated to be 4.6 mm (0.18 in) using the plane stress equation

$$2r_0 = \frac{1}{\pi}\left(\frac{K}{\sigma_0}\right)^2$$

where $2r_0$ is the size of the plastic zone and s_0 is the yield strength of the material.

Loading on the Instron test machine was done at a constant crosshead speed. CT2 was cycled at a rate of 5 complex cycles/min, and CT3 was cycled between 2 to 4 complex cycles/min. Much higher rates of 1 to 2 complex cycles/sec were used in growing the cracks on the MTS machine. The difference in the loading rates was not expected to affect the behavior of the fatigue cracks or the acoustic emissions produced.[8,55]

Laboratory Fatigue Tests

Plots of the *DK* levels for the overload and minor cycles at which AE were measured are shown in Figure D3. Valid AE data were recorded from specimen CT2, starting with the measurements done at a crack length of 19.3 mm (0.76 in). Two other series of AE data acquisition periods, evident in Figure D4(a), were performed at crack lengths of 24.4 mm (0.96 in) and 28.7 mm (1.13 in). During the first series, 118 waveforms from the crack were recorded over a cumulative total of 239 complex load cycles monitored. In the second series of measurements, WD-40 lubricant was sprayed between the crack faces to reduce or eliminate emissions attributable to crack face rubbing. The number of waveforms collected was drastically reduced to 23 over a monitoring period of more than 270 complex cycles. The final series of measurements resulted in the detection of 24 waveforms over 493 cycles monitored.

As in CT2, three series of AE measurements were performed on specimen CT3. These were at 14.2 mm (0.56 in), 16.5 mm (0.65 in), and 25.4 mm (1.0 in). AE were collected over 152 cycles in the first series, resulting in 65 crack-related AE recorded. Only 23 signals from the crack were detected in the second series over a cumulative monitoring period of 386 cycles while the crack grew by 2.3 mm (0.09 in). The final series of measurements were made during more than 600 cycles spread over a period of 7,780 loading cycles in which the crack grew by 3.0 mm (0.12 in).

Cluster analysis using SAS was used to identify repetitive waveforms. Results from this automatic classification process were confirmed or corrected through visual inspection of each waveform. Two types of behavior were noted from the repetitive emissions. The more predominant repetitive waveforms were observed to repeat at generally the same load levels and always on the same side of the load cycle. An example of this type of signal (type 1) is plotted on the load cycle of Figure D4. This signal was observed to occur over 129 complex load cycles (2,580 individual cycles) in CT3 before finally fading from detection. Most repeating signals were not as persistent, however, often occurring less than 10 times over the entire tests. These emissions (type 2) were detected at varying load levels and did not repeat on successive cycles but occurred sometimes more than 100 cycles apart. This load behavior is shown in Figure D5. Repetitive waveforms were detected from minimum load to within 98 percent of maximum load. The waveform of Figure D4, which displayed the most variability in magnitude among repetitive emissions, ranged in amplitude from 24 to 30 dB.

Unique waveforms that occurred on rising loads were identified from both specimens. Twenty-seven emissions from CT2 and 8 from CT3 satisfied both criteria for uniqueness and occurrence on rising loads. Examples of such waveforms are shown in Figure D6. Only 3 of the emissions from CT2 did not occur above 95 percent of maximum load, whereas all 8 emissions from CT3 were detected above 92 percent of maximum load. All of these waveforms were detected on overload cycles. The minimum *DKs* at which these emissions occurred were 34.1 ksi-in$^{1/2}$ (37.5 MPa-m$^{1/2}$) for CT2 and 30.7 ksi-in$^{1/2}$ (33.7 MPa-m$^{1/2}$) for CT3. For both CT2 and CT3, no crack growth emissions were recorded during the first series of measurements. The power spectra of all waveforms were calculated, and the percentage of the area under the curve above a frequency of 500 kHz was determined. Table D1 shows the mean percentages for the

Table D1. Percentage of area under power spectrum above 500 kHz for different types of AE

SPECIMEN	*AE TYPE*	*MEAN % AREA ABOVE 500 kHz*
CT2	Primary	45.28
	Secondary (before WD-40)	14.80
	Secondary (after WD-40)	42.94
CT3	Primary	43.41
	Secondary	29.28

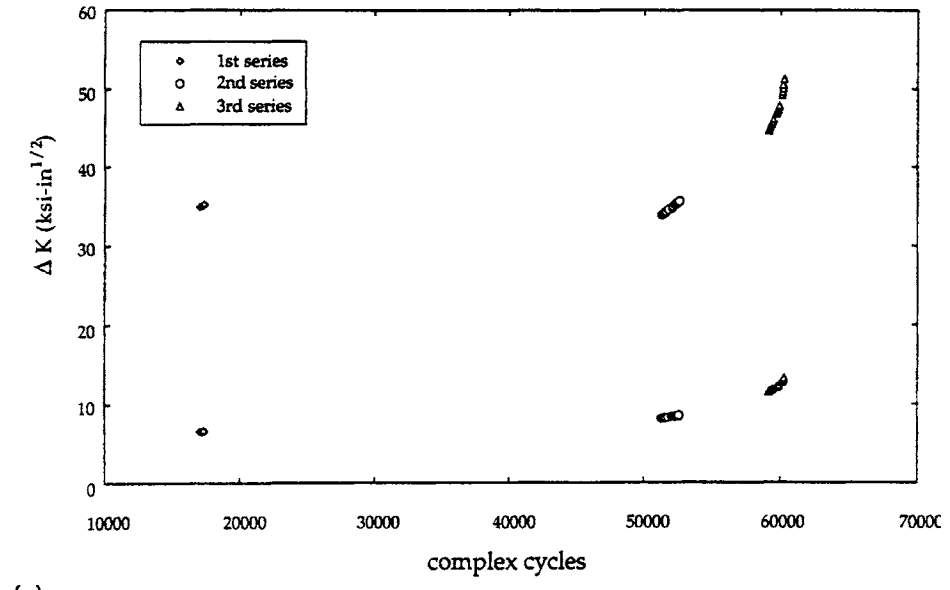

Figure D3. Stress intensity range versus number of complex cycles during AE data acquisition for (a) CT2 and (b) CT3

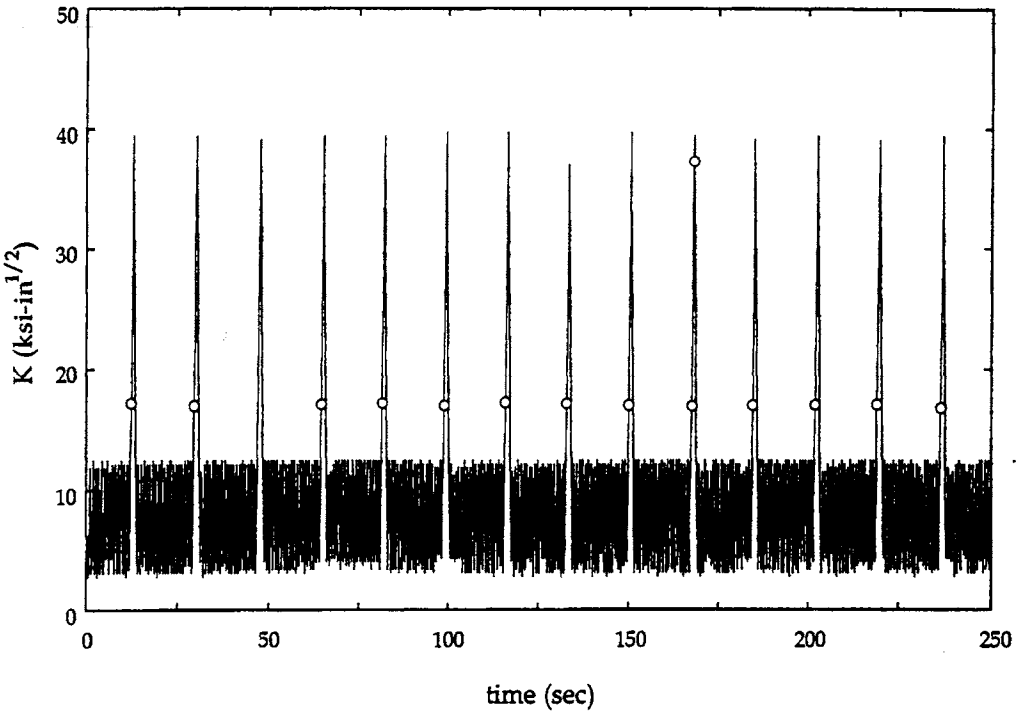

Figure D4. Stress intensity cycle plot of CT3 Type 1 repetitive waveform

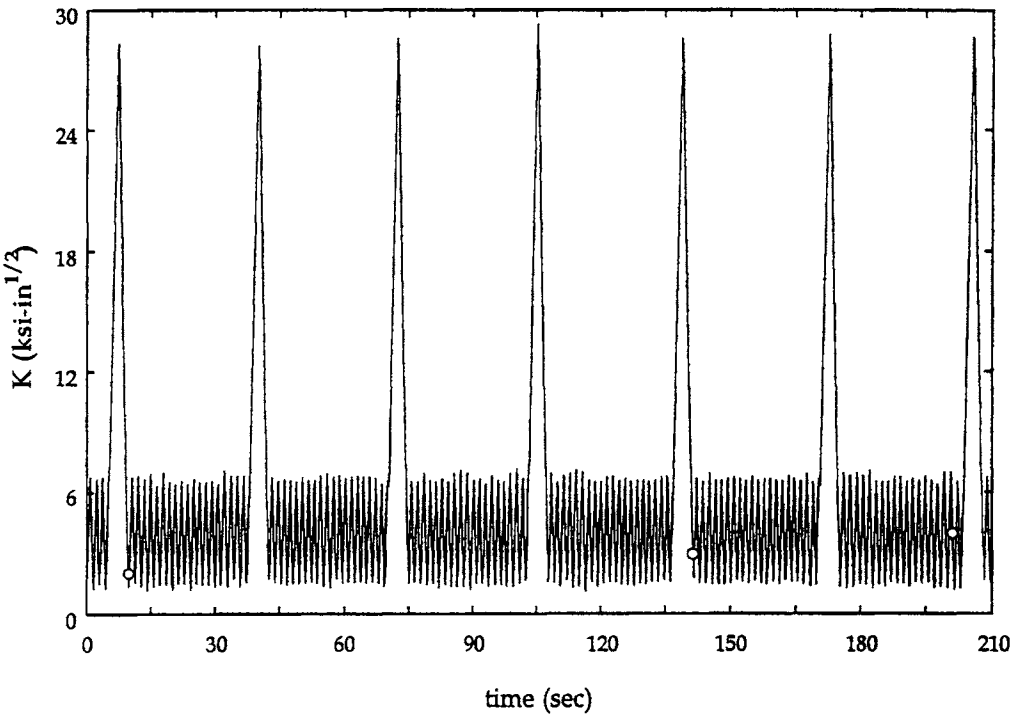

Figure D5. Stress intensity cycle plot of CT3 Type 2 repetitive waveform

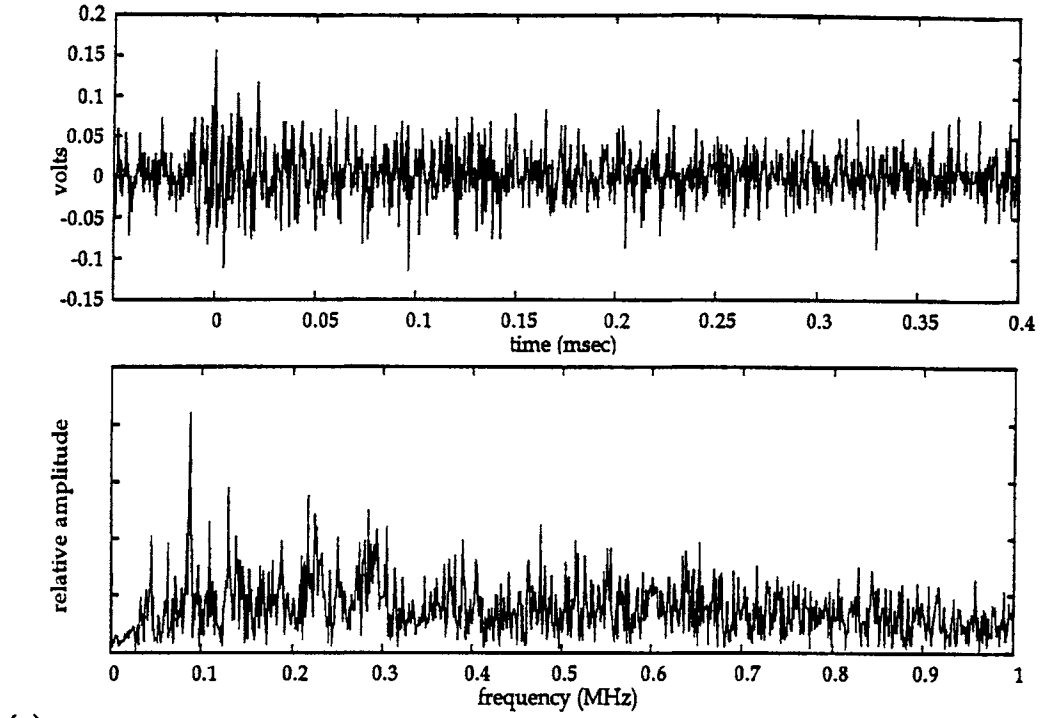

(a)

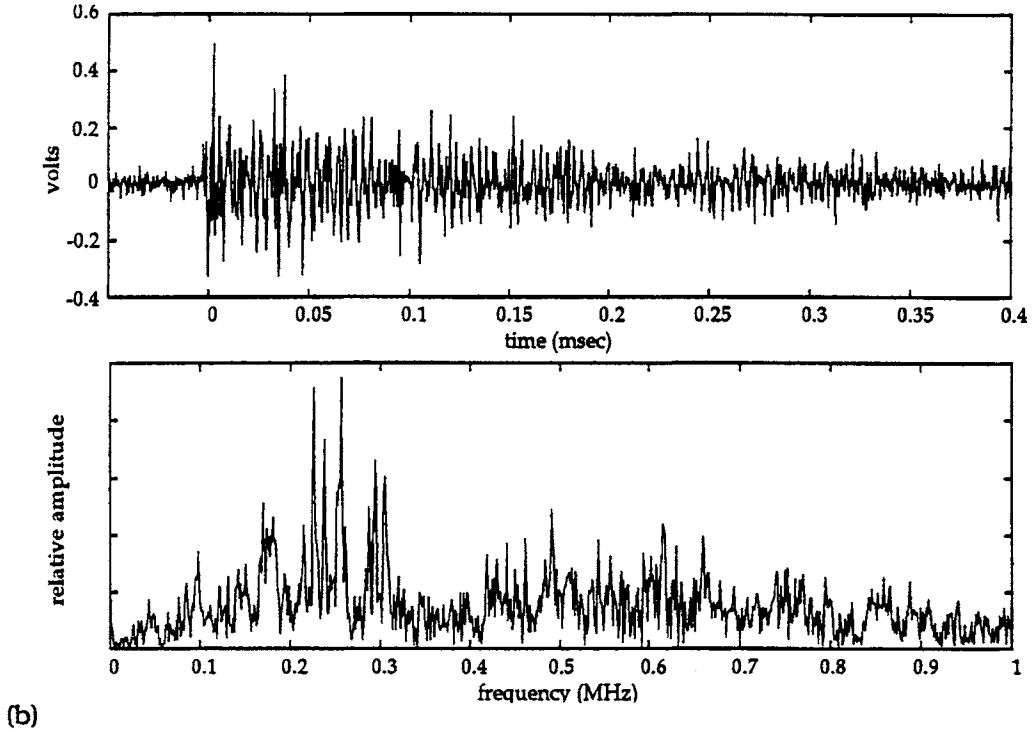

(b)

Figure D6. Crack growth AE (two waveforms and FFT) from compact tension specimens

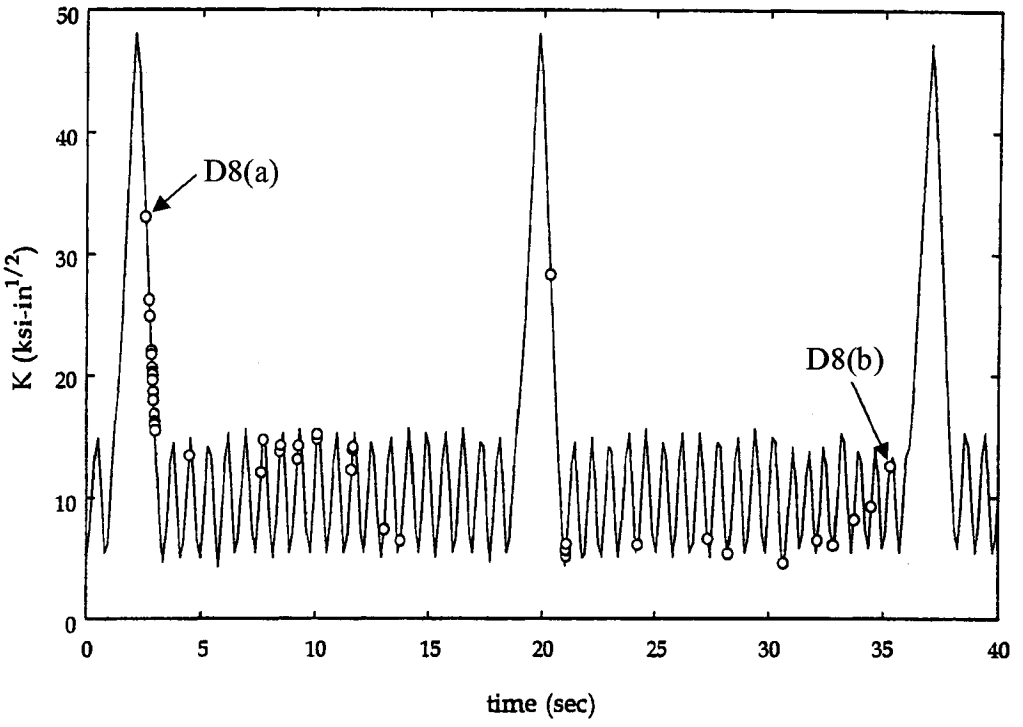

Figure D7. Stress intensity cycle plot of waveforms from crushing of corrosion particles

unique, rising load waveforms believed to be primary emissions attributable to crack growth and for other crack-related, secondary waveforms. Secondary waveforms from CT2 were further grouped in two, based on whether they were detected before or after the application of lubricant to the crack.

To establish the behavior of another source of crack-related AE, crushing of corrosion products between crack faces, a simulated test was set up using specimen CT3. After all regular AE measurements were concluded at a crack length of 1.13 in, hard corrosion scale taken from the bridge hanger was placed at the opening of the crack. The cyclic opening and closing of the crack caused the pieces of rust held on to the crack with vacuum grease to be drawn between the crack faces. CT3 was cycled at the same loading parameters as the regular AE measurements for 833 complex cycles before AE from rust-crushing was recorded. A plot of the location of emissions in the load cycle is shown in Figure D6. All emissions on the plot originated from a single source as evidenced by their nearly identical waveforms. Unlike repetitive AE from crack-face rubbing, the repetitive signals of Figure D6 occurred at widely varying loads, on different sides of the load cycles and several times on a single cycle.

Signal amplitudes of identical waveforms from rust particles also varied widely. The emissions of Figure D7 ranged in peak signal amplitudes of 30 to 58 dB. The repeating waveforms evolved in appearance. Figure D8(a) shows a waveform detected at 2.7 sec in Figure D7, and Figure D8(b) shows a waveform detected at 35.3 sec, 39 minor and overload cycles later. The general waveform appearance was retained, but visible changes were also evident. Such a

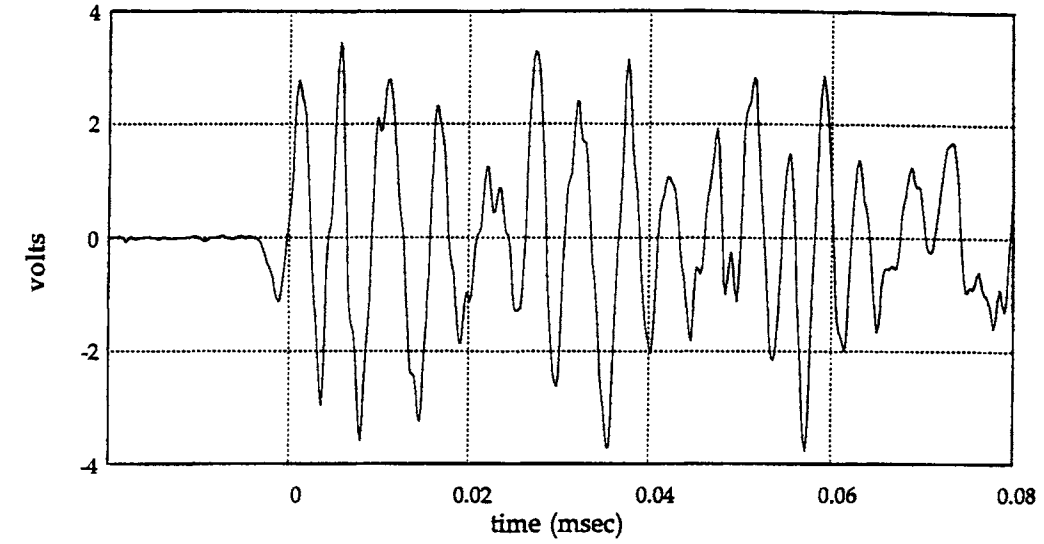

(a)

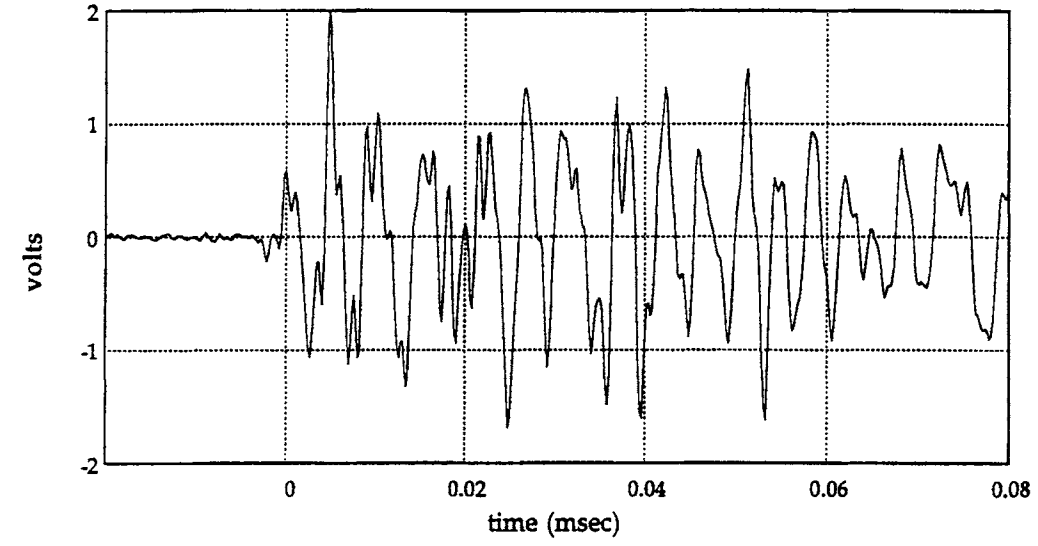

(b)

Figure D8. Two AE waveforms from crushing of corrosion particles showing evolution in appearance of waveforms

rapid change in appearance was not observed from the crack face rubbing emissions. The mean percentage of the area under the power spectrum above 500 kHz for all waveforms from the crushing of corrosion particles was calculated to be 8.56 percent.

APPENDIX E

REMOTE FIELD AE MONITORING

The Executive Summary of the report of a research program jointly sponsored by Sonix, Inc. (Springfield, Virginia), the Virginia Center for Innovative Technology, and the Virginia Transportation Research Council is included here. Requests for copies of the report *Definition of a Bridge Monitoring System,* Final Report to Sonix, Inc., 1995, should be directed to Sonix, Inc., Springfield, Virginia.

Executive Summary

A concept system for acoustic emission (AE) monitoring of steel bridge members has been configured. The system consists of two AE channels, one mechanical strain monitoring channel, that are monitored continuously, and data is periodically reported to a remote location by telephone modem. The system has been installed for extended periods of time on a bridge.

As a result of the field testing the following features are deemed to be critical in a prototype system:

1. capability of booting, from temperature equilibrium, over the range of -10°C - 30°C
2. electrical surge protection on power, communications and data lines
3. ability to periodically, automatically reboot
4. capability to upload and download files (data, executables and parameters) from a remote computer
5. ability to remotely change amplification of AE monitoring channels
6. capability to directly attach a strain gage attached to the bridge, and a temperature compensation gage
7. capability of being easily attached to a bridge substructure
8. RAM: a large allocation sufficient to provide a buffer to allow for data analysis to occur before the final data entry is written to the hard drive
9. hard disk storage if data is analyzed at the remote site 2M/day prior to reporting seems sufficient; if full waveform acquisition and reporting seems impractical for extended periods, memory available would then limit the period of full waveform collection prior to reporting.

The following features are deemed to be desirable:

1. battery powered

2. cellular fax/modem

3. 16 bit voltage resolution.

The above features are in addition to the presently existing features and capabilities of the Sonix STR*825 hardware and software driver routines, when installed in a 386 PC. (Note: The input resistor for the STR*825 board used to monitor the strain was changed to 1 MS.)

Procomm Plus has been used to facilitate communication between the system and the remote reporting site; a comparable software package that could be integrated into the data acquisition software would be essential.

APPENDIX F

PROCEDURAL OUTLINE FOR APPLYING AE MONITORING OF STEEL BRIDGE MEMBERS

As a result of this program, it is recommended that AE monitoring be applied to steel bridge members with forms of deterioration that increase at an uncertain rate such that repeated costly reinspection is necessary to monitor the rate of this deterioration. The appropriate applications for AE monitoring are further limited to those situations for which the deterioration is associated with load redistribution of the structure. Such load redistribution will typically cause AE that can be used to monitor the deterioration. The principal form of deterioration suited to AE monitoring is cracking; however, other situations are also amenable, including the slippage of pins (indicating that the pin is *not* frozen) and the absence of cracking for retrofitted members. Of course, other forms of deterioration are not suitable, e.g., corrosion formation and the associated metal loss.

The application of AE monitoring is recommended for situations where a flaw has been detected during the course of the regular bridge inspection and the extent of the flaw, e.g., a crack, is not sufficiently serious to warrant immediate action to repair or replace the component. In addition, uncertainty concerning the rate of deterioration would exist, making a prediction of when the deterioration of the flaw might progress to a critical point impossible. In such a situation, AE monitoring could be used to "keep tabs" on the flaw with a frequency that could in fact be continuous.

At present, there is no commercially available AE system that can be placed directly onto a bridge structure and left to monitor the flaw; however, such a device is the goal of the FHWA/PAC/VTRC cooperative venture mentioned previously. It is anticipated that the device being developed would be able to operate under the most demanding circumstances without requiring electrical or telephone cable line and report to a remote location.

At present, it is possible to configure a system (using the work described in Appendix E) that is capable of monitoring AE waveforms and strain gage information and reporting this information to a remote location such as a district office. This system, composed of essentially off-the-shelf items, would require support of 110 V electrical service and a standard telephone line.

1. The AE system should be placed in a protected location beneath the bridge in close proximity to the flaw to be monitored.

2. Ideally, two wideband AE sensors should be positioned at locations at known distances from the flaw and away from other possible sources of AE that would be considered noise. If space allows, transducers with integral preamplifiers should be used; otherwise, regular wideband AE sensors should be used along with the separate preamplifiers, which should be located as close as possible to the AE transducer. The

transducers should be held in place with magnetic clamps if a viscous couplant such as vacuum grease is used or bonded using a 5-minute waterproof epoxy.

3. A resistance wire strain gage should be bonded to the structure in a location that will provide an indication of the nature of the loading experienced by the flaw being monitored. The strain gage amplifier should be attached in a convenient, protected location and effectively grounded electrically.

4. The output signal of the AE preamplifiers and the strain gage amplifier should be input to an appropriate datalogging device. This data acquisition system must be capable of recording data for signal variations as high as 2 MHz. Ideally, a computer processing unit incorporating a means of remote communications should be used to power and control these components. Alternatively, a unit that incorporates an FM transmitter might be used to allow for communication with a local computer for uploading control parameters and downloading data.

5. During the initial period of data monitoring, the system should be configured to collected data in as unrestricted a fashion as possible. During the initial period, which may last as long as a week, the collected data should be examined to establish the nature of the AE from the flaw, as well as possible noise sources. This examination should seek to identify a more restrictive monitoring configuration, since often the number of AE collected with unrestricted monitoring is impractical large. Typically, the strain gage output may be used to limit the period of deformation during which AE is stored. (This selection may be very different depending on the location of the strain gage and the circumstances of the monitoring. For example, if a steel pin is being monitored to ensure that the pin is not "frozen," it may be best to select a period during a change in sign of the strain The period of largest positive or negative strain should be monitored for cracks.)

6. The initial monitoring phase should be continued until it is possible to restrict the monitoring configuration. This revised configuration should then be uploaded to the bridge monitoring unit and long-term monitoring commenced.

7. If the system is monitored at a remote site, the data should be periodically considered to determine the rate of "significant" emission. If the data from the system are down-loaded using FM transmission, the period of visitation for transferring the data should be selected as frequently as practical.

8. During the long-term monitoring, it is important to develop a continually increasing history of significant AE activity. When increases in the number of significant AE are observed, consideration should be given to sending an inspector to the bridge. Care should be taken to document as accurately as possible the extent of increased deterioration during the normally scheduled inspections so as to provide a corroborative input for the growing AE database.

During the next few years of using AE monitoring of steel bridge components, each application will provide invaluable input to the database for this NDE procedure. There is no practical substitute for actual inservice monitoring and the experience it will provide because no two flaws behave precisely the same; however, variations within a large database will cause less confusion than when the database is small.

It is highly recommended that the Virginia Transportation Research Council be actively involved, for the near future, in all instances of AE monitoring so as to establish a unified AE database.